NASA CONTRACTOR REPORT

NASA CR-1142

LUNAR ORBITER V

Extended-Mission Spacecraft Operations and Subsystem Performance

Prepared by
THE BOEING COMPANY
Seattle, Wash.
for Langley Research Center

NATIONAL AERONAUTICS AND SPACE ADMINISTRATION • WASHINGTON, D. C. • AUGUST 1968

NASA CR-1142

LUNAR ORBITER V

Extended-Mission Spacecraft Operations and Subsystem Performance

Issued by Originator as Document D2-100755-4 (Vol. IV)

Prepared under Contract No. NAS 1-3800 by
THE BOEING COMPANY
Seattle, Wash.

for Langley Research Center

NATIONAL AERONAUTICS AND SPACE ADMINISTRATION

For sale by the Clearinghouse for Federal Scientific and Technical Information
Springfield, Virginia 22151 – CFSTI price $3.00

Contents

Page

1.0 SUMMARY 1

2.0 INTRODUCTION 3
2.1 Spacecraft Description 3
2.2 Mission Objectives 3
2.3 Operational Organization 5

3.0 FLIGHT OPERATIONS 7
3.1 Spacecraft Control 8
3.1.1 Command Activity 8
3.1.2 Spacecraft Telemetry 8
3.2 Flight Path Control 15
3.2.1 Tracking Data Editing 15
3.2.2 Orbit Determination 15
3.2.3 Guidance Maneuvers 37
3.2.3.1 Orbit Phasing Maneuver for October 1967 Lunar Eclipse Passage 37
3.2.3.2 Terminal Transfer Maneuver 41

4.0 FLIGHT DATA 45
4.1 Environmental Data 45
4.1.1 Radiation 45
4.1.2 Micrometeoroids 45
4.2 Special Experiments 46
4.2.1 Voice Relay Experiment 46
4.2.2 RF Occult Determination Experiment 47
4.2.3 Bistatic Radar Experiment 47
4.2.4 Convolutional Coding/Sequential Decoding Experiment 48
4.2.5 Visual Observation Experiment 48
4.2.6 Manned Space Flight Network/Apollo GOSS Navigational Qualification (MSFN/AGNQ) 49
4.2.7 Perilune Residual Experiment 49

5.0 SPACECRAFT SUBSYSTEM PERFORMANCE 51
5.1 Summary 51
5.2 Subsystem Performance 51
5.2.1 Attitude Control Subsystem 51
5.2.1.1 Inertial Reference Unit (IRU) 60
5.2.1.2 Star Tracker 64
5.2.1.3 Sun Sensors 64
5.2.1.4 Closed-Loop Electronics 64
5.2.1.5 Reaction Control and Nitrogen Usage 69
5.2.1.6 Control Assembly 72
5.2.1.7 Switching Assembly 73
5.2.2 Communications Subsystem 73
5.2.2.1 Transponder 74
5.2.2.2 Traveling-Wave-Tube Amplifier 75
5.2.2.3 Command Decoder 83
5.2.2.4 Modulation Selector 83

Contents - Continued

Page

5.2.2.5 High-Gain Antenna Position Controller 83
5.2.2.6 Radiation 83
5.2.2.7 Micrometeoroid Data 83
5.2.3 Power Subsystem 83
5.2.3.1 Solar Array Performance 83
5.2.3.2 Battery Performance 84
5.2.3.3 Shunt Regulator Performance 87
5.2.3.4 Charge Controller Performance 87
5.2.3.5 Power Subsystem Performance 89
5.2.4 Photo Subsystem 89
5.2.5 Structures and Mechanisms Subsystem 92
5.2.5.1 EMD Thermal Control Coating 92
5.2.5.2 Thermal Control Coating Coupons 92
5.2.6 Velocity and Reaction Control Subsystems 96
5.2.6.1 Reaction Control Subsystem Performance 96
5.2.6.2 Velocity Control Subsystem Performance 96
5.3 Special Flight Tests 100
5.3.1 Battery Discharge Tests 100
5.3.2 Paint Degradation Test 103
5.3.3 Solar Array Performance at High Off-Sun Angles Test 104
5.3.4 Maneuver Accuracy, Pitch and Yaw 105
5.4 Spacecraft Anomaly 105

6.0 EXTENDED-MISSION PROGRAM SUMMARY 111
6.1 Extended-Mission Objectives 112
6.2 Extended-Mission Accomplishments 112
6.3 Flight Operations Summary 114
6.4 Environmental Data 116
6.4.1 Radiation 116
6.4.2 Micrometeoroids 116
6.5 Spacecraft Subsystem Performance 116

Figures

		Page
2-1	Lunar Orbiter Spacecraft	4
2-2	Spacecraft Subsystems	5
3-1	Orbital Inclination History	35
3-2	Perilune Altitude History	35
3-3	Ranging Data Residuals	36
3-4	Predicted Lighting During Lunar Eclipse — OD 6094-10	38
3-5	Predicted Lighting During Lunar Eclipse — OD 8000-10	38
3-6	Predicted Long-Term Variation of Perilune Altitude	39
3-7	Lunar Eclipse Phasing Maneuver	40
3-8	Calculated and Measured Sunlight During Eclipse — Day 291	41
3-9	Terminal Transfer Two-Way Doppler — DSS-41	43
4-1	Radiation Data	46
4-2	Typical Doppler Residuals	50
5-1	Attitude Control Subsystem Functional Block Diagram	52
5-2	Drift Measurement History	61
5-3	EMD (STO3) and Gyro Temperature History Showing Probable Gyro Heater Saturation	62
5-4	EMD (STO3) and Gyro Temperature History During Lunar Eclipse — Day 291	63
5-5	Gyro Temperature Oscillation	63
5-6	Telemetry Data Star Map — Day 270	65
5-7	Telemetry Data Star Map — Day 324	66
5-8	Telemetry Data Star Map — Day 335	67
5-9	Gyro and Acutator Position During Burn — Day 283	69
5-10	Limit Cycle — Day 331, 07:00 to 10:00	70
5-11	Limit Cycle — Day 024, 13:15 to 15:54	70
5-12	Nitrogen Supply History	71
5-13	Communications Subsystem	73
5-14	Transponder Power Output	74
5-15	Transponder Power Output	75
5-16	Transponder Power/Thermal History	76
5-17	TWTA Sunset Performance	77
5-18	TWTA Sunset Performance	78
5-19	TWTA Sunset Performance	79
5-20	Initial TWTA Turn-On	80
5-21	Final TWTA Turn-On	81
5-22	TWTA Performance History	82
5-23	Power Subsystem	83
5-24	Solar Array Performance — Lunar Eclipse of Day 291	85
5-25	Battery Performance — Lunar Eclipse of Day 291	86
5-26	Shunt Regulator Leakage — Day 291	87
5-27	Predicted Light-to-Dark Ratio	88
5-28	Photo Subsystem	89
5-29	Spacecraft Off-Sunline Angle History	93
5-30	EMD Temperature History	94

Figures - Continued

Page

5-31 EMD Temperature History 95
5-32 Velocity and Reaction Control Subsystem 96
5-33 Nitrogen Tank History 97
5-34 Propellant Tankage History 98
5-35 Propellant Pressures – Phasing Maneuver 99
5-36 Propellant Pressures – Terminal Transfer Burn 100
5-37 Battery Discharge Test – Day 270 101
5-38 Battery Discharge Test – Day 012 102
5-39 High Off-Sun Angle Solar Array Performance 104
5-40 Off-Sun Angle 108
5-41 Case I Estimated Array Current versus Mission Time 108
5-42 Case II Estimated Array Current versus Mission Time 109

6-1 Extended-Mission Tracking Summary 111
6-2 Tracking Schedule for Lunar Orbiter Spacecraft 116

Tables

Page

1-1 Orbit Parameter Summary 1

3-1 Programmer Core Map Summary 9
3-2 Spacecraft Telemetry Summary 11
3-3 Tracking Data Summary 16
3-4 Station Timing Synchronization 23
3-5 Master File Tracking Data Tapes 23
3-6 Lunar Harmonic Coefficients 24
3-7 Orbital Elements (Selenographic, True of Date) 25
3-8 Orbit Determination Data Summary 27
3-9 Sun Occultation Times 36

4-1 Radiation Data 45
4-2 MSFN/AGNQ Tracking Summary 49

5-1 Extended-Mission Maneuver Summary 53
5-2 Extended-Mission Attitude Maneuvers 53
5-3 Extended-Mission Maneuver Accuracy 60
5-4 Inertial-Hold Drift Measurements 60
5-5 Gyro Wheel Currents 61
5-6 Limit Cycle Characteristics 68
5-7 Extended-Mission Maneuver Rates 68
5-8 TVC Actuator Position Summary 68
5-9 Postburn Residual Rates 69
5-10 Nitrogen Usage Breakdown 72
5-11 Reaction Control Thruster Performance 72
5-12 Solar Panel Degradation 84
5-13 Power Subsystem Data 89
5-14 Photo Subsystem Temperature and Pressure History 90
5-15 Summary of Photo Subsystem Responses 91
5-16 Major Events Using Nitrogen Gas 97
5-17 Delta V Error Factors 99
5-18 Thermal Coating Experiment Data 103
5-19 Subsystem Status 106

6-1 Extended-Mission Objectives - Lunar Orbiters I through V 113
6-2 Extended-Mission Summary 115
6-3 Extended-Mission Flight Plans 115
6-4 Velocity Maneuvers 117
6-5 Average Orbital Elements 118
6-6 Subsystem Performance 119

Abbreviations

AGNQ	Apollo GOSS Navigation Qualification
ASU	acquire Sun
BOS	bright-object sensor
CAO	Canopus sensor on
CAO*	Canopus sensor off
CDZ	±2.0-degree deadzone
CDZ*	±0.2-degree deadzone
COGL	command generation and programmer simulation program
DACON	data controller
DATL	data alarm summary
DSIF	Deep Space Information Facility
DSN	Deep Space Network
DSS	Deep Space Station
EMD	equipment-mount deck
EMM	execute magnitude minus
FAT	flight acceptance test
FPAC	Flight Path Analysis and Control
GMT	Greenwich Mean Time
GOSS	Ground Operation Support System
IH	inertial hold
IRU	inertial reference unit
JPL	Jet Propulsion Laboratory
LRC	Langley Research Center
MDE	mission-dependent equipment
MSFN	Manned Space Flight Network
NASA	National Aeronautics and Space Administration
ODGX	orbit data generation
ODPL	orbit determination
OMS	optical-mechanical scanner
OSR	optical solar reflectors
PIM	pitch minus
PIP	pitch plus
ROM	roll minus
ROP	roll plus
RTC	real-time command
SFOF	Space Flight Operations Facility
SLOE	Senior Lunar Orbiter Engineer
SPA	stored-program address
SPAC	Spacecraft Performance Analysis and Command
SPC	stored-program command
TDPX	tracking data validation
TRJL	trajectory program
TSF	Track Synthesizer Frequency
TTY	telemetry

Abbreviations - Continued

TVC	thrust vector control	V/H	velocity-height
TWT	traveling-wave tube	YAP	yaw plus
TWTA	traveling-wave-tube amplifier	YAM	yaw minus
VCO	voltage controlled oscillator	ΔV	velocity change

1.0 Summary

The Lunar Orbiter V spacecraft was tracked from the start of its extended mission on August 28, 1967 (GMT Day 240) until it was intentionally crashed into the Moon's nearside on January 31, 1968 (GMT Day 031). During this period, the primary objectives of selenodetic data acquisition and lunar environment sampling were accomplished by ranging, tracking, and spacecraft telemetry monitoring. All high-priority secondary objectives, which included four special exercises and seven experiments, were accomplished prior to mission termination.

From August 28, 1967 (GMT Day 240) until October 9, 1967 (GMT Day 282), Lunar Orbiter III, which had been inserted into an Apollo-type orbit, was designated as the prime spacecraft for selenodesy studies. Lunar Orbiters II and V were tracked only to obtain a brief subsystem status check during this period. Following the termination of the Lunar Orbiter II and III missions, Lunar Orbiter V was maneuvered to survive the October 18, 1967 (GMT Day 291) lunar eclipse. Selenodesy data were acquired approximately every three days from October 11, 1967 (GMT Day 284) until the end of the mission. Orbit parameters before and after transfer maneuvers are shown in Table 1-1.

Of significance in lunar environmental data were proton events starting on November 1, 1967 (GMT Day 305) and December 1, 1967 (GMT Day 335), which caused increases of 1.5 and 3.5 rads, respectively, on the looper radiation dosage counter. Five micrometeoroid hits were sustained by the spacecraft's detectors during the extended mission.

The special exercises that were conducted provided the results summarized below.

- On September 27, 1967 (GMT Day 270) a battery discharge test was conducted after a 51-day period of constant overcharge. The test was repeated on January 12, 1968 (GMT Day 012) after the battery had experienced approximately 750 discharge cycles. Both tests confirmed that the battery characteristics had not been detrimentally affected.
- The maneuver accuracy test in the pitch and yaw axes showed that the attitude control subsystem performed within the mission tolerance of 0.3%.
- Absorptivity and emissivity data on several experimental paint samples were gathered and used in studies of paint degradation caused by the solar environment.

Table 1-1: Orbit Parameter Summary

Event	Day GMT	Calendar	Perilune Altitude (km)	Apolune Altitude (km)	Inclination (deg)	Period (min)	Comments
Start extended mission	240	Aug 28, 1967	105	1,490	85	191	
Eclipse phasing maneuver Δ V= 67.5 m/sec	283	Oct 10, 1967	113 199	1,480 1,985	85	191 225	Prepare for lunar eclipse on Day 291
Terminal transfer maneuver Δ V=29.14 m/sec	031	Jan 31, 1968	164 −7.4	2,023	85	225 215	Designed for lunar impact
Lunar impact	031	Jan 31, 1968	–	–	–	–	Impact time 075808.27 Lat 2.79° S Long 83.04° W

- The performance of the solar array at high off-Sun angles was measured dynamically and checked with three static points. The test showed that the array output departs from the cosine function at higher angles of incident illumination.

The following special experiments were performed to support the MSFN and to obtain additional data of a scientific nature.

- The MSFN employed Lunar Orbiter V to acquire two-way tracking data, conduct time correlations, range, develop procedures, and train network personnel. The network also used the spacecraft to develop farfield antenna patterns and in preliminary qualification of the basic real-time computer complex (RTCC) navigational concepts.
- The bistatic radar experiments were conducted to obtain information concerning lunar topography from reflected RF signals.
- Voice messages of excellent quality were relayed from Earth through the spacecraft and back to Earth.
- Accurate measurements of the occultation of the spacecraft's RF signal were made as an independent correlation point for orbit determination and as a possible data source for measuring lunar surface characteristics such as conductivity.
- Convolution coding/sequential decoding experiments were conducted to confirm theoretical calculations and ground simulations of this information transfer technique.
- On January 21, 1968 (GMT Day 021) the spacecraft was visually tracked from an Earth-based telescope located at the Lunar and Planetary Laboratory, Tucson, Arizona.
- The spacecraft was tracked in one-way lock by DSS-12 and DSS-41 at apolune and perilune to provide additional Doppler data that might eliminate uplink lock as the source of perilune residuals in the orbit determination solutions.

In general, all of the spacecraft's subsystems performed satisfactorily through January 26, 1968 (GMT Day 026), and from January 29, 1968 (GMT Day 029) to the end of the mission. In the intervening period a spacecraft anomaly occurred that resulted in depletion of the nitrogen attitude control gas to an unsatisfactorily low level. The cause of the situation could not be conclusively established. The out-of-tolerance conditions that were observed consisted of a shunt regulator leakage in the power subsystem, which cleared itself; gyro drift rates in yaw and roll; and the pitch plus deadband. None of these conditions adversely affected the extended-mission operation.

Because of the excessive loss of nitrogen gas, the spacecraft was maneuvered to a controlled impact on the lunar surface on January 31, 1968 (GMT Day 031). Actual impact was calculated to have occurred at 07:58:08.27 GMT at 83.04° W longitude and 2.79° S latitude.

2.0 Introduction

This volume describes spacecraft control and flight path analysis and control operations conducted during this extended mission and discusses spacecraft performance during these operations. Complete data packages have been prepared for each experiment and special exercise under separate cover and forwarded to the requestor via the NASA experiment coordinator. The highlights of each special exercise and experiment are summarized herein.

Transition from the photographic mission to the extended-mission phase was completed on Day 240 (August 28, 1967). All spacecraft systems were operational, with the exception of the photo subsystem, which had malfunctioned after successfully completing the photographic mission. The spacecraft was in an orbit inclined 85 degrees to the lunar equator with an apolune altitude of 1,490 kilometers, a perilune altitude of 105 kilometers, and a period of 191 minutes. The spacecraft was operating in wide deadzone (2.0 degrees) and pitched off the sunline at plus 53 degrees for thermal relief. The communications subsystem was operating in Mode III.

2.1 SPACECRAFT DESCRIPTION

The 853-pound Lunar Orbiter spacecraft is 6.83 feet high, spans 17.1 feet from the tip of the rotatable high-gain dish antenna to the tip of the low-gain antenna, and measures 12.4 feet across the solar panels. Figure 2-1 shows the spacecraft in the flight configuration with all elements fully deployed (the mylar thermal barrier is not shown). Major components are attached to the largest of three deck structures, which are interconnected by a tubular truss network. Thermal control is maintained by controlling emission of internal energy and absorption of solar energy through the use of one-inch-square mirrors and a special paint covering the bottom side of the deck structure. The entire spacecraft periphery above the large equipment-mounting deck is covered with a highly reflective aluminum-coated mylar shroud, providing an adiabatic thermal barrier. In addition to its structural functions, the tank deck is designed to withstand radiant energy from the velocity control engine to minimize heat losses. Three-axis stabilization is provided by using the Sun and Canopus as primary angular references, and by a three-axis inertial system when the vehicle is required to operate off celestial references, during maneuvers, or when the Sun and/or Canopus are occulted by the Moon. The spacecraft subsystems are shown in block diagram form in Figure 2-2.

2.2 MISSION OBJECTIVES

The primary objective of this extended mission was to secure information that could be used to increase scientific knowledge of the size and shape of the Moon, the properties of its gravitational field, and the lunar environment. Secondary objectives were to conduct special experiments and exercises, and explore the use of Lunar Orbiter subsystems for other applications. During this extended mission the following exercises and experiments were included.

- *Voice relay experiment* to test the feasibility of relaying voice by a lunar orbiting spacecraft.
- *Battery discharge test* to determine battery performance.
- *Paint degradation test* to measure the degradation of four types of thermal control paints when exposed to space environments.
- *MSFN/Apollo GOSS navigational qualification* support to qualify the Apollo tracking-data acquisition system.
- *RF occultation experiment* to evaluate the fundamental nature of lunar occultation of an RF signal.
- *Bistatic radar experiment* to investigate methods of obtaining scientific information about the surface of celestial bodies using radar techniques.
- *Solar array performance* test to establish solar array performance at high angles of incident illumination.
- *Convolutional coding/sequential decoding experiment* to verify theoretical calculations using a spacecraft RF link.
- *Visual observation experiment* to determine whether the Lunar Orbiter V spacecraft can be observed with Earth-based optics.
- *Doppler residual (perilune) experiment* to eliminate ground transmitter signals as a cause of perilune residuals.

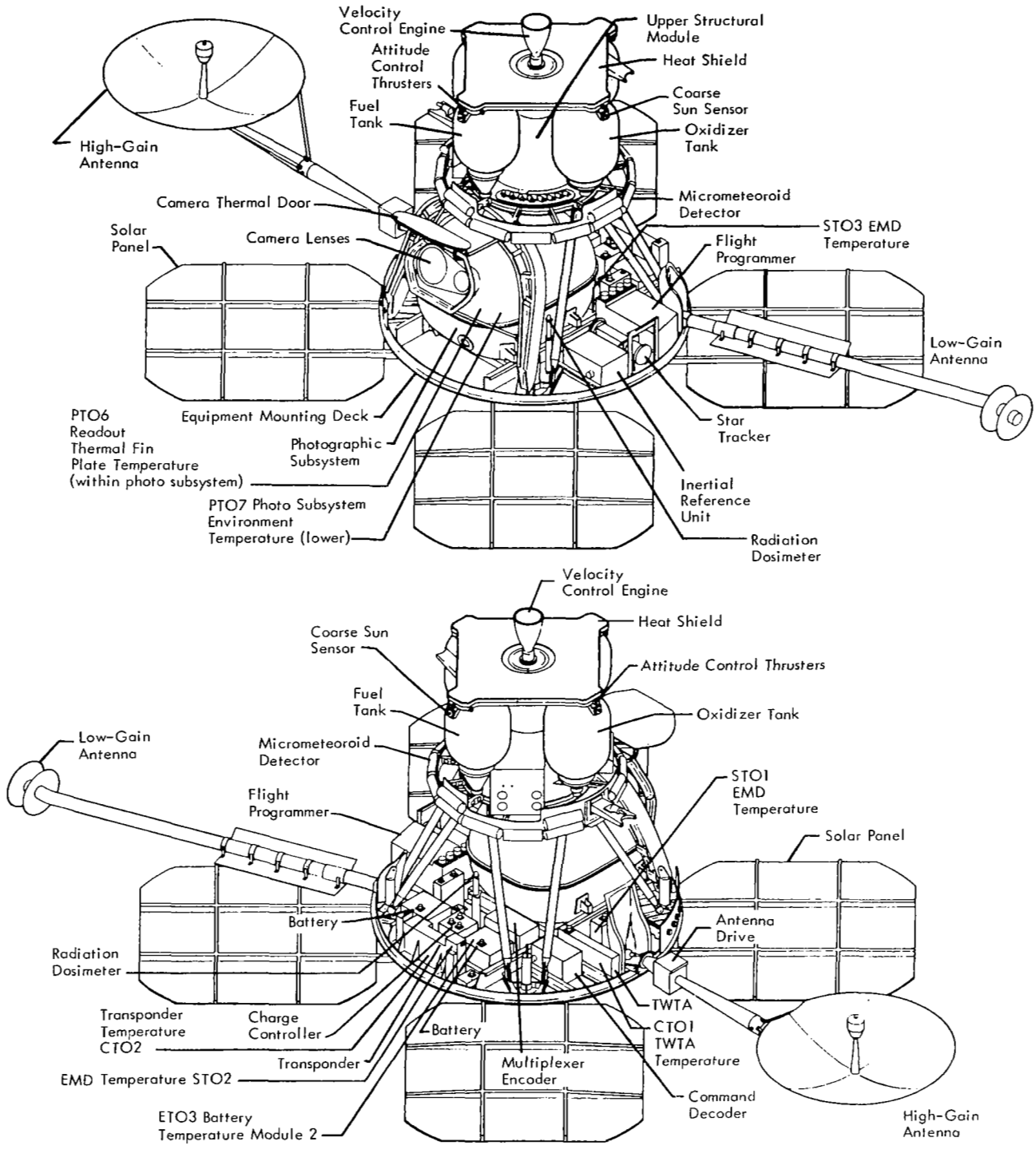

Note: Shown with Thermal Barrier Removed

Figure 2-1: Lunar Orbiter Spacecraft

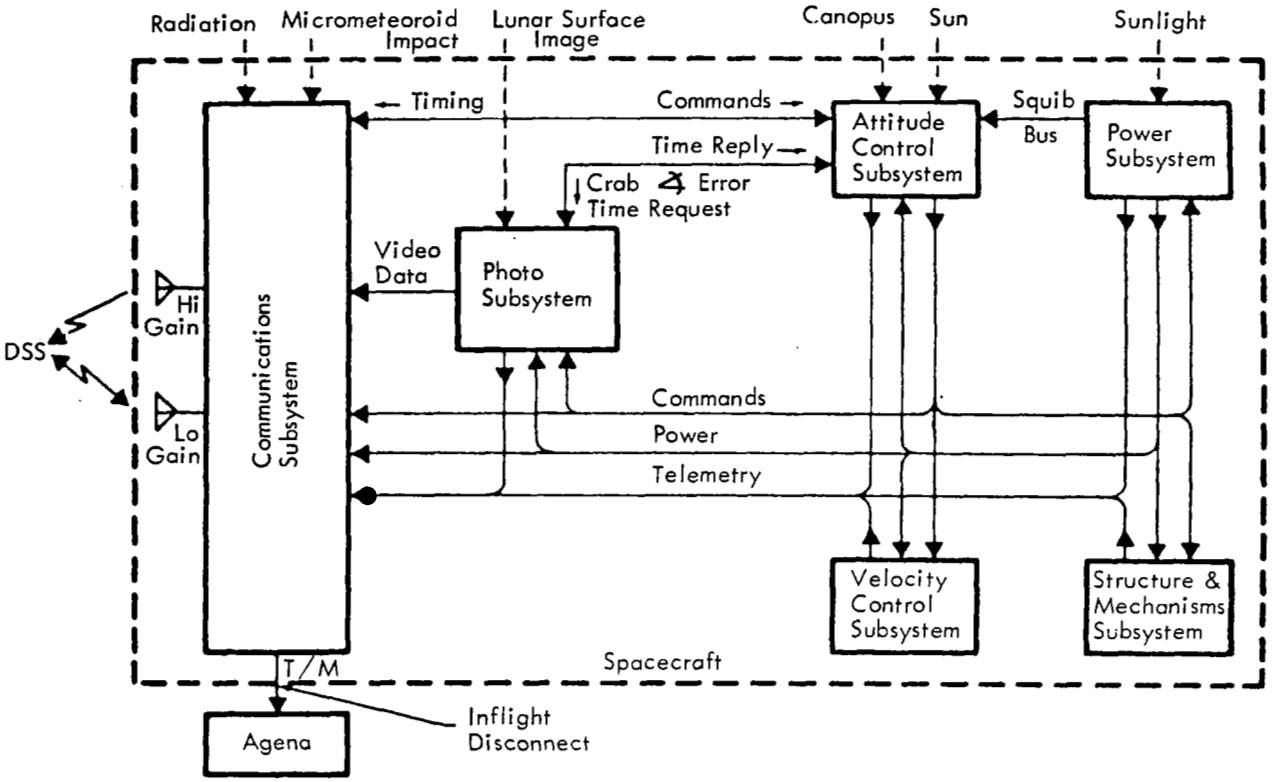

Figure 2-2: Spacecraft Subsystems

- *Maneuver accuracy test* to determine the maneuver accuracy of the attitude control subsystem.

2.3 OPERATIONAL ORGANIZATION

The extended mission of Lunar Orbiter V was conducted using a centralized method of control from the Space Flight Operations Facility at Pasadena, California, that was similar to that adopted for the photographic missions. Primary differences between extended and photographic mission activities are described in the following paragraphs.

Manning at the SFOF and at the DSS's was at a significantly reduced level during the extended mission than during the photographic mission. Manning at the DSS's was reduced by limiting the MDE personnel to the Senior Lunar Orbiter Engineer (SLOE) provided by the DSN. During the photographic mission, the additional services of a video engineer, assistant SLOE, MDE systems engineer, supporting film processing personnel, and telemetry operators were required. Manning at the SFOF was reduced in several areas. The NASA mission advisors were no longer required; however, a small NASA scientific team located at the Langley Research Center was available for selenodetic studies and consultation. The Mission Director also was no longer required at the SFOF, but was available at Langley for key decisions. It was possible to reduce the size of the operational teams because of shorter tracking periods and a decrease in the level of operational activity. For those periods of increased activity such as preparation for and during a velocity maneuver, personnel from the contractor's facility were sent to the SFOF to augment the extended-mission team. During long (but infrequent) tracking periods such as MSFN tracks, which lasted up to 28 hours, the extended-mission team was also augmented by personnel from the contractor's facility.

A list of the manning provided by the contractor at the SFOF for extended-mission tracks is shown below. In addition to these personnel, the space flight operations director and a reduced (from the photographic mission) complement of JPL personnel such as track chief and communications personnel were required to support the tracking periods.

- Assistant space flight operations director
- SPAC
  1) Command programmer analyst
  2) Attitude control analyst
  3) Power/thermal analyst
  4) Communications system analyst
  5) SPAC software analyst
  6) Photo subsystem analyst
  7) Command coordinator
- DACON
  Data controller
- FPAC
  1) Flight chief
  2) Orbit determination analyst
  3) Guidance analyst

3.0 Flight Operations

An extended-mission flight operations plan was developed within the constraints of (1) DSN commitment for tracking coverage, (2) nitrogen gas available for attitude control, (3) preservation of capability for positive mission termination (lunar impact), and (4) maximization of selenodesy data acquisition.

The tracking commitment during the first 30 days consisted of a track every other day of three orbits' duration (approximately 11 hours) to be shared by the active spacecraft. After the first 30-day period, the tracking commitment was reduced to a two-orbit track (approximately 7 hours) every third day. In addition, three tracks per month, on an average, were extended to approximately 27 hours' duration to support the MSFN effort.

The spacecraft had 5.4 pounds of nitrogen at the end of the photographic mission, which was enough to complete a nominal 11-month extended mission with the experiments and special exercises then specified. At that time it appeared that Lunar Orbiter II could complete an 11-month extended mission if maneuvering were limited; Lunar Orbiter III also had promise of getting almost 11 months of extended mission if maneuvering were limited. The wide-attitude control deadzone, 2.0 degrees, was used whenever possible to conserve the supply of nitrogen gas. Thermal control of the spacecraft was maintained by using the appropriate off-Sun angle within power constraints. Gyro drift, and the need to keep spacecraft temperatures within satisfactory operating limits were the prime considerations in determining off-Sun angle and the update cycle stored in the flight programmer.

In the initial stage of the Lunar Orbiter V extended mission, Lunar Orbiter III was inserted into an Apollo-type orbit. As this nearly circular orbit could provide significant new selenodesy data, Lunar Orbiter III was designated the prime spacecraft for tracking purposes and MSFN support. During this period Lunar Orbiter V and Lunar Orbiter II were tracked briefly during each pass to determine subsystem status. Lunar Orbiter V, however, was used to support the voice relay experiments during this early extended-mission phase.

Preparations for the October 18 lunar eclipse consisted of terminating the extended missions of Lunar Orbiters II and III and orbital phasing of Lunar Orbiter V. At that time, the propellant remaining was inadequate to alter the orbital geometry sufficiently to survive the eclipse, maintain an impact reserve, and prevent the predicted light-to-dark ratio from discharging the battery after Day 121 (reference paragraph 5.2.3.4). The plan was therefore modified to (1) survive the eclipse, (2) perform additional experiments commensurate with the time and nitrogen gas available, and (3) monitor the actual and predicted perilune altitude to determine the latest impact opportunity.

Implementation of the flight plan was accomplished by operations directives, which were prepared for each tracking period and defined the support requirements and the sequence of events to be followed. The primary considerations used in preparing these directives included:

- Amount of nitrogen available for attitude control;
- Thermal history and temperature trends;
- Electrical power loads and array capability at various off-Sun angles;
- Requirements for special exercises and experiments.

The spacecraft was operated according to the flight plan until Day 029 (January 29), when the nitrogen gas supply was discovered at DSS acquisition of signal to be below the safe operating level. At that time, the perilune altitude consideration predicted mission termination in late February or March. Because of the low nitrogen supply, however, the spacecraft was maneuvered for a controlled impact on the near-side of the lunar surface at the earliest opportunity, Day 031 (January 31).

3.1 SPACECRAFT CONTROL

Until the missions of Lunar Orbiters II and III were terminated, spacecraft control required that multiple-spacecraft operation techniques be used to avoid interference with other extended-mission spacecraft using approximately the same best-lock frequency. Multiple-spacecraft operation was accomplished by a variety of techniques, including tracking at offset frequency to prevent the acquisition of an undesired spacecraft, programming command transmission to occur when secondary spacecraft were occulted from the Earth, and delaying command transmission until inadvertent uplink lock was prevented by orbital geometry. In addition, the secondary spacecraft were tracked for a brief period, after all command activity on the prime spacecraft had been completed, to verify flight programmer operation and to monitor other subsystem status. After the other missions were terminated, special control techniques were no longer required or used.

After spacecraft acquisition, real-time telemetry readout was obtained at the SFOF via high-speed data line and 60-wpm teletype. The telemetry data were processed in real time by an IBM 7044 computer or in conjunction with an IBM 7094 computer, and then displayed on 100-wpm teletype machines, X-Y plotters, and bulk printers for analysis.

Commands used to change the spacecraft programmer memory were normally generated by the COGL program, sent to the DSS, and transmitted to the spacecraft. Such programmer commands were used to perform housekeeping functions and to conduct experiments and special exercises. The programmer maps were supplemented by RTC updates as required, which did not necessitate use of the COGL program.

3.1.1 Command Activity

Initially, the programmer core map used to update the Sun reference consisted of acquiring the Sun every 72 hours and pitching plus 53 degrees for thermal relief. As shown in Table 3-1, this map was revised on Day 242, and at other times during the course of the extended mission as required, to compensate for changing gyro drift rates and thermal conditions. The table also shows real-time jump commands that initiated stored-program sequences for special activities, such as Sun occultation recording, and which returned the programmer to the cruise map.

Real-time commands were employed to supplement stored sequences whenever the desired spacecraft activity was not sufficiently predictable to be stored or when a spacecraft reaction had to be evaluated prior to proceeding to the next command. Virtually all activity concerned with star acquisitions was accomplished by real-time commands due to the possibility of interference by glint with the star tracker operation. Real-time commands were also typically used to overstore discrete programmer locations, to rotate the high-gain antenna, to cycle the star tracker on and off to break lock on glint, to initiate velocity maneuver sequences, as a backup terminate for velocity maneuvers, and to orient the spacecraft as dictated by real-time situations.

A total of 670 RTC's and a total of 241 SPC's were executed during the extended mission.

3.1.2 Spacecraft Telemetry

A total of 471.6 hours of telemetry data was processed for 65 Lunar Orbiter V tracking passes. Table 3-2 contains a summary of telemetry data by station and includes a listing of the significant activities accomplished during each pass. The DSS-14 and DSS-72 ranging checkouts listed in Table 3-2 consisted of two-way tracking and ranging by the stations in preparation for Mariner '67 activities.

During quick-look tracking periods the spacecraft was analyzed to determine subsystem performance. Of primary interest was the detection of detrimental spurious commands that may have been received during command transmissions to another spacecraft. When possible, the quick-look tracking periods were scheduled to make possible the observation of predicted events such as sunrise, sunset, and earthset to evaluate the validity and error magnitudes in the current predicted orbital parameters. This information was used to up-

Table 3-1: Programmer Core Map Summary

Map Number	Time Transmitted to spacecraft Day:Hr:Mn	Time Span Effectivity Day:Hr:Mn/Day:Hr:Mn	Purpose	COGL Run Number
59		239:22:55/240:00:00	Flight plan-(acquire Sun, wait approximately 60 min, pitch plus 53°, wait approximately 72 hours, repeat)	238-02-1
--	244:13:45	240:00:00/260:00:00	New flight plan (acquire Sun, wait approximately 60 min, pitch minus 53°, wait approximately 72 hours, repeat)	254-02
60	264:07:49	260:00:00/270:00:00	New flight plan-(acquire Sun, wait approximately 60 min, pitch minus 53°, wait approximately 49 hours, repeat)	264-000
61	270:10:16	270:00:00/271:00:00	1) Battery discharge test	270-01A
62	270:10:39		2. Antenna rotation sequences	
63	270:18:57		3) Revise flight plan to pitch minus 50° on Days 272, 274 and 276 only	
64	----	271:00:00/280:01:02	Reflects RTC jump command	274-02
65	283:02:47	280:01:02/283:04:00	Preparations for lunar-eclipse-phasing velocity maneuver	283-01
65 Update	283:17:06	283:04:00/284:00:00	Parameter update for velocity maneuver	283-02
66	291:12:14	284:00:00/295:00:00	Lunar eclipse emergency sequences (transmitted to spacecraft, but not used during lunar eclipse)	291-01
--	----	295:00:00/310:00:00	Reflect RTC jump command	296-01
66U & RTC JMP	321:19:20	310:00:00/335:00:00	1) Reflects four RTC jump commands 2) Over stores lunar eclipse emergency sequences (IRU off, etc)	324-01
--	----	335:00:00/345:00:00	Reflects four RTC jump commands	340-01C

Table 3-1 (Continued)

Map Number	Time Transmitted To Spacecraft Day:Hr:Mn	Time Span Effectivity Day:Hr:Mn/Day:Hr:Mn	Purpose	COGL Run Number
67	345:20:44	345:00:00/346:00:00	Sequence to configure the programmer to store Sun occultation times	347-01A
68	349:22:30	346:00:00/360:00:00	Reflects real-time jump commands and TWTA "off" sequence for MSFN pass	355-01
--	----	360:00:00/365:24:00	Reflects real-time jump commands	361-01
68 Update	009:00:43	365:24:00/010:00:00	Extends Sun occultation sequence and reflects RTC's	373-01
69	012:17:30	010:00:00/016:00:00	1) Battery discharge test 2) Solar array performance	380-01
--	----	016:00:00/020:00:00	Reflects RTC's	383-01
70	021:11:30	020:00:00/024:09:43	New flight plan-(acquire Sun, wait approximately 30 min, pitch minus 53°, wait approximately 49 hours, repeat)	386-01
--	----	024:09:43/025:00:00	Reflects RTC's	024-01
71	026:19:22	025:00:00/027:00:00	New flight plan-(acquire Sun, wait approximately 30 min, pitch minus 60°, wait approximately 49 hours, repeat)	026-01
72	030:08:30	027:00:00/030:00:00	1) Telemeter Memory 2) Readjustment due to halt mode 3) Camera test sequence	029-01
72 Update	031:04:38	030:00:00/031:07:59	Terminal velocity maneuver	

Table 3-2: Spacecraft Telemetry Summary

Day	Period (GMT)	Deep Space Station	Activities
242	02:47-03:05	62	*
242	22:30-22:50	41	*
243	00:40-01:00	41	*
243	04:46-05:18	62	*
244	13:39-13:53	12	*
248	15:50-16:04 15:50-18:55 18:00-18:40	62 14 12	a. DSS 14 planetary ranging checkout b. *
250	18:03-18:45	62	*
253	07:13-07:55	41	*
254	18:10-18:50	62	*
255	15:32-15:38	41	*
256	22:36-23:10	62	*
258	22:30-23:07	62	*
261	11:35-12:11	41	*
262	09:23-10:00	12	*
264	07:47-07:51	12	*
265	07:08-10:00 07:20-10:00	12 14	a. DSS 14 planetary ranging checkout b. *
267	18:35-18:45	41	*
270	10:15-20:30 16:57-20:30	12 41	a. Voice relay experiment b. Battery discharge test c. Selenodesy
272	15:17-15:52	12	*
273	01:46-01:52	41	*
274	12:06-18:20	12	a. Voice relay experiment b. Selenodesy

Table 3-2 (Continued)

Day	Period (GMT)	Deep Space Station	Activities
275	11:04-17:00 17:12-21:00	62 12	a. Voice relay experiment b. Selenodesy
276	12:06-17:31 13:32-24:00 20:45-23:05	62 12 41	a. Voice relay experiment b. Selenodesy
277	14:01-17:19	62	DSS 72 ranging checkout
279	07:25-08:00	41	*
282	10:36-10:42	41	*
282 282-283 283	18:00-21:20 21:00-05:03 02:33-06:00	62 12 41	Selenodesy
283 283-284 284	14:52-22:39 22:10-05:20 03:29-04:15	62 12 41	a. Lunar-eclipse-phasing velocity maneuver b. Selenodesy
284	07:15-07:20	41	*
286	16:45-21:00	62	Selenodesy
289	11:00-14:00	41	Selenodesy
291	05:01-13:23 09:03-15:32	12 41	a. Lunar eclipse monitoring b. Selenodesy
294	19:35-21:41	62	*
296	14:00-16:50	41	Selenodesy
300	14:03-20:48 17:38-24:00	12 41	a. Selenodesy b. Paint degradation test
303	12:01-15:26 12:01-22:28	62 12	Selenodesy
305-306	22:04-00:15 22:04-08:00	12 41	Selenodesy
309	11:39-19:20 18:33-19:20	62 12	Selenodesy

Table 3-2 (Continued)

Day	Period (GMT)	Deep Space Station	Activities
312	15:45-22:45 20:57-22:45	62 12	Selenodesy
315	14:58-16:59 15:01-22:00	41 62	Selenodesy
318 318-319	17:15-18:24 17:14-00:11	41 62	Selenodesy
320-321 321	18:06-01:00 01:37-13:38 10:05-19:47	62 12 41	a. Selenodesy b. MSFN
324 324-325 325	14:01-22:00 21:50-10:13 07:02-17:00 14:32-17:00	41 62 12 41	a. MSFN b. RF occultation experiment c. Selenodesy
326 326-327	21:46-23:57 21:57-05:30	41 62	Selenodesy
331	06:33-13:53 10:20-13:56	62 12	Selenodesy
333	07:32-14:57 12:20-14:57	62 12	Selenodesy
335	13:17-15:55 14:47-23:37	62 12	a. Bistatic radar experiment b. Selenodesy c. Paint degradation test
339 339-340 340	00:04-12:26 12:00-20:29 19:20-04:30 00:52-04:30	41 62 12 41	a. MSFN b. Selenodesy
340-341 341	19:57-05:28 00:48-14:07 12:46-22:42	12 41 62	a. MSFN b. Selenodesy
345	15:14-22:17	62	Selenodesy
349	17:01-23:56	62	Selenodesy
352-353 353	19:07-09:04 03:42-15:50	62 12	a. Selenodesy b. MSFN

Table 3-2 (Continued)

Day	Period (GMT)	Deep Space Station	Activities
355-356	22:02-00:20 22:02-05:00	41 62	Selenodesy
361	05:01-11:48	62	Selenodesy
363 363-364	21:18-22:43 21:18-03:45	12 41	Selenodesy
002	12:00-19:00 17:28-19:00	62 12	Selenodesy
005-006	19:07-01:00	12	Selenodesy
008-009	20:37-01:00	12	a. Selenodesy b. Maneuver accuracy test – pitch and yaw
012	17:24-23:45	62	a. Selenodesy b. Paint degradation test c. Solar array performance test d. Battery discharge test
015	03:00-06:58 03:00-12:31	62 12	a. Selenodesy b. Convolutional coding experiment
018	04:04-08:00 04:12-14:00	62 12	a. Selenodesy b. Convolutional coding experiment c. Visual observation experiment
021	06:53-10:22 06:56-14:30	62 12	a. Selenodesy b. Visual observation experiment
024	09:27-11:58 10:34-19:37 14:10-19:37	62 12 14	a. Selenodesy b. Bistatic radar experiment
026	14:01-20:50	12	a. Selenodesy b. Convolutional coding experiment
029-030 030 030-031 031	15:16-00:50 21:25-09:13 08:55-18:06 16:01-02:04 22:12-07:58 06:00-07:58	12 41 62 12 41 51	a. Selenodesy b. MSFN c. Doppler residual (perilune) experiment d. Postterminal velocity maneuver tracking

*Quick-look monitoring – see discussion in Section 3.1.2, page 8.

date the DSS predict information just prior to each tracking period.

Problems encountered, such as minor communications outages and computer internal restarts, were typical of those experienced during the prime missions. Standard workaround methods, such as processing of TTY data and use of raw hexidecimal data, were employed to minimize data problems. The communications processor caused the raw TTY data to lag behind real time, which resulted in frequent deletion of data in order to return to real time.

A data and alarm summary (DATL) containing a majority of the telemetry channels for each frame was processed for all tracking passes to provide a permanent record of the telemetry data.

3.2 FLIGHT PATH CONTROL

Flight path control of the spacecraft during the extended mission is the responsibility of the FPAC portion of the flight team. The functions carried out by this team are identical to those during the primary mission (i.e., tracking data editing, orbit determination, and guidance maneuver calculations). The processes used to perform these functions are the same as in the prime mission, except that data quantity is less due to decreased tracking time.

3.2.1 Tracking Data Editing

Tracking data editing is the process of monitoring, analyzing, and judging the quality of the Doppler and range radar tracking data transmitted to the SFOF from the DSN. The data, provided by three DSN stations – Madrid, Spain (DSS-62); Woomera, Australia (DSS-41); and Goldstone, California (DSS-12) – are of three types: continuous-count Doppler, ranging units, and antenna-pointing angles. The pointing angles were not used because of the small arc traversed by the spacecraft in lunar orbit. Table 3-3 is a summary of the tracking data obtained during the extended mission. Computer programs TDPX and ODGX were used to edit and process the tracking data. Tables 3-3 and -4 provide information used for this editing and processing. Table 3-5 contains a list of master file (tracking data) tapes generated by TDPX; both tapes sent to Langley Research Center and those kept in the Jet Propulsion Laboratory tape library are listed.

3.2.2 Orbit Determination

Orbit determination is a best-fit technique of computing the spacecraft trajectory from actual tracking data. The computer program used during the extended mission, identical to that used during the primary mission, is identified as ODPL and calculates orbit determinations from the tracking data prepared by the editing programs. ODPL uses a seventh-order spherical harmonic expansion of the lunar potential field. NASA provided the coefficients for the lunar model on July 28, 1967 (see Table 3-6). The following general procedures were used in the orbit determination procedures.

- Use at least two orbits of Doppler data. Both two-way (CC3) and three-way (C3) Doppler are to be used with data weights of 0.1 cycle per second.
- Use Doppler data from at least two different stations when available.
- Use range units calculated only for visual assistance of the determination.
- Do not use perilune data in the determination. This can be accomplished by omitting all data from 20 minutes before to 20 minutes after perilune. After ODPL converges to a solution, the perilune data are to be restored, but a rejection sigma of 0.1 cycle per second effectively is to be used to keep these data from being used.
- Converge on a solution for state vector and Doppler bias; then converge on a solution for state vector, Doppler bias, and eight or ten high-order harmonic coefficients.
- True anomaly of spacecraft at epoch as close to 180 degrees (apolune) as possible and keep sufficient data for a good orbit determination.

The Keplerian state vectors resulting from the orbit determination are summarized in Table 3-7. Table 3-8 describes the data used in each determination and the resulting data statistics. Figures 3-1 and -2 show the calculated orbital elements versus time.

Table 3-3: Tracking Data Summary

Day of Pass	Sta	Doppler Type	Doppler Start Time	Doppler Stop Time	Doppler Amount (hrs)	Doppler Transmitter "on" Time	Ranging Start Time	Ranging Stop Time	Ranging Amount (hrs)	Ranging Sta Delay	Ranging Transponder Temp °F	*Syn-Freq.
239	62	CC3	08:01	08:57	0.94	08:01						5100
239	12	C3	08:01	08:57	0.94							
		CC3	09:38	18:30	8.55	09:38						
239	41	C3	17:43	18:30	0.58							
239/40	41	CC3	19:11	00:52	4.85	19:11						
239/40	62	C3	23:03	00:52	1.76							
240	62	CC3	01:35	02:24	0.82	01:35						5100
270	12	CC3	10:17	20:29	8.35	10:17	17:54	18:56	0.95	N.A.	65	5660
270	41	C3	16:57	20:29	3.52							5660
274	12	CC3	12:08	16:40	3.75	12:08						5640
274	62	C3	16:19	16:40	0.35							5300
275	62	CC3	11:08	13:00	1.86	11:08						5640
		C3	13:04	17:00	3.78							
275	12	C3	12:45	13:00	0.25							
		CC3	13:04	21:00	7.94	13:04	16:51	21:00	3.55	N.A.	73	
276	62	CC3	12:10	14:10	2.00	12:10						
		C3	14:16	17:30	3.22							
276	12	C3	13:40	14:06	0.44							
		CC3	14:13	23:48	8.42	14:13	19:50	22:45	1.46	N.A.	72	
276	41	C3	20:45	23:00	2.08							
282	62	CC3	18:04	21:10	2.42	18:04						
		C3	21:15	21:19	0.06							
282	12	C3	21:02	21:08	0.10							
282/3		CC3	21:15	05:00	6.92							5640

*Synfreq=204XXXX.0

Table 3-3 (Continued)

Day of Pass	Sta	Doppler Type	Doppler Start Time	Doppler Stop Time	Doppler Amount (hrs)	Doppler Transmitter "on" Time	Ranging Start Time	Ranging Stop Time	Ranging Amount (hrs)	Ranging Sta Delay	Ranging Transponder Temp °F	*Syn-Freq
283	41	C3	02:38	04:56	2.25							5640
		CC3	05:05	05:58	0.88	05:05						5640
283	62	CC3	14:53	18:00	5.84	14:53						5640
			18:00	22:10		14:53	19:53	21:32	1.65	280	65	5650
283	12	C3	22:01	22:08	0.08							5640
283/4	12	CC3	22:14	04:14	6.84	22:14	22:34	04:12	5.64	280	68	5640
			04:15	05:07		22:14						5300
284	41	C3	03:40	04:13	0.55							5640
291	12	CC3	05:03	11:04	5.32	05:03						
		C3	11:37	13:20	1.70							
291	41	C3	09:05	11:04	1.98							
		CC3	11:38	15:32	3.34	11:38						
294	62	CC3	20:32	21:37	1.08	20:32						
296	41	CC3	14:02	16:46	2.00	14:02	14:24	15:02	0.65	297	72	
300	12	CC3	14:07	19:50	5.72	14:07	14:13	19:45	5.25	290	78	
		C3	19:55	20:47	0.86							
300	41	C3	17:39	19:47	2.16							
		CC3	19:53	24:00	4.12	19:53	20:06	24:00	3.60	292	82	
303	62	CC3	12:34	14:35	1.92	12:34	12:55	14:05	1.58	284	58	
303	12	C3	12:43	14:45	1.90							
		CC3	14:57	22:22	6.64	14:57	15:56	22:22	5.46	283	64	
305/6	12	C3	22:07	00:15	2.12							
305/6	41	CC3	22:06	07:58	9.66	22:06	00:40	07:58	7.00	288	68	
309	62	CC3	11:42	19:20	5.62	11:42	11:55	19:20	4.34	279	58	5640

*Synfreq=204 XXXX.0

Table 3-3 (Continued)

Day of Pass	Sta	Doppler Type	Doppler Start Time	Doppler Stop Time	Doppler Amount (hrs)	Doppler Transmitter "on" Time	Ranging Start Time	Ranging Stop Time	Ranging Amount (hrs)	Ranging Sta Delay	Ranging Transponder Temp °F	*Syn-Freq.
309	12	C3	18:36	19:20	0.72							5640
312	62	CC3	15:49	22:43	6.90	15:49	15:56	22:43	6.60	320	62	
312	12	C3	21:00	22:45	1.75							
315	41	CC3	15:00	16:30	1.50	15:00	15:12	16:23	1.08	302	57	
		C3	16:30	16:57	0.45							
315	62	C3	15:03	16:25	1.86							
		CC3	16:35	22:00	5.42	16:35	16:37	22:00	5.38	287	55	
318	41	C3	17:17	18:25	1.14							
318/9	62	CC3	17:16	00:12	5.92	17:16	17:28	00:08	4.95	290	62	
320	62	CC3	18:10	19:48	1.64	18:10						
320/1	62	C3	20:02	00:59	4.20							
321	12	C3	01:47	08:05	5.66							
		CC3	08:13	12:15	3.34	08:13						
		C3	13:00	13:37	0.62							
321	41	C3	10:05	12:15	2.16							
		CC3	12:57	19:47	6.00	12:57	13:07	13:39	0.54	298	62	
324	41	CC3	14:05	16:48	2.08	14:05						
		C3	16:53	22:00	4.48							
324/5	62	C3	21:55	02:43	3.68							
325	62	CC3	03:20	03:38	0.30	03:20						
		C3	03:42	06:05	2.25							
		CC3	06:13	06:29	0.26	06:13						
		C3	07:12	10:13	2.88							
325	12	CC3	07:10	14:00	6.25	07:10	07:13	13:58	5.50	274	65	5640

*Synfreq=204 XXXX.0

Table 3-3 (Continued)

Day of Pass	Sta	Doppler Type	Doppler Start Time	Doppler Stop Time	Doppler Amount (hrs)	Doppler Transmitter "on" Time	Ranging Start Time	Ranging Stop Time	Ranging Amount (hrs)	Ranging Sta Delay	Ranging Transponder Temp °F	*Syn-Freq.
325	12	C3	14:36	16:58	2.34							5640
325	41	CC3	14:36	17:00	2.38	14:36	14:44	15:59	1.26	299	65	
326	41	CC3	21:48	23:58	2.18	21:48	22:03	23:57	1.80	295	59	
326	62	C3	21:53	23:58	1.98							
327	62	CC3	00:18	05:28	4.96	00:18	00:24	05:28	4.14	280	59	
331	62	CC3	06:35	13:51	7.28	06:35	06:44	13:51	5.25	280	62	
331	12	C3	10:23	13:50	3.45							
333	62	CC3	07:34	14:48	6.42	07:34	07:45	14:48	5.75	292	63	
333	12	C3	12:23	14:46	1.35							
335	62	CC3	13:31	15:56	2.42	13:31	15:36	15:55	0.32	280	83	
335	12	C3	14:52	15:55	1.06							
		CC3	17:06	23:18	3.64	17:06						
339	41	CC3	00:06	00:58	0.86	00:06						
		C3	01:05	05:56	4.84							
		CC3	06:03	06:27	0.40	06:03						
		C3	07:02	12:25	5.38							
339	62	C3	12:00	15:33	3.55							
		CC3	15:43	16:58	1.25	15:43	16:15	16:45	0.50	278	68	
		C3	17:03	19:15	2.20							
		CC3	19:23	19:38	0.25	19:23						
		C3	19:43	20:29	0.76							
339	12	C3	19:32	19:35	0.04							
339/40	12	CC3	19:42	04:29	8.80	19:42	19:50	03:40	7.42	258	66	
340	41	C3	00:56	04:29	3.54							5640

*Synfreq=204XXXX.0

Table 3-3 (Continued)

Day of Pass	Sta	Doppler Type	Doppler Start Time	Doppler Stop Time	Doppler Amount (hrs)	Doppler Transmitter "on" Time	Ranging Start Time	Ranging Stop Time	Ranging Amount (hrs)	Ranging Sta Delay	Ranging Transponder Temp °F	*Syn-Freq.
340/1	12	CC3	20:00	21:00	0.88	20:00						5640
		C3	21:02	02:00	4.90							
341	12	CC3	02:02	04:30	2.46	02:02	02:09	04:23	1.94	277	68	
		C3	04:40	05:27	0.78							
341	41	C3	01:22	04:23	2.98							
		CC3	04:37	10:58	6.35	04:37	05:38	06:13	0.68	299	68	
		C3	11:01	12:17	1.36		09:15	10:58	1.74	299	68	
341	62	C3	18:19	21:58	3.64							
		CC3	22:02	22:40	0.64	22:02	22:21	22:38	0.28	N.A.	68	
345	62	CC3	15:22	22:07	6.25	15:22	15:34	22:06	4.26	N.A.	65	
349	62	CC3	17:06	23:52	6.42	17:06	17:13	23:52	4.54	266	67	
352	62	CC3	22:03	23:08	1.08	22:03						
		C3	23:12	23:23	0.18							
353	62	CC3	03:43	06:55	3.20	03:43	04:14	06:02	1.80	283	71	
		C3	07:26	09:03	1.60							
353	12	C3	03:45	06:53	3.14							
		CC3	07:26	10:43	3.28	07:26	08:07	10:43	2.54	N.A.	71	
		C3	11:09	13:30	2.34							
355	41	CC3	22:04	23:58	1.92	22:04	23:08	23:58	0.74	297	65	
356	41	C3	00:05	00:14	0.15							
355	62	C3	22:05	23:58	1.88							
356	62	CC3	00:05	04:55	4.84	00:05	01:00	04:53	2.05	284	65	
361	62	CC3	05:05	11:48	5.75	05:05	05:15	11:38	3.68	281	66	
363	12	C3	21:19	22:40	1.35							5640

*Synfreq=204XXXX.0

Table 3-3 (Continued)

Day of Pass	Sta	Doppler Type	Doppler Start Time	Doppler Stop Time	Doppler Amount (hrs)	Doppler Transmitter "on" Time	Ranging Start Time	Ranging Stop Time	Ranging Amount (hrs)	Ranging Sta Delay	Ranging Transponder Temp °F	*Syn-Freq.
363/4	41	CC3	20:46	03:45	5.42	20:46	21:36	03:44	4.58	293	67	5640
002	62	CC3	12:05	19:00	6.90	12:05	12:50	18:55	5.52	N.A.	69	
002	12	C3	17:30	19:00	1.50							
005/6	12	CC3	19:13	00:58	5.58	19:13	19:42	00:58	4.65	280	66	
008/9	12	CC3	20:48	00:37	3.18	20:48						
012	62	CC3	17:27	23:43	5.66	17:27	18:00	20:10	1.92	277	72	
015	12	CC3	03:07	12:31	7.92	03:07	10:34	10:46	0.20	288	77	
015	62	C3	03:07	06:57	3.12							
018	12	C3	04:15	05:08	0.88							
		CC3	05:15	13:45	7.92	05:15	13:08	13:30	0.36	291	85	
018	62	CC3	04:13	05:10	0.78	04:13						
		C3	05:17	08:00	2.72							
021	12	C3	06:58	07:10	0.20							
		CC3	07:15	14:30	7.25	07:15						
021	62	CC3	06:58	07:10	0.20	06:58						
		C3	07:15	10:20	3.08							
024	62	CC3	09:33	11:30	1.94	09:33						
		C3	11:36	11:58	0.36							
024	12	C3	10:37	11:27	0.84							
		CC3	11:36	14:12	1.14	11:36						
		C3	14:13	14:50	0.66							
		CC3	14:51	17:50	1.84	14:51						
		C3	17:54	18:29	0.58							
024	12	CC3	18:31	19:33	1.04	18:31						5640

*Synfreq=204XXXX.0

Table 3-3 (Continued)

Day of Pass	Sta	Doppler Type	Doppler Start Time	Doppler Stop Time	Doppler Amount (hrs)	Doppler Transmitter "on" Time	Ranging Start Time	Ranging Stop Time	Ranging Amount (hrs)	Ranging Sta Delay	Ranging Transponder Temp °F	*Syn-Freq.
026	12	CC3	14:07	20:48	5.94	14:07	19:35	20:45	1.14	N.A.	86	5640
029	12	CC3	15:20	18:30	3.14	15:20						
		C3	18:32	20:29	1.95							
		CC3	20:32	22:30	1.98	20:32	20:45	22:30	1.88	278	80	
029/030	12	C3	22:33	00:50	2.28							
029	41	C3	21:26	22:27	1.02							
029/030	41	CC3	22:33	09:12	10.64	22:33	23:05	03:40	4.48	289	80	
030	62	C3	08:52	09:12	0.36							
		CC3	09:23	16:59	7.60	09:23						
		C3	17:03	18:05	1.04							
030	12	C3	16:04	16:57	0.88							
		CC3	17:03	22:17	4.25	17:03						
030/131	12	C3	23:08	02:03	2.34							
030	41	C3	22:12	22:17	0.08							
030/031	41	CC3	23:08	03:52	4.02	23:08	23:30	00:13	0.72	286	80	5640
		CC3	03:52	05:57	2.08							5620
		CC3	06:07	07:59	1.88							5617
031	51	C3	05:55	06:05	0.16							5576.5
			06:05	07:58	1.70							5620

*Synfreq=204XXXX.0

Table 3-4: Station Timing Synchronization

Time (GMT)	DSS Station	Timing Bias*
1967 242:21:20	41	254 ± 4
264:04:25	62	−612 ± 0.8
296:18:50	41	669 ± 1
300:19:30	41	667.95 + 0.3
303:15:00	62	−711.8 ± 1
305:22:50	41	770.95 ± 0.3
306:20:00	41	775.1 ± 1
309:19:00	62	265.3 ± 0.2
312:22:00	62	532.0 ± 0.5
321:11:30	41	718.2 ± 0.3
325:08:00	62	439.1 ± 0.1
331:11:55	62	459.5 ± 0.3
333:14:25	62	471.1 ± 0.2
363:22:00	41	1,344 ± 3
1968 002:18:00	62	541.9 ± 0.5
030:17:40	62	585.7 ± 0.3
031:23:55	41	1,581.6 ± 0.3

*Deviation from DSS-12's clock in microseconds.

Table 3-5: Master File Tracking Data Tapes

Time Interval		LRC	JPL
Start Time Day:Hr:Min	Stop Time Day:Hr:Min	Tape Number	Tape Number
239:08:00	284:05:07	516	11691,7296
239:08:00	291:15:31	517	11691,7926
239:08:00	303:22:22	518	11691,7926
239:08:00	312:22:45	519	11691,7926
239:08:00	331:13:56	520	11691,7926
239:08:00	364:03:45	521	11691,7926
002:12:02	015:12:21	522	7206,7734
002:12:02	031:07:59	523	7206,7734

Table 3-6: Lunar Harmonic Coefficients

LRC 7/28B		
KM = 4902.58	S66 = −0.6016E-8	S42 = −0.7879E-6
J20 = 0.2092E-3	C31= 0.2272E-4	C72= −0.2053E-5
J30 = −0.1738E-4	S31 = −0.1355E-4	S72 = −0.9328E-6
J40 = −0.3793E-4	C61= 0.5216E-5	C53= −0.2503E-6
J50 = 0.3176E-4	S61 = 0.2231E-5	S53 = 0.9193E-6
J60 = Zero	C32= 0.7405E-5	C44= −0.4731E-7
J70 = Zero	S32 = 0.2090E-5	S44 = 0.1580E-7
C21= −0.1571E-6	C62= −0.1715E-5	C74= 0.5499E-7
S21 = −0.5515E-5	S62 = 0.5328E-6	S74 = −0.1402E-7
C51= −0.7216E-5	C43= −0.4107E-6	C75= −0.6878E-8
S51 = −0.6547E-6	S43 = −0.9379E-6	S75 = 0.6343E-9
C22= 0.1766E-4	C73= 0.1342E-6	C77= −0.2571E-9
S22 = −0.1667E-5	S73 = −0.2469E-6	S77 = 0.3969E-9
C52= 0.4039E-5	C64= 0.9962E-7	
S52 = 0.1951E-5	S64 = −0.1047E-6	
C33= 0.3755E-5	C65= −0.3961E-8	
S33 = 0.3523E-6	S65 = −0.2166E-7	
C63= −0.5840E-6	C76= −0.1945E-9	
S63 = −0.1616E-6	S76 = 0.5396E-9	
C54= 0.1076E-6	C41= −0.3263E-5	
S54 = 0.9155E-7	S41 = 0.6798E-5	
C55= −0.4162E-7	C71= 0.1305E-4	
S55 = 0.4836E-7	S71= 0.3413E-5	
C66= 0.4314E-8	C42= 0.9158E-7	

Table 3-7: Orbital Elements (Selenographic, True of Date)

OD	Epoch (GMT) Day:Hr:Mn:Sc	Semimajor Axis a(km)	Eccentricity e	Argument of Perilune ω (deg)	Long. of Asc. Node Ω (deg)	Inclination i(deg)	Time from Periapsis Tp(sec)
6098	239:08:00:00	2,536.08	0.273245	192.034	.0515	85.3987	−4,528.6
7001-10	270:10:40:00	2,535.12	0.270531	140.664	356.849	85.1976	2,897.75
7002-10	275:11:30:00	2,534.52	0.271876	74.084	355.551	84.7100	2,597.82
7003-10	276:13:00:00	2,534.84	0.272793	59.998	355.082	84.8307	2,761.36
7004-10	282:18:30:00	2,534.73	0.270480	337.735	355.868	85.2883	2,527.47
8000-10	283:19:40:00	2,831.10	0.315381	323.871	12.062	85.1452	1,187.77
8001-10	291:05:05:00	2,831.79	0.316195	226.148	10.271	85.0353	4,372.13
8002-10	300:14:05:00	2,831.29	0.317201	102.294	10.591	84.8004	2,983.73
8003-10	303:13:00:00	2,831.00	0.317940	63.217	9.477	84.8295	1,384.10
8004-10	305:22:00:00	2,831.83	0.319346	31.826	9.242	85.2192	3,750.44
8005-10	309:11:45:00	2,830.94	0.320188	344.722	10.384	85.2757	1,385.18
8006-10	312:15:50:00	2,831.84	0.319732	302.783	10.635	84.9002	4,824.86
8007-10	315:15:00:00	2,831.95	0.319888	263.549	9.729	84.7551	4,117.38
8008-10	318:17:15:00	2,831.79	0.320483	222.726	9.142	85.2615	975.39
8009-10	321:09:10:00	2,830.88	0.320325	187.588	9.218	85.3923	1,177.55
8010-10	325:07:10:00	2,830.72	0.320698	135.808	9.636	85.1751	1,488.04
8011-10	326:21:50:00	2,831.95	0.321033	114.523	9.646	84.9083	5,460.72
8012-10	331:06:35:00	2,831.70	0.322372	56.802	8.116	84.8884	3,969.32
8013-10	333:07:35:00	2,831.83	0.323305	29.822	7.969	85.7074	4,580.27
8014-10	335:13:35:00	2,831.52	0.324107	0.180	8.827	85.4268	−3,887.06
8015-10	339:19:20:00	2,831.35	0.323416	304.126	9.464	84.8890	−2,721.12
8016-10	341:02:30:00	2,831.39	0.323332	286.933	9.034	84.7544	1,309.63

Table 3-7 (Continued)

OD	Epoch (GMT) Day:Hr:Mn:Sc	Semimajor Axis a(km)	Eccentricity e	Argument of Perilune ω (deg)	Long. of Asc. Node Ω (deg)	Inclination i (deg)	Time from Periapsis T_p (sec)
8017-10	345:15:25:00	2,831.64	0.324260	226.910	8.672	85.9506	1,278.85
8018-10	349:17:10:00	2,830.56	0.323453	172.800	8.618	79.7846	1,567.70
8019-10	353:03:45:00	2,830.91	0.324182	127.745	8.484	85.0497	1,352.64
8020-10	355:22:10:00	2,831.39	0.324745	91.161	7.841	84.7142	−2,941.63
8021-10	361:05:45:00	2,831.20	0.326947	20.910	7.049	85.5286	−3,385.88
8022-10	363:21:20:00	2,831.65	0.327140	345.988	7.786	85.3121	−4,401.19
8023-10	002:12:05:00	2,831.52	0.326351	298.163	8.060	84.8150	−3,121.85
8024-10	005:19:15:00	2,831.17	0.326605	254.552	6.907	84.7035	−2,061.17
8025-10	012-17-30-00	2,830.56	0.326247	162.753	7.597	82.5029	1,444.08
8026-10	015:03:05:00	2,831.53	0.326879	131.384	7.217	85.0962	5,895.70
8027-10	018:04:55:00	2,830.76	0.326914	90.708	6.493	84.6936	1,265.14
8028-10	021:06:55:00	2,831.31	0.328458	49.931	5.587	84.9326	−2,756.63
8029-10	024:09:35:00	2,831.64	0.329294	8.862	6.074	85.3249	−4,423.85
8030-10	026:15:45:00	2,831.09	0.328904	339.131	6.625	85.3220	1,233.98
8031-10	029:20:40:00	2,831.87	0.328195	296.696	6.736	84.7710	−5,839.80
8032-10	030:08:55:00	2,831.33	0.328260	289.936	6.630	84.7182	−2,302.87
8033-10	030:15:50:00	2,831.79	0.328306	286.125	6.498	84.7002	−4,444.29
8034-10	030:18:00:00	2,831.64	0.328359	284.928	6.461	84.6948	3,356.10
9000-10	031:06:13:20	2,746.57	0.369872	278.189	6.489	84.6626	−6,431.46

Table 3-8: Orbit Determination Data Summary						
OD	Station	Data Type	Start Time (GMT) Day:Hr:Mn	End Time (GMT) Day:Hr:Mn	Number of Points	Standard Deviation
6098	62	C3	239:08:00	239:08:56	52	.107
	41	C3	239:17:43	239:18:29	47	.122
	12	C3	239:08:01	239:08:56	52	.125
	12	CC3	239:09:38	239:18:29	435	.107
7001-10	41	C3	270:16:57	270:20:27	167	.0545
	12	CC3	270:10:40	270:20:26	448	.065
7002-10	62	C3	275:13:04	275:16:59	163	.0147
	62	CC3	275:11:30	275:12:58	87	.0105
	12	C3	275:12:44	275:12:56	13	.0066
	12	CC3	275:13:04	275:20:59	302	.0286
7003-10	62	C3	276:14:16	276:17:29	148	.0385
	62	CC3	276:13:00	276:14:08	58	.0339
	41	C3	276:20:48	276:22:59	84	.0558
	12	C3	276:13:40	276:14:06	23	.0075
	12	CC3	276:14:13	276:23:48	387	.0431

Table 3-8 (Continued)

OD	Station	Data Type	Start Time (GMT) Day:Hr:Mn	End Time (GMT) Day:Hr:Mn	Number of Points	Standard Deviation
7004-10	62	C3	282:21:15	282:21:15	1	0
	62	CC3	282:18:30	282:21:09	82	.0379
	41	C3	283:02:33	283:04:56	93	.0322
	41	CC3	283:05:04	283:05:57	51	.0313
	12	CC3	282:21:14	283:04:59	310	.0390
8000-10	62	CC3	283:19:40	283:22:09	134	.0268
	41	C3	284:03:40	284:04:13	28	.0273
	12	C3	283:22:01	283:22:06	6	.0060
	12	CC3	283:22:13	284:05:06	318	.0354
8001-10	41	C3	291:09:05	291:11:03	110	.0332
	41	CC3	291:11:38	291:15:27	162	.0260
	12	C3	291:11:37	291:13:21	88	.0239
	12	CC3	291:05:05	291:11:01	272	.0279
8002-10	41	C3	300:17:39	300:19:47	121	.0249
	41	CC3	300:19:53	300:23:58	197	.0270
	12	C3	300:19:53	300:20:46	24	.0328
	12	CC3	300:14:06	300:19:49	287	.0298

Table 3-8 (Continued)						
OD	Station	Data Type	Start Time (GMT) Day:Hr:Mn	End Time (GMT) Day:Hr:Mn	Number of Points	Standard Deviation
8003-10	62	CC3	303:13:00	303:14:35	85	.0176
	12	C3	303:13:00	303:14:46	90	.0254
	12	CC3	303:14:56	303:22:21	329	.0244
8004-10	41	CC3	305:22:06	306:07:58	479	.0356
	12	C3	305:22:09	306:00:13	101	.0273
8005-10	62	CC3	309:11:45	309:19:19	321	.1553
	12	C3	309:18:36	309:19:19	42	.2563
8006-10	62	CC3	312:15:50	312:22:43	346	.0331
	12	C3	312:21:00	312:22:44	89	.0547
8007-10	62	C3	315:15:04	315:16:25	79	.0186
	62	CC3	315:16:34	315:21:58	251	.0254
	41	C3	315:16:34	315:16:57	23	.0183
	41	CC3	315:15:01	315:16:28	86	.0157
8008-10	62	CC3	318:17:16	319:00:10	339	.0639
	41	C3	318:17:18	318:18:24	58	.0899

Table 3-8 (Continued)						
OD	Station	Data Type	Start Time (GMT) Day:Hr:Mn	End Time (GMT) Day:Hr:Mn	Number of Points	Standard Deviation
8009-10	41	C3	321:10:05	321:12:15	123	.1813
	41	CC3	321:12:57	321:19:46	287	.1753
	12	C3	321:13:02	321:13:36	21	.1917
	12	CC3	321:09:12	321:12:15	165	.1760
8010-10	62	C3	325:07:12	325:10:12	134	.0279
	41	CC3	325:14:36	325:16:57	127	.0286
	12	C3	325:14:37	325:16:57	113	.0394
	12	CC3	325:07:20	325:13:59	317	.0250
8011-10	62	C3	326:21:53	326:23:56	83	.0335
	62	CC3	327:00:19	327:05:26	250	.0329
	41	CC3	326:21:50	326:23:56	118	.0360
8012-10	62	CC3	331:06:35	331:13:51	306	.0243
	12	C3	331:10:23	331:13:49	144	.0263
8014-10	62	CC3	335:13:35	335:15:54	83	.0453
	12	C3	335:14:52	335:15:54	49	.0475
	12	CC3	335:17:06	335:23:16	166	.0463

Table 3-8 (Continued)

OD	Station	Data Type	Start Time (GMT) Day:Hr:Mn	End Time (GMT) Day:Hr:Mn	Number of Points	Standard Deviation
8015-10	62	C3	339:19:43	339:20:28	28	.0451
	62	CC3	339:19:23	339:19:37	11	.0127
	41	C3	340:00:59	340:04:27	154	.0257
	12	C3	339:19:32	339:19:34	3	.0030
	12	CC3	339:19:42	340:04:28	449	.0248
8016-10	41	C3	341:02:30	341:04:23	108	.0214
	41	CC3	341:04:38	341:10:58	293	.0285
	12	C3	341:04:41	341:05:26	38	.0277
	12	CC3	341:02:30	341:04:26	106	.0227
8017-10	62	CC3	345:15:25	345:22:06	333	.1623
8018-10	62	CC3	349:17:10	349:23:52	343	1.9777
8019-10	62	C3	353:07:26	353:09:02	78	.0197
	62	CC3	353:03:45	353:06:55	180	.0154
	12	C3	353:03:45	353:06:55	178	.0186
	12	CC3	353:07:26	353:10:41	156	.0219

Table 3-8 (Continued)						
OD	Station	Data Type	Start Time (GMT) Day:Hr:Mn	End Time (GMT) Day:Hr:Mn	Number of Points	Standard Deviation
8020-10	62	C3	355:22:10	355:23:53	69	.0259
	62	CC3	356:00:05	356:04:53	245	.0219
	41	C3	356:00:05	356:00:18	14	.0072
	41	CC3	355:22:10	355:23:58	74	.0226
8021-10	62	CC3	361:05:45	361:11:48	218	.1740
8022-10	41	CC3	363:21:20	364:03:43	250	.0243
	12	C3	363:21:20	363:22:40	52	.0348
8023-10	62	CC3	002:12:05	002:18:58	314	.0228
	12	C3	002:17:30	002:18:58	84	.0167
8024-10	12	CC3	005:19:15	006:00:58	323	.6172
8025-10	62	CC3	012:17:30	012:23:43	314	1.0907
8026-10	62	C3	015:03:07	015:06:56	147	.0339
	12	CC3	015:03:06	015:12:20	363	.0387

Table 3-8 (Continued)

OD	Station	Data Type	Start Time (GMT) Day:Hr:Mn	End Time (GMT) Day:Hr:Mn	Number of Points	Standard Deviation
8027-10	62	C3	018:05:14	018:07:59	148	.0307
	62	CC3	018:04:56	018:05:07	4	.0340
	12	C3	018:04:57	018:05:06	5	.0175
	12	CC3	018:05:14	018:13:44	376	.0391
8028-10	62	C3	021:07:13	021:10:20	134	.0255
	62	CC3	021:06:57	021:07:08	12	.0330
	12	C3	021:06:58	021:07:07	10	.0418
	12	CC3	021:07:13	021:14:29	308	.0274
8029-10	62	C3	024:11:31	024:11:57	22	.0308
	62	CC3	024:09:35	024:11:29	85	.0780
	12	C3	024:10:37	024:11:26	41	.1654
	12	CC3	024:11:36	024:19:31	197	.0677
8030-10	12	CC3	026:15:45	026:20:48	249	.1019
8031-10	41	C3	029:21:26	029:22:26	51	.0352
	41	CC3	029:22:33	030:08:39	508	.0335
	12	C3	029:22:34	030:00:48	127	.0280
	12	CC3	029:20:42	029:22:28	77	.0343

Table 3-8 (Continued)

OD	Station	Data Type	Start Time (GMT) Day:Hr:Mn	End Time (GMT) Day:Hr:Mn	Number of Points	Standard Deviation
8032-10	62	C3	030:08:55	030:18:05	55	.0313
	62	CC3	030:09:25	030:16:58	345	.0286
	41	CC3	030:08:55	030:09:11	13	.0293
	12	CC3	030:17:03	030:20:18	168	.0291
	12	CC3	030:16:04	030:16:56	35	.0513
8033-10	62	C3	030:17:23	030:18:05	41	.0252
	62	CC3	030:15:50	030:16:42	51	.0403
	41	CC3	030:23:11	030:03:59	234	.0305
	12	C3	030:16:04	031:02:03	153	.0398
	12	CC3	030:17:23	030:22:17	217	.0247
8034-10	62	C3	030:18:00	030:18:05	6	.0057
	41	CC3	030:23:11	031:05:57	302	.0296
	12	C3	030:23:10	031:02:03	117	.0311
	12	CC3	030:18:00	030:22:17	182	.0231
9000-10	41	CC3	031:06:15	031:07:55	84	.1529
	51	C3	031:06:22	031:07:55	125	.1466

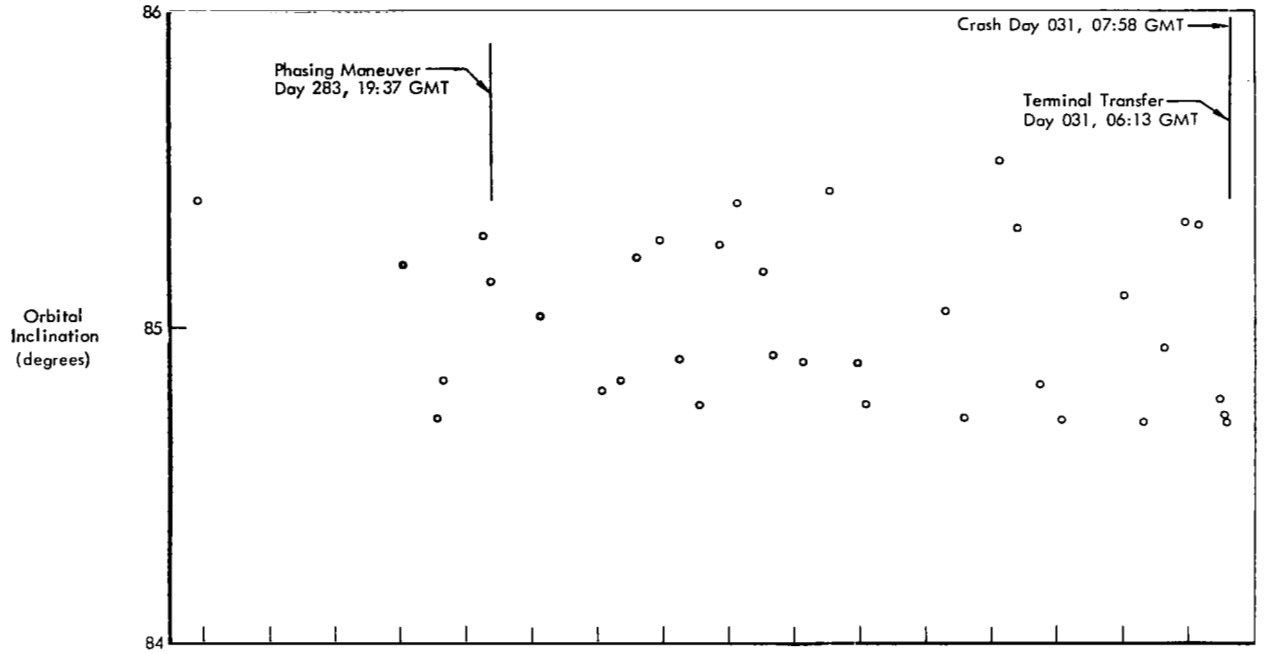

Figure 3-1: Orbital Inclination History

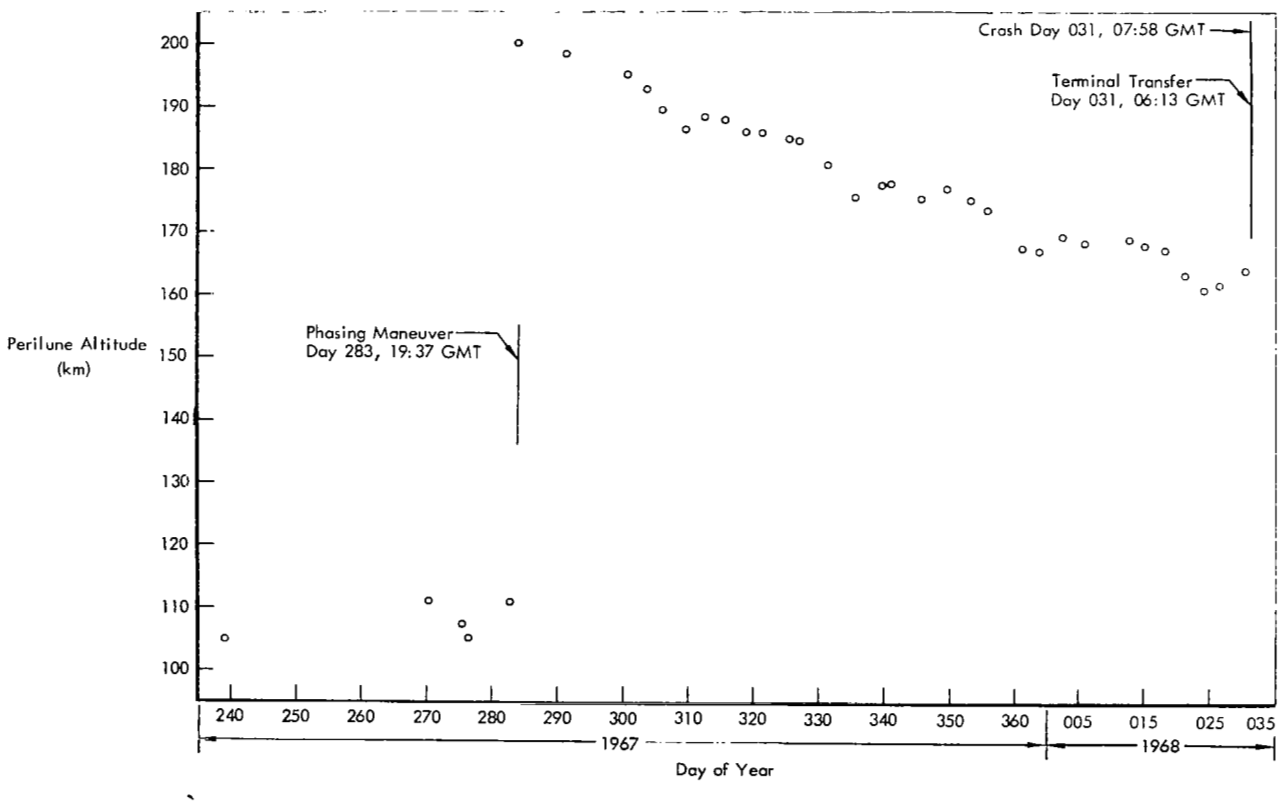

Figure 3-2: Perilune Altitude History

During a period from Day 349, 1967 to Day 026, 1968 spacecraft sunsets were recorded using the flight programmer. These data were used in the orbit determination process as a confirmation of convergence. A summary of the recorded sunset times, along with the OD identification number and the residuals (difference between recorded time and OD-computed sunset time), is presented in Table 3-9. From an investigation of the residuals the advantage of multistation tracking is evident.

Ranging data taken during the latter portion of the extended mission were used for comparison of the recently generated integrated lunar ephemeris. Figure 3-3 indicates the agreement between the OD ranging residuals and the range difference between current and integrated ephemeris tapes. The indication is that the new ephemeris contains a more accurate representation of the lunar position.

Table 3-9: Sun Occultation Times

Recorded Sunsets Day:Hr:Min:Sec	OD	OD Solution Residual	Recorded Sunsets Day:Hr:Min:Sec	OD	OD Solution Residual
349:20:10:41.83	8018	−18.264*	002:16:26:50.84	8023	0.552
353:06:49:36.86	8019	1.968	005:19:34:58.22	8024	7.237*
355:22:41:24.59	8020	2.178	005:23:20:22.72	8024	7.778*
356:02:26:47.99	8020	2.088	015:05:00:33.81	8025	8.910*
361:06:24:53.55	8021	7.975*	015:08:46:00.21	8025	8.758*
361:10:10:18.75	8021	8.351*	018:11:54:40.43	8027	5.247
363:22:17:01.68	8022	2.140	026:15:19:11.10	8030	N.A.
364:02:02:26.78	8022	1.928	026:19:04:42.70	8030	19.58 *
002:12:41:26.54	8023	0.197	* One Station OD		

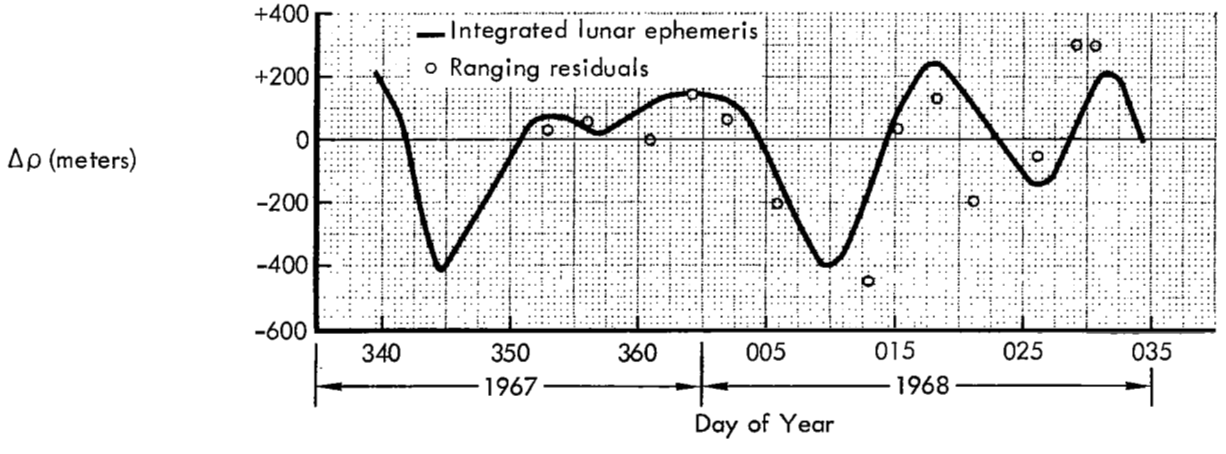

Figure 3-3: Ranging Data Residuals

3.2.3 Guidance Maneuvers

When the orbit determination process defines a trajectory, the trajectory is analyzed to determine if a maneuver is required. A maneuver may be needed for many reasons (e.g., to offset the effects of a lunar eclipse, to increase or terminate orbital lifetime, or to fulfill planned or functional objectives). The process of designing the maneuver during the extended mission did not differ from that of the primary mission; basically, the purpose of the maneuvers was different. During the Lunar Orbiter V extended mission there were two guidance maneuvers planned and executed.

3.2.3.1 Orbit Phasing Maneuver for October 1967 Lunar Eclipse Passage

In preparation for the October 18, 1967 lunar eclipse, studies were made to determine detrimental effects on Lunar Orbiter V. Figure 3-4 shows the sunlight conditions for the spacecraft during the period of interest. The time in total darkness was 205 minutes and the time below 30% sunlight was 260 minutes. Consequently the ampere-hour capacity of the battery would have been exceeded, resulting in loss of the spacecraft. The following general objectives were to be met by executing the engine burn.

- The sunlight conditions at the spacecraft during the eclipse were to be adequate to limit the battery depth of discharge to 12 ampere-hours.
- The spacecraft orbital lifetime was to be greater than the expected nitrogen lifetime.
- A Δ V reserve was to be retained that would be sufficient to produce a controlled impact during the next 5 months.
- The maneuver was to be executed within the view of the Earth.

Because of the high orbital inclination (85 degrees), which resulted in orbital motion perpendicular to the eclipse shadow passage, it was not possible to obtain favorable lighting conditions with a simple phasing maneuver. Three alterations to orbital parameters were necessary to obtain proper lighting: (1) an increase in apolune altitude, (2) a southerly rotation of the latitude of apolune, and (3) proper phasing of the spacecraft in the orbit. This sequence was successful due to the fact that the Earth's shadow was displaced toward the lunar North Pole and a southerly displacement of the spacecraft would result in passage outside the umbral eclipse.

Using this design approach, a study of the Δ V required to minimize the depth of discharge while maintaining the desired orbital lifetime was investigated. The analysis showed that all constraints could be satisfied with an expenditure of 67.5 meters per second.

This maneuver design was based on OD 7004-10, which appears in Table 3-7.

To demonstrate the successful accomplishment of all design constraints, the following are presented.

- Figure 3-5 contains the predicted illumination during the eclipse. The resultant battery discharge based on this prediction is less than 12 ampere-hours.
- Figure 3-6 presents a sketch of the expected long-term perilune altitude variation. The lifetime, based on the prediction capability of the LRC 7/28B lunar model, appears to be several years. This is several times longer than the anticipated nitrogen lifetime.
- Also indicated in Figure 3-6 are the intervals during which a controlled impact is possible. The calculation of these periods assumed a ΔV capability of 30 m/sec and a ∂ Rp/∂ ΔV sensitivity of 5.8 km/m/sec.
- The true anomaly of maneuver execution (68.11 degrees) was within view of the Earth.

Therefore, all objectives were satisfied by the maneuver design.

The star Canopus was used as the roll reference for the maneuver.

The results of the maneuver design were as follows.

- Engine ignition time: Day 283, 19:37:6.75
- Magnitude of ΔV required: 67.5 m/sec
- Attitude maneuvers:
  HRoll = 31.33° (sunline roll)
  Pitch = −50.96°
- Designed change in orbital elements (selenographic of-date coordinates)

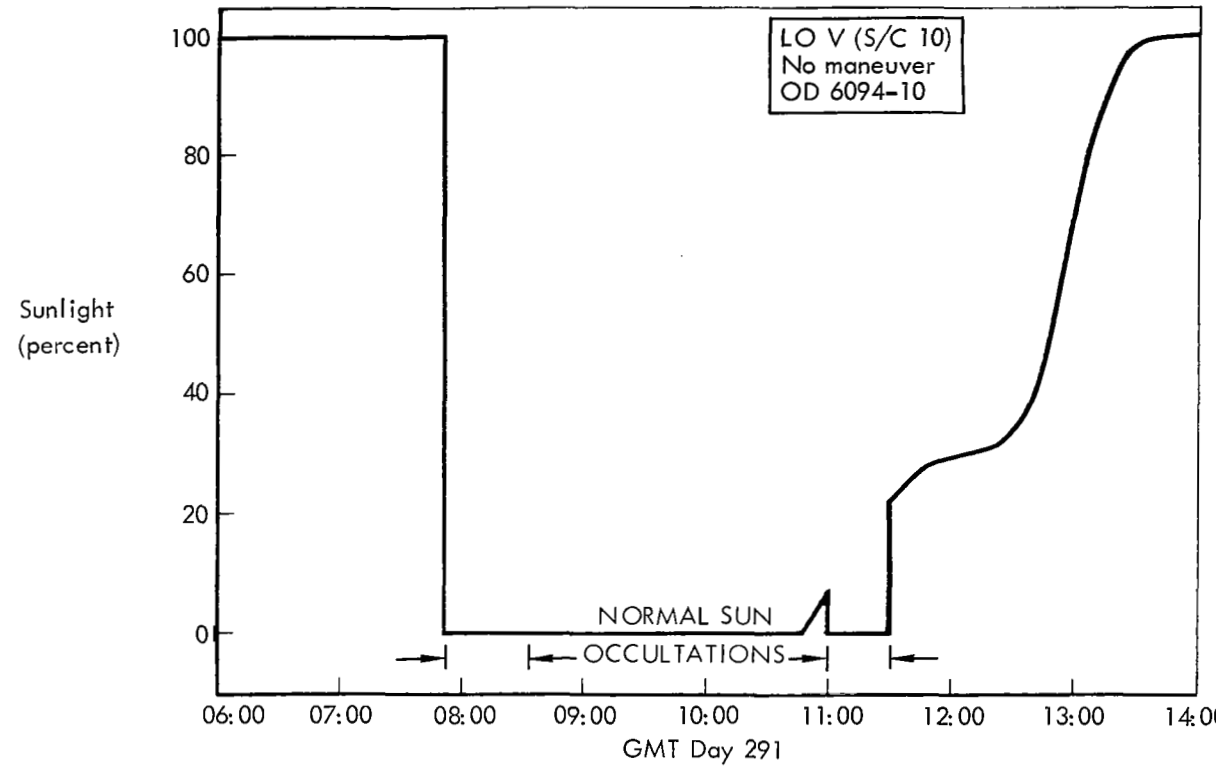

Figure 3-4: Predicted Lighting During Lunar Eclipse – OD 6094-10

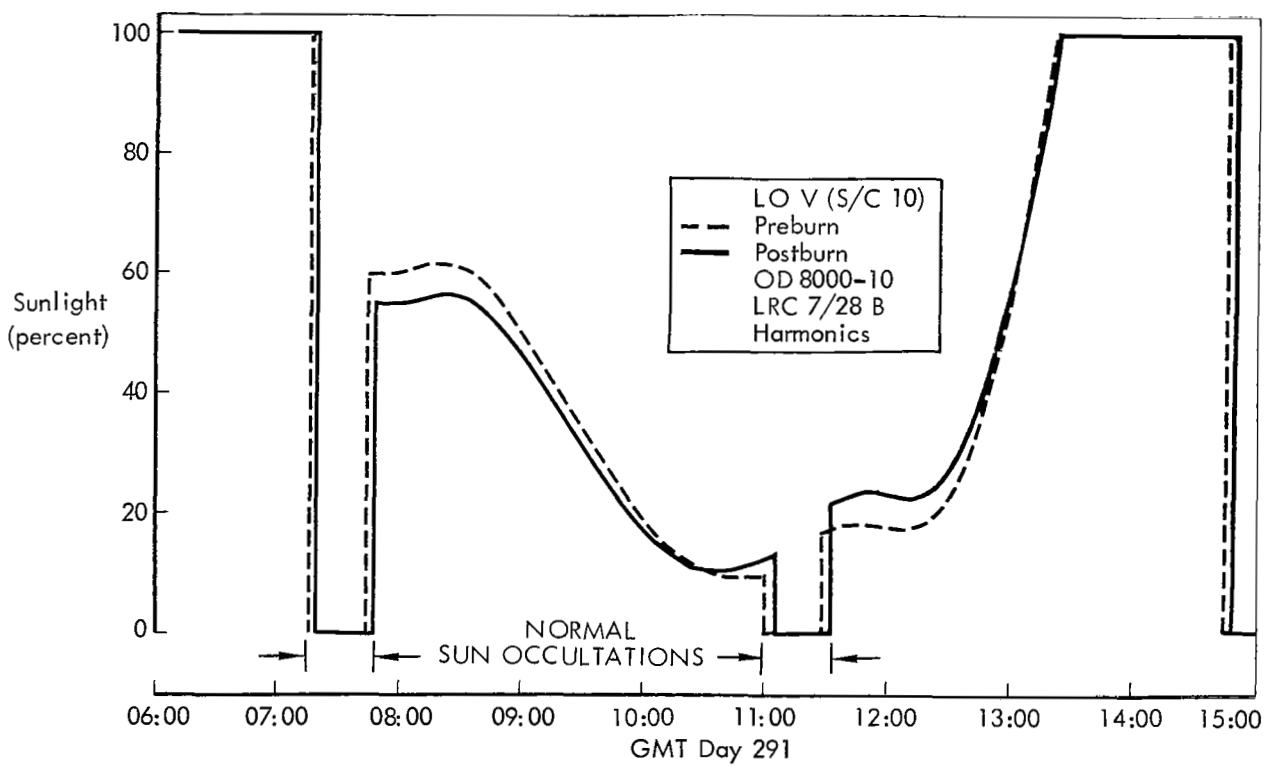

Figure 3-5: Predicted Lighting During Lunar Eclipse – OD 8000-10

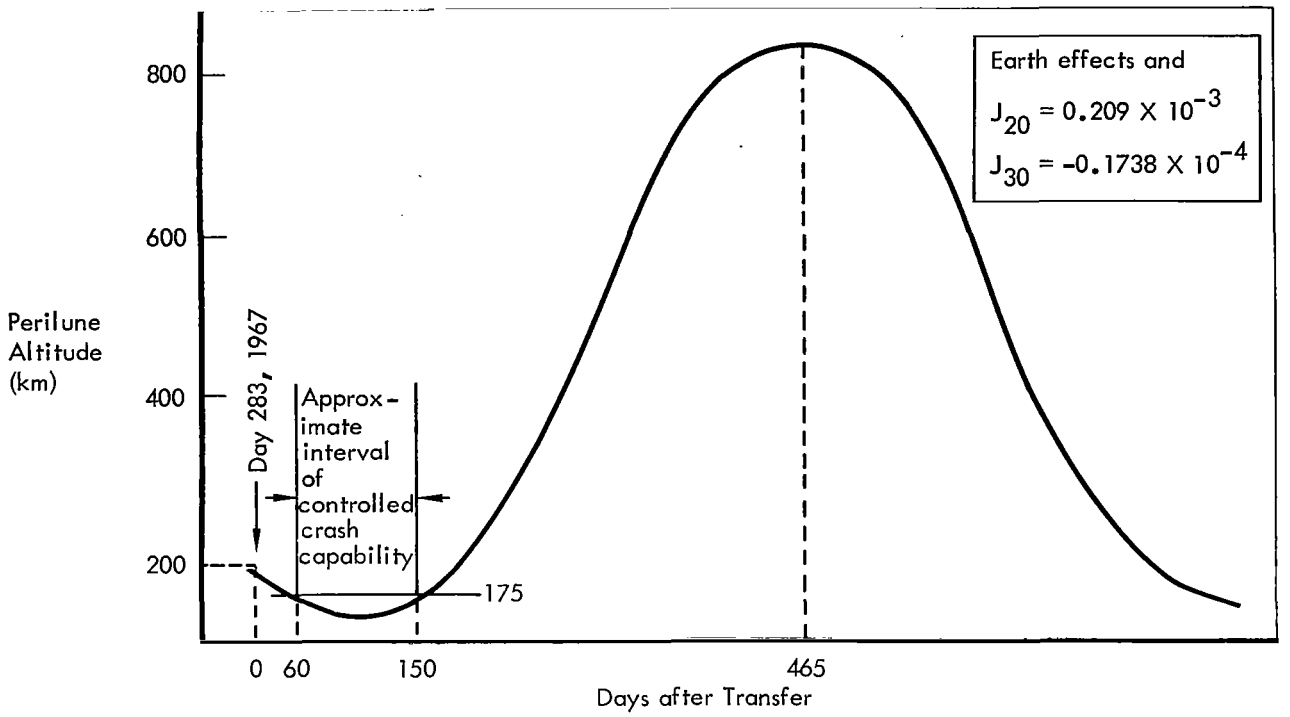

Figure 3-6: Predicted Long-Term Variation of Perilune Altitude

	Elements Prior to Maneuver	Elements Following Maneuver
Semimajor axis (km)	2,534.76	2,830.65
Eccentricity	0.26948	0.31541
Argument of perilune (deg)	356.12	12.03
Longitude of ascending node (deg)	323.89	323.91
Inclination (deg)	85.15	85.15
Orbital period (min)	190.86	225.24
Apolune altitude (km)	1,479.73	1,985.36
Perilune altitude (km)	113.61	199.76

- True anomaly of transfer maneuver 68.11 degrees

Monitoring of the velocity maneuver was accomplished using Doppler data from DSS-62. The predicted and actual two-way Doppler data are plotted in Figure 3-7. The total shift of 1,031.2 Hz agreed closely with the predicted value. The bias (42 Hz) between the two curves was caused by the epoch forwarding of the orbit determination state vector (OD 7004-10) to the time of the engine burn (a period of 25 hours).

A better determination of engine performance can be gained from examination of the post-maneuver orbital elements and the expected "percent sunlight" history during the eclipse period. The first of these data appear in the following table, which contains a comparison of the designed orbital elements with those calculated after the maneuver in OD 8000-10. The altitudes of perilune and apolune, and the argument of perilune, are sufficiently close to the values desired to meet the design constraints. Only the effect of the 3-second deviation in orbital period required further consideration.

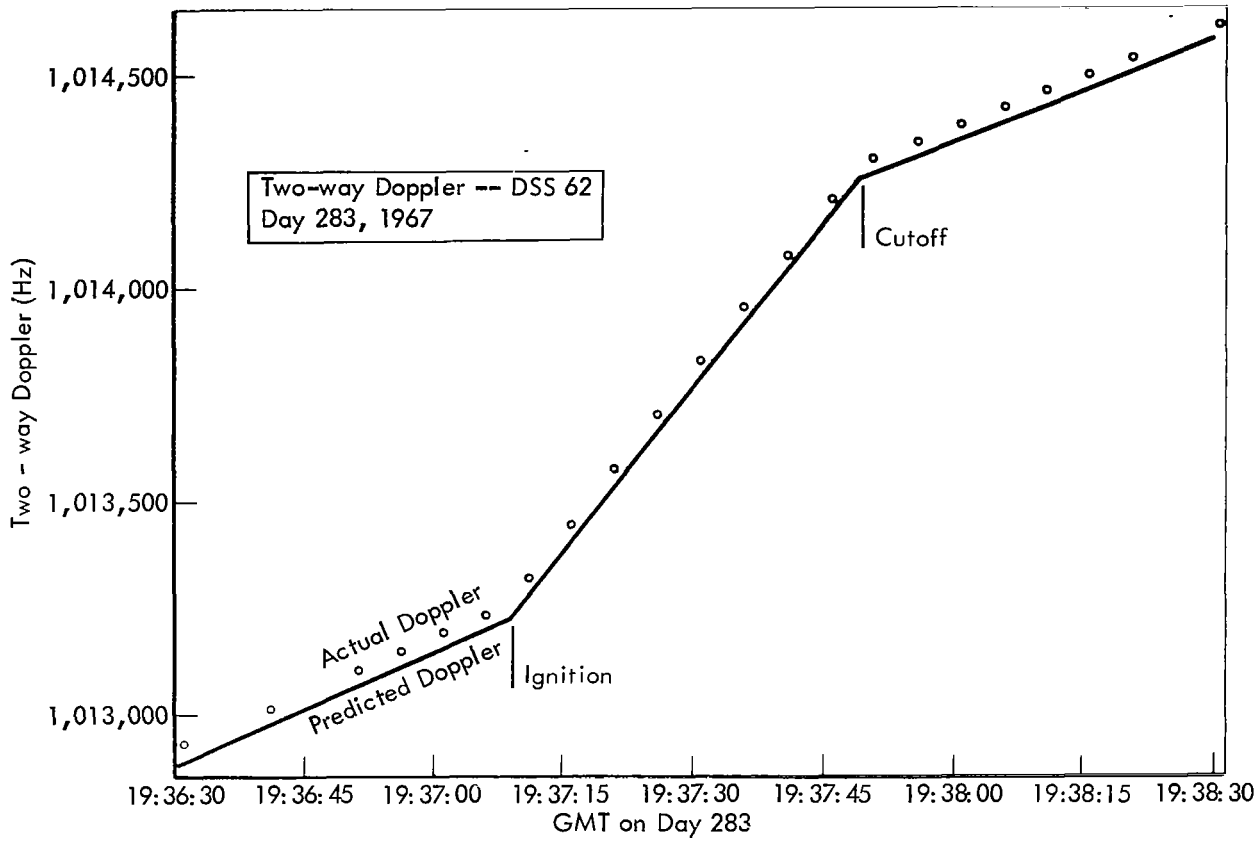

Figure 3-7: Lunar Eclipse Phasing Maneuver

	Postmaneuver Orbital Elements	
	Predicted	Actual
Semimajor axis (km)	2,830.65	2,831.10
Eccentricity	0.31541	0.31538
Argument of perilune (deg)	12.03	12.06
Longitude of ascending node (deg)	323.91	323.87
Inclination (deg)	85.15	85.15
Orbital period (min)	225.24	225.29
Apolune altitude (km)	1,985.36	1,985.88
Perilune altitude (km)	199.76	200.13

The integrated effect of the error in period alters the sequence of events at the time of the eclipse by 2.5 minutes. Figure 3-5 shows the lighting conditions in this interval of interest. Comparison of the pre- and postburn predictions indicates a slight degradation at the start of the eclipse, but shows improved conditions just before and after the period of Sun occultation, at 11:05 and 11:32 GMT, respectively. Therefore, the total effect did not violate the 12 ampere-hour discharge constraint. Consequently it can be concluded that all design criteria were met by the maneuver.

During the eclipse, telemetry measurements of the solar array current were monitored. This gave an indication of the percentage of sunlight visible to the spacecraft. Figure 3-8 contains a composite of these data and the lighting history calculated with OD 8001-10.

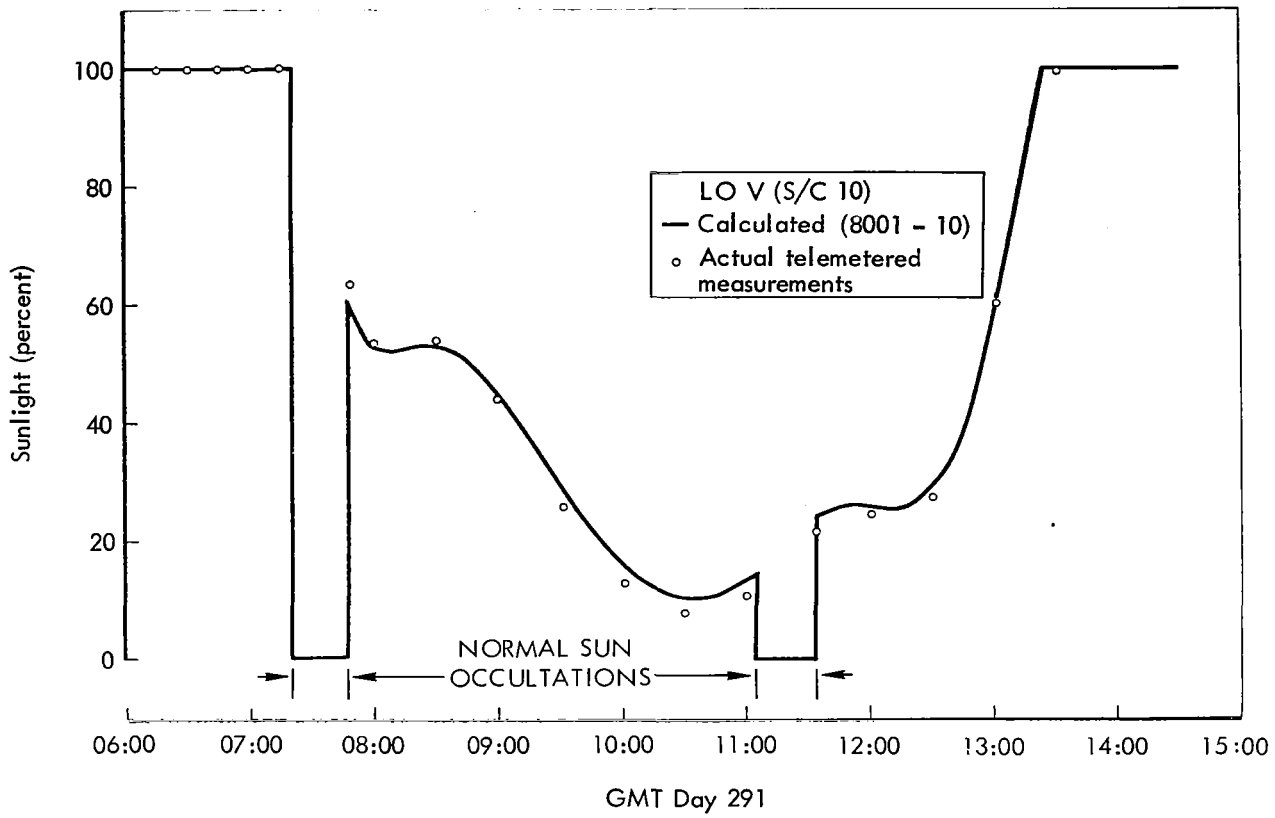

Figure 3-8: Calculated and Measured Sunlight During Eclipse — Day 291

3.2.3.2 Terminal Transfer Maneuver

On January 29, 1968 (GMT Day 029) telemetry measurements received from Lunar Orbiter V indicated a very low supply of the nitrogen used for attitude control of the spacecraft. Therefore, before control was lost, a decision was made to transfer the spacecraft to an impact trajectory. The object of the maneuver was to produce a crash on the lunar surface within view of the Deep Space Tracking Stations. Although the ΔV supply was estimated to be only 30 meters per second, this was considered sufficient to accomplish the objective.

The maneuver design was accomplished using orbit determination solution Number 8032-10, which is summarized in Table 3-7. This state vector was mapped forward to the maneuver time with the LRC 7/28B lunar harmonic model.

The radius of perilune was selected as the only critical targeting parameter. The objective was to make it coincident with the lunar surface. The average lunar radius is normally considered to be 1,738.1 kilometers. However, to ensure an impact, it was necessary to target to a lower value. Calculations showed that a minus 6-kilometer adjustment was sufficient to account for any uncertainty in the lunar radius and for errors arising from navigation and control considerations.

Since Canopus was out of the field of view of the star tracker and no other bright stars were available, an antenna map of DSIF signal strengths was made to establish the roll attitude reference. Maneuver angles for the burn were specified from Sun-Canopus lock by FPAC, and were adjusted by the attitude control analyst to agree with the known premaneuver attitude.

The results of the maneuver design were as follows.

- Engine ignition time: Day 031, 06:13:03.04
- Burn duration: 16.73 sec
- Magnitude of ΔV required: 29.14 m/sec
- Attitude maneuvers (Sun-Canopus reference):
  HRoll (sunline roll) = −88.84°
  Pitch = +93.61°
- Expected spacecraft and engine performance parameters:
  Thrust = 104.5 lb
  Initial weight = 586.0 lb
  Specific impulse = 276.0 sec
  Weight flow rate = 0.3785 lb/sec
  Average acceleration = 1.77m/sec^2
- True anomaly of transfer: 180.0 deg
- Resulting change in orbital elements (selenographic true-of-date coordinates)

	Elements Prior to Maneuver	Elements Following Maneuver
Semimajor axis (km)	2,832.22	2,747.05
Eccentricity	0.32834	0.36952
Argument of perilune (deg)	6.25	6.30
Longitude of ascending node (deg)	278.19	278.19
Inclination (deg)	84.69	84.69
Apolune altitude (km)	2,024.04	2,024.04
Perilune altitude (km)	164.20	−6.00

NOTE: Altitudes are referred to a lunar radius of 1,738.1 kilometers.

- Predicted postmaneuver events:
  Sun occultation Day 031, 07:51:41.55
  Impact Day 031, 07:57:56.72
  Longitude = 83.17° W
  Latitude = 4.35° S

Therefore, the impact was expected to occur within the view of two DSIF sites, Woomera, Australia and Johannesburg, South Africa.

Monitoring of the velocity maneuver was accomplished using Doppler data from DSS-41 (Woomera). The predicted and actual two-way Doppler data are plotted in Figure 3-9. The total shift of 76.5 Hz agreed closely with the predicted value of 75.2 Hz. The resulting deviation can be attributed to slight differences in the engine performance parameters. The slight bias (0.8 Hz) between the two curves at ignition resulted from the epoch forwarding of OD 8032-10 to the burn time, a period of 21 hours.

A postburn analysis of the tracking data prior to impact was accomplished using Doppler data from Stations 41 and 51. The results, OD 9000-10, are summarized in Table 3-7. The slight differences in the predicted and actual postmaneuver orbital elements can again be attributed to inadequate premaneuver knowledge of engine performance, as mentioned before.

The DSIF received signal intensity (CEC) recordings were carefully examined to determine the exact time of impact on the lunar surface. The recordings exhibited very sharp discontinuities at the "receiver out-of-lock" time. The patterns differed significantly from those taken during normal spacecraft/Earth occultations, thus indicating the first impact of a Lunar Orbiter within DSIF view and successful completion of the maneuver objective. OD 9000-10 was then mapped to the measured impact time to establish the location on the surface of the Moon; in addition, telemetry data were examined for the occurrence of a Sun occultation on the descent trajectory.

From all these data the following sequence of events was established:

Sun occultation Day 031, 07:51:28.7 $\pm$03 sec
Impact Day 031, 07:58:08.27
Longitude = 83.04° W
Latitude = 2.79° S

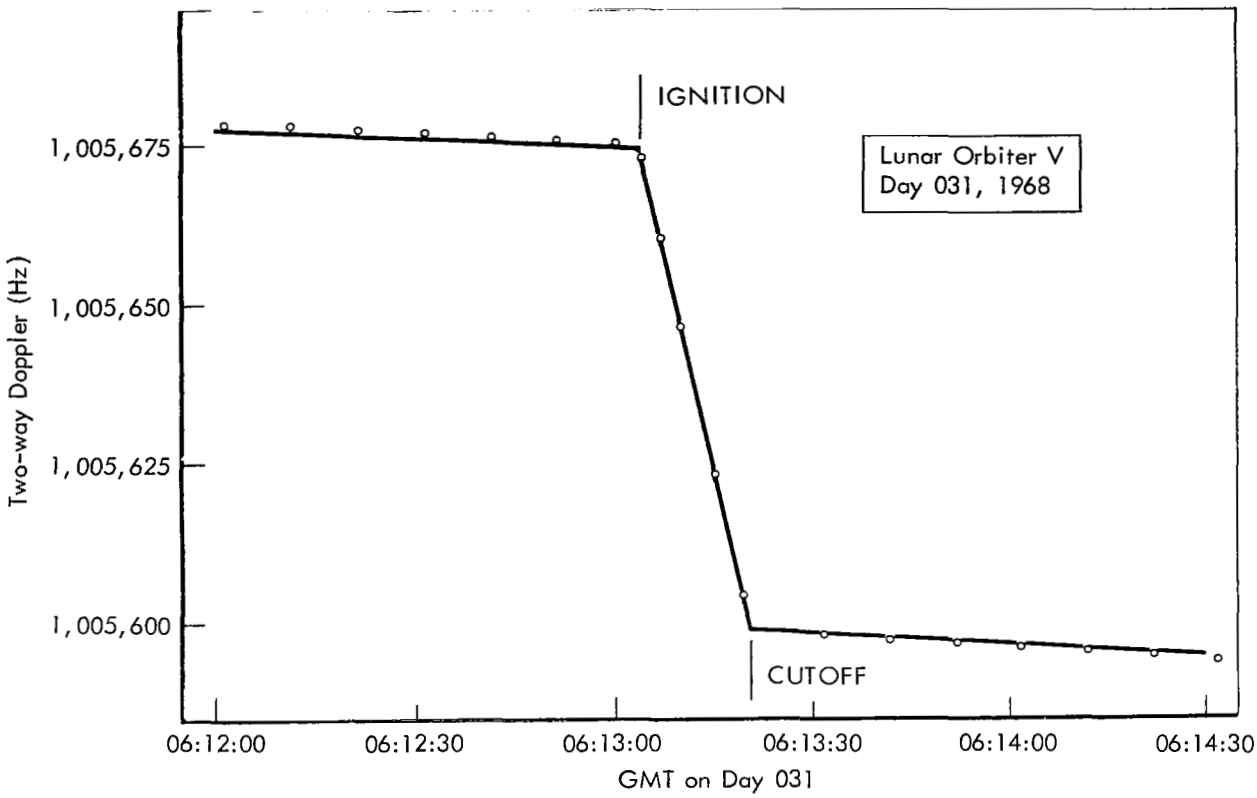

Figure 3-9: Terminal Transfer Two-Way Doppler – DSS-41

4.0 Flight Data

4.1 ENVIRONMENTAL DATA

A primary objective of the extended mission was to collect lunar environmental data during long periods of lunar flight. Spacecraft telemetry was monitored during each tracking period to determine if there had been any increase in radiation flux or micrometeoroid activity. However, because the spacecraft was not tracked continuously, the exact location or time was generally unknown.

4.1.1 Radiation

Table 4-1 shows radiation data collected during the extended mission. The scintillation counters located outside the photo subsystem in the vicinity of the film cassette and the film looper recorded 1.5 and 1.0 rads, respectively, at the beginning of the extended mission. Figure 4-1 illustrates the increasing radiation trend.

4.1.2 Micrometeoroids

The spacecraft sustained a total of six micrometeoroid hits, five of which occurred during the extended-mission phase. Again, only the period between which the hits were recorded can be reported.

Table 4-1: Radiation Data

Tracking Period Day GMT	Cassette Radiation DF04 (Rads)	Looper Radiation DF05 (Rads)	Tracking Period Day GMT	Cassette Radiation DF04 (Rads)	Looper Radiation DF05 (Rads)
242	1.50	1.0	318	3.50	3.5
244	1.50	1.0	320/321	3.50	4.0
248	1.75	1.0	324/325	3.75	4.5
255	1.75	1.0	333	3.75	4.5
256	1.75	1.5	335	4.00	4.5
258	2.00	1.5	339/340	4.25	6.5
265	2.00	1.5	340/341	4.25	6.5
267	2.25	1.5	345	4.25	7.0
274	2.25	1.5	349	4.50	7.0
275	2.25	2.0	352/353	4.50	7.5
276	2.50	2.0	355/356	4.75	8.0
284	2.50	2.0	361	4.75	8.0
286	2.75	2.0	363/364	5.00	8.0
294	2.75	2.0	008/009	5.00	8.0
296	3.00	2.5	012	5.25	8.5
303	3.00	2.5	015	5.25	8.5
305	3.25	2.5	018	5.50	8.5
309	3.25	3.0	021	5.50	8.5
312	3.25	3.0	024	5.75	9.0
315	3.50	3.5	029/030/031	5.75	9.0

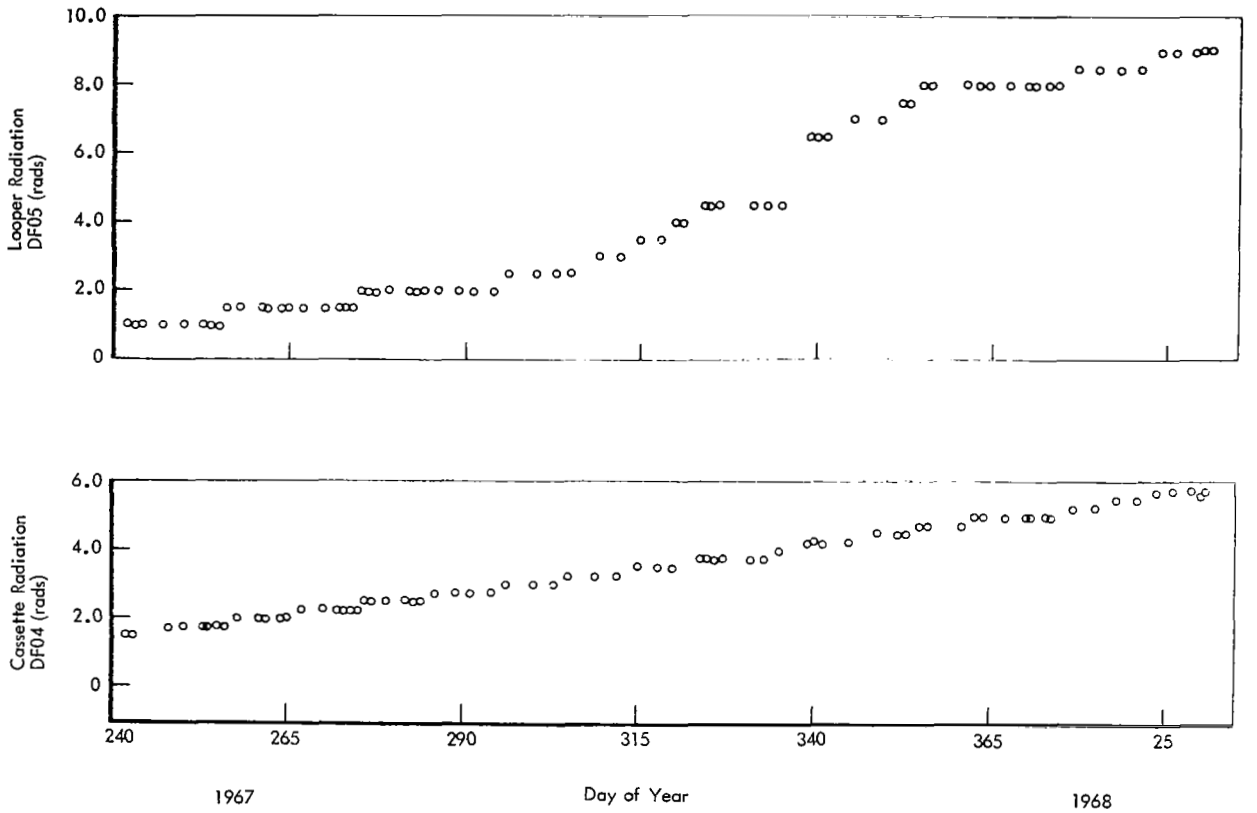

Figure 4-1: Radiation Data

Detector Number	Hit Recorded Between	
	Day:Hr:Min	Day:Hr:Min
09	264:07:51	265:07:08
19	319:00:11	320:18:06
10	324:14:01	325:17:00
03	356:05:00	361:05:01
17	018:14:00	021:06:53

4.2 SPECIAL EXPERIMENTS

During the extended mission, the spacecraft was used to obtain scientific data and as a tool to conduct special experiments. Only the purpose of the experiment and the type of data collected are given in this report. Data analysis is the responsibility of the requesting agency.

4.2.1 Voice Relay Experiment

The experiment was conducted to investigate the feasibility of relaying voice communications by a lunar orbiting spacecraft. Voice data were transmitted to the spacecraft, detected by the transponder receiver, passed through the ranging module, retransmitted to Earth, and received by the DSIF.

The experiment was conducted in three phases. Phase I was to evaluate the RF performance of the spacecraft/DSIF voice relay system and to select optimum parameters (i.e., subcarrier deviation, type of modulation, amplifier and attenuator settings, etc.). Phase II of the experiment was to review and rehearse procedures for setting up, checking out, and adjusting levels of the complete spacecraft/DSIF/ground communication system to be used during Phase III. Phase III was then, logically, a demonstration of the voice relay technique that could be employed via a lunar orbiting spacecraft. This use of the Lunar Orbiter spacecraft as a communication satellite was demonstrated in conjunction with the Langley Research Center's 50th anniversary celebration on Days 275 and 276.

Two transmission methods were attempted during Phase I. The essential difference in these methods was the technique used to modulate and detect the subcarrier.

Method A (FM/PM) – Audio data (voice recorded on magnetic tape to ensure uniform test conditions) were frequency modulated onto a 52.5 kHz subcarrier with a peak frequency deviation of 7.9 kHz. The 52.5 kHz subcarrier was then phase modulated onto the S-band RF carrier with a modulation index of 1.5 radians. The DSIF receiver with a 12-Hz tracking loop bandwidth and telemetry bandwidth of 420 kHz was then phase locked to the downlink carrier. The audio subcarrier as obtained from the receiver phase detector output was demodulated by a 52.5 kHz discriminator, recorded on magnetic tape, and monitored on a speaker.

Method B (PM/PM) – Audio data were phase modulated onto a 52.5 kHz subcarrier with a modulation index of 1.8 radians. The 52.5 kHz subcarrier was then phase modulated onto the S-band RF carrier with a modulation index of 1.5 radians. The DSIF receiver with tracking loop bandwidth of 12 Hz and telemetry bandwidth set to 20 kHz was then phase locked to the first upper and lower audio sideband (52.5 kHz above and below the carrier). The audio data from the phase detector output were then recorded on magnetic tape and monitored on a speaker.

The spacecraft for both Methods A and B was configured with the TWTA on, the ranging module on (Mode I), and the high-gain antenna pointed to the DSIF. To minimize the noise in the received audio data, the uplink S-band modulation index was increased from 1.5 to 1.8 radians and the spacecraft modulation mode was commanded to Mode 2 (ranging module obviously was left on). Method A with these changes was selected for the Phase II and III tests (Method A, modified).

In Phases II and III the audio data originated at the Langley Research Center and was relayed to the DSIF facility (DSS-12) via land lines. The audio data consisted of a 1 kHz tone and a telephone handset (voice). The spacecraft and the DSIF were configured according to Phase I, Method A, modified.

The quality of the voice relayed through the system was reported to be excellent.

4.2.2 RF Occult Determination Experiment

The purpose of the experiment was to obtain data for evaluation of the fundamental nature of lunar occultation of an RF signal. It was anticipated that these data could make possible determination of certain physical lunar characteristics, such as surface conductivity, as an independent correlation point for orbit determination programs.

The experiment consisted of recording the DSIF-received signal intensity as the spacecraft was occulted from Earth view. The recordings were made over the largest possible dynamic range of signal levels and are summarized below.

Orbit Number	DSS	Perilune or Apolune	Spacecraft Configuration		
			TWTA On/Off	Modulation Mode III/IV	Uplink Lock Yes/No
744	41	Perilune	On	IV	No
748	12	Perilune	Off	IV	Yes
749	12	Perilune	Off	IV	No
1171	12	Apolune	Off	III	Yes
1172	12	Apolune	Off	III	Yes

Along with the signal intensity recordings, predictions of Earth occultation time and the orbital geometry at Earth occultation time were computed to support the data analysis.

All data for the experiment were compiled and transmitted to the requesting agency.

4.2.3 Bistatic Radar Experiment

The purpose of the experiment was two-fold: (1) to measure the bistatic radar cross section of selected areas of the lunar surface, and (2) to apply side-looking radar techniques to obtain a radar image of portions of the Moon.

Part 1 of the experiment, conducted on Days 334 and 024, consisted of aiming the spacecraft

high-gain antenna at the lunar surface while transmitting with the TWTA. The transmitted signal, which is right-circularly-polarized and narrow beamed, illuminated a fairly small spot on the surface. The reflected signal from this illuminated spot is composed of a strong polarized (left-circular) component and a weak depolarized (right-circular) component. The DSS station was configured to receive the polarized component of the reflected signal and record this signal for later analysis. The power in this reflected signal is a function of the bistatic radar cross section of the area illuminated; therefore, this parameter can be derived from the recorded signal. The attitude control subsystem was operated in the narrow (0.2 degree) deadband and no maneuvers were performed during the measurement period. The data recordings were compiled and transmitted to the requesting agency.

Part 2 of the experiment, conducted concurrent with Part 1 on Day 024, consisted of transmitting a high-speed ranging signal from DSS-14 to the spacecraft, through the ranging channel, the TWTA, high-gain antenna, and back to the DSS. DSS-14 was configured to record the polarized (left-circular) component of the received signal. The data recordings were collected at DSS-14 by the requesting agency, the Jet Propulsion Laboratory, for analysis and reporting.

4.2.4 Convolutional Coding/Sequential Decoding Experiment

The objective of the experiment was to demonstrate the use of convolutional coding and sequential decoding on a spacecraft link and to confirm the results of theoretical calculations and ground simulations of such systems. It was anticipated that demonstration of this system would lead to the use of convolutional coding and sequential decoding in future telemetry systems.

The Lunar Orbiter spacecraft was used only as a transponder during the experiment. The encoded data, biphase modulated on a 3.75 to 15.0 kHz subcarrier, were transmitted to the spacecraft on the ranging channel. The signal was transponded by the spacecraft and detected by the DSS telemetry receiver with the output taken from the video amplifier. This signal was then synchronized, demodulated and detected with special equipment, and finally decoded on the DSS-12 SDS 930 computer. The code used was a rate one-third convolutional code with 2,048 tree-size bits (6,144 symbols). Of the 2,048 bits only 32 were used for tree synchronization by the decoder; the rest were used for information. It was expected that the system could operate essentially error-free at signal-to-noise (SNR) ratios as low as 2.2 db at the decoder and data rates up to 1,000 bits per second, although about 1% of the data is erased at this SNR. In demonstrations prior to this experiment no errors or erasures had been observed at SNR of 4.0 db. Higher data rates could not be accommodated only because of limited computation speed.

The experiment was conducted at DSS-12 on Days 015, 018 and 026. Data from the experiment were compiled by the experimenter at that time. The preliminary results were reported to be favorable.

4.2.5 Visual Observation Experiment

The purpose of the experiment was to determine whether a spacecraft the size of Lunar Orbiter, when suitably oriented, could become visible from Earth (as a star-like object) by specular reflection of sunlight.

The experiment was conducted on Days 018 and 021 when the spacecraft attitude was maneuvered to a position such that sunlight was reflected off the solar panels and equipment-mounting deck mirrors toward Earth. Specular reflection was detected photographically at an apparent stellar magnitude of about 12 by the Lunar and Planetary Laboratory, Tucson, Arizona, on Day 021. More than 80 photographs were exposed at that time, so optical tracking data are available over about 90 degrees of the orbit.

The apparent success of the experiment suggests that it may be possible to optically track vehicles to Mars and Venus with reflecting surfaces designed specifically for that purpose.

4.2.6 Manned Space Flight Network/Apollo GOSS Navigational Qualification (MSFN/AGNQ)

Lunar Orbiter V was utilized to support Phase C of the MSFN/AGNQ program, which was part of the network's overall preparation for the Apollo mission. Phase C required that the spacecraft be operated in Mode 4 (video modulation) and with the TWTA on to provide adequate signal margin for ranging using the network's 30-foot antennas. During the extended mission, the following stations participated in station-to-station handovers, two- and three-way Doppler tracking, ranging and time correlations: Ascension, Antigua, Bermuda, Canberra, Carnarvon, Canary Island, Grand Bahama, Goldstone, Goldstone (WING), Guam, Guaymus, Hawaii, Madrid, Madrid (WING), Merrit Island, Texas, and Woomera (WING). The tracking data acquired by the stations were transmitted via high and low speed data lines to the real-time computer complex (RTCC) for processing. Table 4-2 is a chronological listing of the MSFN/AGNQ tracking periods.

4.2.7 Perilune Residual Experiment

The purpose of the experiment was to eliminate one possible cause (uplink lock) of the relatively high residuals observed in the orbit determination program near perilune. A typical example of two- and three-way Doppler residuals is shown in Figure 4-2.

The experiment consisted of recording the ground receiver VCO frequency and static phase error while the spacecraft was tracked in

Table 4-2: MSFN/AGNQ Tracking Summary

Day	Total Tracking Time (GMT)	MSFN Three-Way Tracking (GMT)	MSFN Two-Way Tracking (GMT)	Number of Handovers
320/1	18:06-19:47	18:10-19:50 08:11-12:16	19:50-08:11 12:16-19:47	8
324/5	14:01-17:00	14:01-16:50 03:18-03:40 06:11-17:00	16:50-03:18 03:40-06:11	11
339/40	00:04-04:30	00:05-02:00 06:00-06:30 15:40-17:00 19:20-04:30	02:00-06:00 06:30-15:40 17:00-19:20	11
340/1	19:57-22:42	19:57-21:00 02:00-11:00 22:00-22:20	21:00-02:00 11:00-22:00	12
352/3	19:07-15:50	19:07-23:10 03:42-11:30 15:30-15:50	23:10-03:42 11:30-15:30	5
029/30	15:16-18:00	15:16-18:30 20:30-18:00	18:30-20:30	2
				49

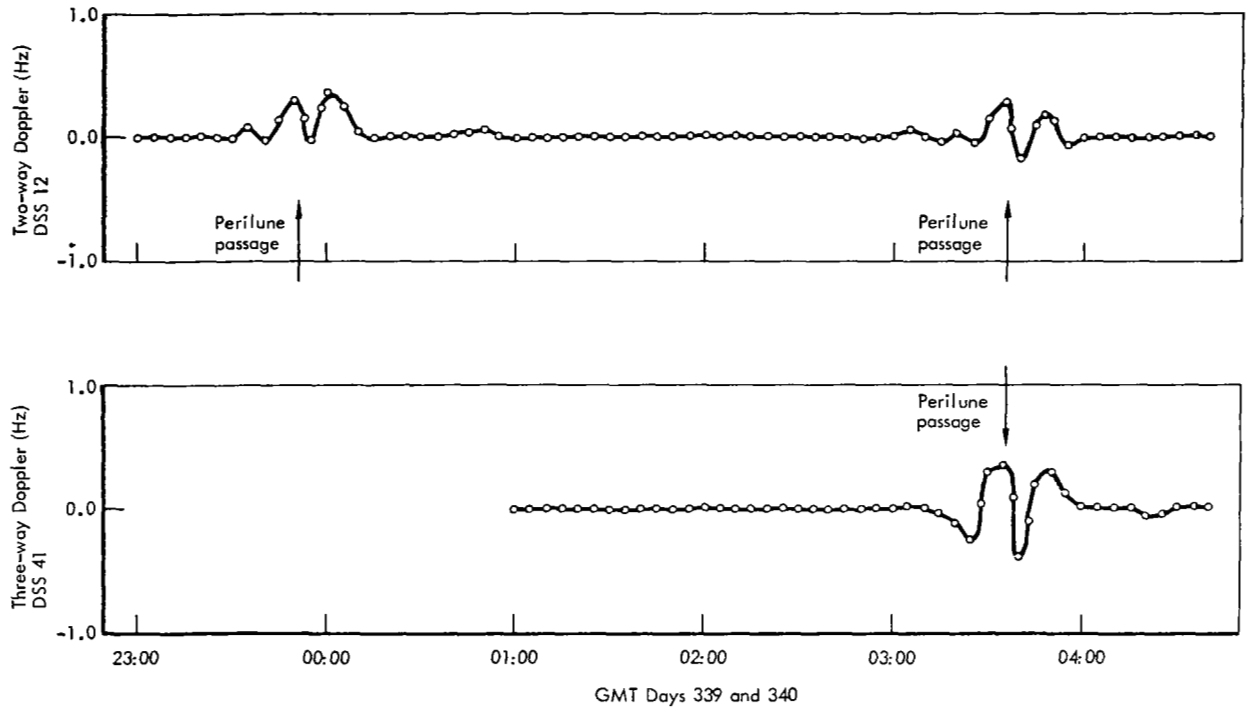

Figure 4-2: Typical Doppler Residuals

one-way lock (DSS transmitter off). These data, recorded for two successive perilune periods and the apolune period intervening, are summarized below.

GMT Day:Hr:Mn/ Day:Hr:Mn	Perilune/ Apolune	Deep Space Station
030:20:20/030:21:20	Perilune	DSS - 12
030:22:20/030:23:00	Apolune	DSS - 12 & DSS - 41
031:00:15/031:00:45	Perilune	DSS - 12 & DSS - 41

The spacecraft was configured in Modulation Mode I (ranging module on) with the TWTA off during the data recording period. The only attitude maneuvers performed consisted of normal limit cycling and the communications subsystem temperatures were relatively stable during the recording period.

The data recorded during the experiment were forwarded to the requestor for analysis.

5.0 Spacecraft Subsystem Performance

Periodic monitoring of spacecraft telemetry data provided information that was used to determine subsystem performance. The data were analyzed to show trends in performance in an attempt to establish what are the detrimental effects on components or subsystems after exposure to space environment. The data and results are presented in this section.

5.1 SUMMARY

Individual subsystem performance was generally within design requirements; there was very little evidence of subsystem or component degradation.

The attitude control subsystem operated normally during the extended mission with the exception of the roll and yaw gyro drift rates, which exceeded the design specification limit of 0.5 degrees per hour, and the pitch plus threshold detector, which triggered at 1.1 volts versus a nominal 2.0 volts. Although the latter anomaly resulted in higher-than-planned nitrogen consumption, neither condition adversely affected the overall conduct of the mission. Two hundred thirty-five maneuvers and 119 Sun acquisitions were performed. The sun sensors and star tracker operated as planned; however, glint remained a problem during initial celestial reference acquisitions. When Canopus moved out of the tracker field of view, lesser stars were successfully acquired to provide a roll reference when required. Nitrogen usage was within the predicted limits for the maneuvers and the deadbands maintained.

Although the flight programmer performed nominally during all observed operations, a halt mode condition was a probable explanation for the loss of attitude control that led to premature mission termination.

The communications subsystem performed within specification requirements; however, the transponder RF power telemetry circuit displayed a significant change in output versus temperature after the lunar eclipse.

The power subsystem provided sufficient power to operate the spacecraft during all observed tracking periods, although the solar array predictably degraded 3.1% and the shunt regulator leaked current for a period of time. The battery was discharged 11.8 ampere-hours (98.3%) during the lunar eclipse, which indicated that negligible degradation had occurred since launch.

The photo subsystem was used only during the investigation of the nitrogen depletion anomaly. The environmental conditions were as expected for the off-Sun attitude of the spacecraft and the pressurization system indicated no leakage.

The velocity and reaction control subsystem performed satisfactorily. Two velocity maneuvers were conducted during the extended mission, accumulating 57.2 seconds of operating time and providing 96.6 meters per second of energy.

With the exception of the EMD thermal-control coating, the structures and mechanisms subsystem performed as predicted. Degradation of the thermal-control coating occurred as anticipated, requiring that the spacecraft be oriented off-Sun to maintain proper thermal control.

5.2 SUBSYSTEM PERFORMANCE

5.2.1 Attitude Control Subsystems

The attitude control subsystem consists of inertial reference, control assembly, star tracker and sun sensor units, and a switching assembly. The inertial reference unit is a three-axis, strapdown gyro system with an accelerometer for differential velocity derivation. Inertial reference outputs consist of angular rates and position data about each of the spacecraft's three orthogonal axes, and spacecraft velocity change in line with the X axis. Subsystem control and integration is furnished by the control assembly, which consists of a memory core, a clock oscillator, a logic system, input circuitry, and closed-loop electronics. The primary purpose of the control assembly is to command the spacecraft either from stored commands or real-time commands and, through the logic system and closed-loop electronics, control the position

thrusters and the engine pointing angle. The star tracker contains a photo-multiplier tube for sensing Canopus presence; a bright-object sensor to operate a sun shade for protection of the photo-multiplier tube; light baffles and optics; and associated electronics. Its purpose is to furnish spatial roll axis references. The sun sensors are silicon solar cells that provide spatial yaw and pitch axis reference. The switching assembly contains high-power switching circuitry and is controlled by the control assembly (see Figure 5-1).

During the extended mission 235 maneuvers and 119 Sun acquisitions were performed. Limit cycle, with the exception of positive pitch deadband, was normal and consistent throughout the mission. An apparent change in the pitch-

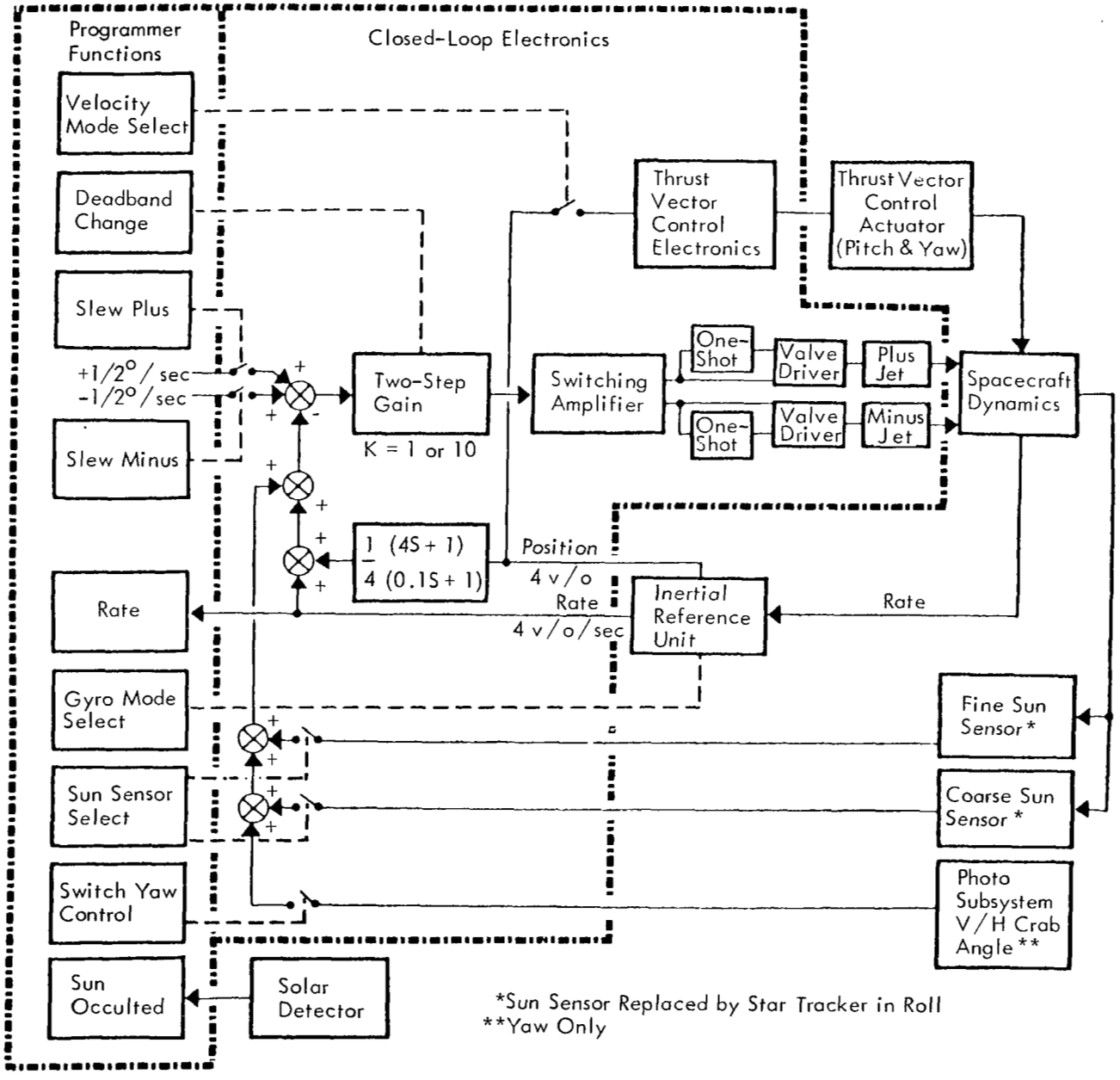

Figure 5-1: Attitude Control Subsystem Functional Block Diagram

minus threshold detector resulted in a pitch-limit cycle of +1/−2 degrees (typical in wide deadzone) and a pitch-minus maneuver rate of 0.27 degree per second in wide deadband. Narrow deadband maneuver rates remained within the design tolerance of 0.55 ±0.05 degree per second.

Table 5-1 summarizes extended-mission maneuvers.

Roll error signal from the tracker was never used in the closed-loop attitude control of the spacecraft. On 18 occasions, "Acquire Canopus" was commanded with the tracker off in order to store Sun occultation times with the programmer.

Table 5-2 consists of a listing of attitude maneuvers performed during the extended

Table 5-1:
Extended-Mission Maneuver Summary

Type of Maneuver	0.2-Degree Deadband	2.0 Degree Deadband
Roll	29	48
Pitch	26	109
Yaw	13	10
ASU, acquire Sun	13	106
ACA, acquire Canopus	0	18
CDZ*, close deadband	----	11
VEL, velocity	----	2

Table 5-2: Extended-Mission Attitude Maneuvers

Day:Hr:Min:Sec	Event	Mag	Comment
240:02:00:00.1	ASU		
03:01:27.0	PIP	53.0 deg	
243:03:19:08.2	ASU		
04:20:35.1	PIP	53.1 deg	
246:04:38:18.3	ASU		
05:39:45.2	PIM	53.0 deg	
249:05:57:26.4	ASU		
06:58:53.3	PIM	53.1 deg	
252:07:16:36.5	ASU		
08:18:03.4	PIM	53.0 deg	
255:08:35:44.6	ASU		
09:37:11.5	PIM	53.1 deg	
258:09:54:54.7	ASU		
10:56:21.6	PIM	53.0 deg	
261:11:14:02.8	ASU		
12:33:11.7	PIM	53.1 deg	
264:12:33:12.9	ASU		
264:13:34:39.8	PIM	53.0 deg	
266:14:10:16.1	ASU		
15:11:42.8	PIM	53.1 deg	
268:15:47:21.3	ASU		
16:48:48.2	PIM	53.0 deg	
270:10:23	CDZ*		
10:28	PIM	50.0 deg	
10:38	PIM	5.0 deg	
11:42	PIP	95.0 deg	Discharge test
11:45	ASU		
12:19	ROP	360 deg	
12:41	ROM	90.0 deg	
13:29	PIM	43.0 deg	
270:13:30	CDZ		
18:25	PIM	6.0 deg	
272:12:05:16.3	ASU		
13:06:43.2	PIM	53.1 deg	

Table 5-2 (Continued)

Day:Hr:Min:Sec	Event	Mag	Comment
274:12:40	ASU		
12:50	ROP	15.0 deg	
13:02	ROM	30.0 deg	
13:18	PIM	43.0 deg	
13:51	ROP	5.0 deg	
14:03	ROM	10.0 deg	
275:12:05	PIM	10.0 deg	
12:19	ROM	10.0 deg	
12:36	YAM	5.0 deg	
14:48	ROM	5.0 deg	
276:12:32	ASU		
12:41	PIM	43.0 deg	
13:02	ROM	10.0 deg	
13:19	ROP	15.0 deg	
13:35	YAM	5.0 deg	
277:07:59:38.6	ASU		
09:01:05.5	PIM	50.1 deg	
279:09:35:43.8	ASU		
10:37:10.7	PIM	49.99 deg	
281:11:11:47.0	ASU		
17:13:13.9	PIM	53.0 deg	
282:20:30	ASU		
21:29	PIM	43.0 deg	
23:07	ASU		
23:18	ROM	40.0 deg	
23:36	ROP	12.0 deg	To Canopus
23:49	PIM	50.0 deg	
283:15:51	ROM	6.0 deg	
18:31:47.7	ASU		
18:45:27.1	CDZ*		

Day:Hr:Min:Sec	Event	Mag	Comment
283:19:16	ROP	34.3 deg	
19:18	PIM	51.0 deg	
19:37	CDZ		
19:37	ΔV	221.5 ft/sec	
19:38	PIM	2.0 deg	
284:14:49:40.6	ASU		
15:51:07.5	PIM	53.0 deg	
286:16:12:06.7	ASU		
17:13:33.6	PIM	53.1 deg	
288:17:34:32.8	ASU		
18:39:02.7	PIM	53.0 deg	
290:18:56:58.9	ASU		
19:58:25.8	PIM	53.1 deg	
291:05:30	ASU		
08:26	PIM	.011 deg	
13:38	PIP	48.0 deg	
292:20:19:25.0	ASU		
21:20:51.9	PIM	53.0 deg	
294:21:41:51.1	ASU		
22:43:18.0	PIM	53.1 deg	
296:21:37:08.2	ASU		
22:38:35.1	PIM	53.0 deg	
298:22:59:34.3	ASU		
299:00:01:01.2	PIM	53.1 deg	
300:16:15	ASU		
19:59	PIP	35.0 deg	
301:00:22:00.4	ASU		
01:23:27.3	PIM	53.0 deg	
303:01:44:26.5	ASU		
02:45:53.4	PIM	50.0 deg	

Table 5-2 (Continued)

Day:Hr:Min:Sec	Event	Mag	Comment
305:03:06:41.6	ASU		
04:08:08.5	PIM	50.1 deg	
307:04:28:57.7	ASU		
05:30:24.6	PIM	49.99 deg	
309:05:51:12.8	ASU		
06:52:39.7	PIM	53.0 deg	
311:07:13:38.9	ASU		
08:15:05.8	PIM	53.1 deg	
313:08:36:05.1	ASU		
09:37:31.9	PIM	53.0 deg	
315:09:58:31.1	ASU		
10:59:58.0	PIM	53.1 deg	
317:11:20:57.2	ASU		
12:22:24.1	PIM	53.0 deg	
319:10:23:24.0	ASU		
11:24:50.9	PIM	53.1 deg	
320:18:12:41.0	ASU		
18:21:08.0	ROM	120.0 deg	
19:31:00.0	PIM	50.0 deg	
321:14:05:20.0	YAM	6.0 deg	
14:19:16.0	ROM	7.0 deg	
19:25:00.0	ROP	.03 deg	
322:07:08:19.0	ASU		
08:09:46.0	PIM	53.0 deg	
324:08:30:45.0	ASU		
09:32:12.0	PIM	53.0 deg	
14:08:09.0	ASU		
14:19:22.0	ROM	20.0 deg	
14:35:00.0	ROM	20.0 deg	
14:46:00.0	ROM	20.0 deg	

Day:Hr:Min:Sec	Event	Mag	Comment
324:15:02:14.0	CDZ*		
15:04:14.0	ROP	360.0 deg	
16:08:33.0	CDZ		
16:13:19.0	ROM	23.0 deg	
16:32:00.0	PIM	50.0 deg	
325:10:04	ROP	4.0 deg	
326:16:44:52.2	ASU		
17:46:19.1	PIM	53.0 deg	
328:18:07:18.3	ASU		
19:08:45.2	PIM	53.1 deg	
330:19:29:44.4	ASU		
20:31:11.3	PIM	53.0 deg	
332:20:52:10.5	ASU		
21:53:37.4	PIM	53.1 deg	
334:22:14:36.6	ASU		
23:16:03.5	PIM	53.0 deg	
335:13:30	ASU		
13:40	ROP	60.0 deg	
14:10	CDZ*		
14:31	ROM	360.0 deg	
15:25	ROM	98.0 deg	
15:31	PIM	50.0 deg	
17:10	ROP	19.0 deg	Canopus
17:25	PIP	50.0 deg	
17:29	ASU		
17:35	ROP	103.8 deg	
17:41	PIP	.011 deg.	
21:01	PIM	50.0 deg	
21:30	PIP	50.0 deg	
21:35	ASU		

Table 5-2 (Continued)

Day:Hr:Min:Sec	Event	Mag	Comment
335:22:52	ROM	120.0 deg	
22:58	CDZ		
23:20	PIM	53.0 deg	
337:23:41:14.4	ASU		
338:00:42:41.3	PIM	53.0 deg	
339:00:10	ASU		
00:20	ROM	20.0 deg	
00:34	ROM	20.0 deg	
00:50	ROP	60.0 deg	
01:26	ROM	20.0 deg	
01:36	PIM	50.0 deg	
06:21	YAM	5.0 deg	
15:55	YAM	5.0 deg	
340:20:00	ASU		
20:19	PIM	50.0 deg	
342:21:03:51.2	ASU		
22:05:18.1	PIM	53.1 deg	
344:22:26:17.3	ASU		
23:27:44.2	DIM	53.0 deg	
345:21:19:51.5	ASU		All eyes off
21:19:51.5	ACA		Tracker off
21:33:31.0	PIP	.011 deg	
21:34:22.4	ROP	.011 deg	
346:16:47:18.5	ASU		
17:48:45.4	PIM	53.0 deg	
348:18:09:44.6	ASU		
19:11:01.5	PIM	53.1 deg	
20:03:03.5	ASU		All eyes off
349:20:03:03.5	ACA		Tracker off
20:16:43.0	PIP	.011 deg	
349:20:17:34.5	ROP	.011 deg	
20:52	ASU		
21:13	PIM	53.0 deg	
351:21:34:04.4	ASU		
22:35:31.3	PIM	53.1 deg	
352:19:11	ASU		
19:16	ROM	50.0 deg	
20:35	PIM	50.0 deg	
22:06	ASU		
22:27	ROP	40.0 deg	
22:55	PIM	50.0 deg	
353:06:07	YAM	6.0 deg	
06:46:03.5	ASU		All eyes off
06:46:03.5	ACA		Tracker off
06:59:00.0	PIP	.011 deg	
06:59:51.2	ROP	.011 deg	
07:49	YAM	7.0 deg	
07:53	PIM	6.0 deg	
11:22	YAM	5.0 deg	
354:10:47:27.7	ASU		
11:48:54.4	PIM	53.0 deg	
355:22:33:03.5	ASU ACA		Occultation test
22:46:43.0	PIP	.011 deg	
22:47:34.5	ROP	.011 deg	
356:02:24:00.1	ASU ACA		Occultation test
02:37:43.0	PIP	.011 deg	
02:38:34.4	ROP	.011 deg	
03:15	ASU		
03:26	PIM	53.0 deg	

Table 5-2 (Continued)

Day:Hr:Min:Sec	Event	Mag	Comment
358:03:46:54.4	ASU		
04:48:21.3	PIM	53.0 deg	
360:05:09:20.5	ASU		
06:10:47.4	PIM	53.1 deg	
361:06:18:00.0	ASU ACA		Occultation test
06:31:43.0	PIP	.011 deg	
06:34:34.5	ROP	.011 deg	
10:07:00.1	ASU ACA		Occultation test
10:20:43.0	PIP	.011 deg	
10:21:34.5	ROP	.011 deg	
10:47	ASU		
10:54	PIM	53.0 deg	
363:11:15:13.4	ASU		
12:16:40.3	PIM	53.1 deg	
22:13:00.1	ASU ACA		Occultation test
22:46:43.0	PIP	.011 deg	
22:47:35.0	ROP	.011 deg	
364:02:01:00.1	ASU ACA		Occultation test
02:14:43.0	PIP	.011 deg	
02:15:35.0	ROP	.011 deg	
21:50:18.5	ASU		
22:51:45.4	PIM	53.0 deg	
1968 001:23:12:44.6	ASU		
002:00:14:11.5	PIM	53.1 deg	
12:38:00.1	ASU ACA		Occultation test
12:51:43.0	PIP	.011 deg	

Day:Hr:Min:Sec	Event	Mag	Comment
002:12:52:35.0	ROP	.011 deg	
16:25:00.1	ASU ACA		Occultation test
16:38:43.0	PIP	.011 deg	
16:39:35.0	ROP	.011 deg	
003:12:40:18.5	ASU		
13:41:45.4	PIM	53.0 deg	
005:14:02:44.6	ASU		
15:04:11.5	PIM	53.1 deg	
19:34:00.1	ASU ACA		Occultation test
19:47:43.0	PIP	.011 deg	
19:48:35.0	ROP	.011 deg	
23:17:00.1	ASU ACA		Occultation test
23:30:00.1	PIP	.011 deg	
23:31:35.0	ROP	.011 deg	
008:00:47:56.0	ASU		
01:49:23.1	PIP	53.0 deg	
21:07	ASU		
21:12	CDZ*		
21:22	YAM	360.0 deg	
21:39	ASU		
21:43	YAP	360.0 deg	
22:00	ASU		
22:05	PIM	360.0 deg	
23:26	ASU		
23:28	PIP	360.0 deg	
23:44	CDZ		
23:59	ROM	20.0 deg	
009:00:13	ROP	40.0 deg	

Table 5-2 (Continued)

Day:Hr:Min:Sec	Event	Mag	Comment
009:00:28	PIM	53.0 deg	
010:21:20:01.2	ASU		
22:21:28.1	PIM	53.1 deg	
012:17:34	ASU		
17:51	ROP	190.0 deg	
19:30	PIP	95.0 deg	
21:16	PIM	95.0 deg	
21:24	ASU		
21:27	CDZ*		
21:38	PIP	70.0 deg	
22:15	PIP	7.0 deg	
22:30	PIP	8.0 deg	
22:42	ROM	45.0 deg	
22:50	ROM	17.0 deg	
22:52	PIM	110.0 deg	
23:07	ROP	5.0 deg	
23:15	CDZ		
23:21	ASU		
013:00:22	PIM	53.0 deg	
015:00:43:08.2	ASU		
01:44:35.1	PIM	53.1 deg	
04:51:03.5	ASU ACA		Occultation test
05:04:43.0	PIP	.011 deg	
05:05:34.5	ROP	.011 deg	
08:40:03.5	ASU ACA		Occultation test
08:53:43.0	PIP	.011 deg	
08:54:34.5	ROP	.011 deg	
21:16:17.0	ASU		

Day:Hr:Min:Sec	Event	Mag	Comment
015:22:17:43.9	PIM	53.0 deg	
017:22:38:43.1	ASU		
23:40:10.0	PIM	53.1 deg	
018:04:09	ASU		
04:33	CDZ*		
04:35	ROP	360.0 deg	
04:45	ASU		At sunrise
05:17	ROP	99.0 deg	
05:21	PIM	50.0 deg	
07:24	PIP	50.0 deg	
07:28	ASU		
07:37	ROP	12.0 deg	
08:02	ROP	3.0 deg	
08:30	ASU		At sunrise
08:39	ROP	113.3 deg	
08:45	YAP	40.0 deg	
09:37	YAM	24.0 deg	
10:40	CDZ		
10:42	ASU		
10:46	PIM	53.0 deg	
11:53:03.4	ASU ACA		Occultation test
12:06:43.0	PIP	.011 deg	
12:07:34.5	ROP	.011 deg	
020:12:26:56.2	ASU		
13:28:23.1	PIM	53.1 deg	
021:07:14	ASU		
07:25	CDZ*		
07:32	ROM	130.0 deg	
07:48	PIM	50.0 deg	

Table 5-2: (Continued)

Day:Hr:Min:Sec	Event	Mag	Comment
021:07:55	ROP	90.0 deg	
10:25	YAM	50.0 deg	
10:28	ASU		
10:33	ROM	43.0 deg	
10:38	YAP	20.0 deg	
11:01	YAM	20.0 deg	
11:04	ASU		
11:36	ASU		At sunrise
11:50	ROM	95.76 deg	
11:54	YAM	37.15 deg	
12:33:53.0	YAM	0.5 deg	
12:30:50.0	PIM	0.5 deg	
12:42:55.0	YAP	0.5 deg	
12:52:30.0	PIP	1.0 deg	
12:58:24.0	YAM	0.6 deg	
13:00:33.0	PIM	0.9 deg	
13:03:19.0	ROP	360.0 deg	
13:29	YAP	37.15 deg	
13:35	CDZ		
13:41	PIM	58.0 deg	
023:07:39:34.1	ASU		
08:13:42.7	PIM	53.0 deg	
024:10:01	ASU		
10:09	CDZ*		
10:15	ROP	120.0 deg	
10:29	ROM	45.4 deg	
10:32	PIM	53.0 deg	
10:39	ROP	20.0 deg	
13:49	PIP	50.0 deg	

Day:Hr:Min:Sec	Event	Mag	Comment
024:13:57	ASU		
14:00	PIM	50.0 deg	
14:03	ROM	7.2 deg	
17:02	YAM	4.3 deg	
17:05	ROM	3.0 deg	
17:07	PIM	2.2 deg	
18:36	CDZ		
026:14:00:14.2	ASU		
14:11	PIP	53.0 deg	
15:18:03.5	ACA ASU		Occultation test
15:31:43.0	PIP	.011 deg	
15:32:34.5	ROP	.011 deg	
19:04:03.5	ACA ASU		Occultation test
19:17:43.0	PIP	.011 deg	
19:18:34.5	ROP	.011 deg	
030:03:46	YAM	2.0 deg	
031:01:01	YAM	61.0 deg	
01:22	ASU		
01:24	CDZ*		
01:27	ROP	360.0 deg	
02:12	ROP	91.0 deg	
02:26	CDZ		
02:29	PIP	50.0 deg	
05:31	ROM	4.8 deg	
05:45	PIP	42.2 deg	
06:12	CDZ*		
06:13	CDZ		
06:13	ΔV	95.6 ft/sec	
06:21	PIM	42.2 deg	

mission. Maneuver accuracy tests were performed in pitch and yaw; Table 5-3 shows the results of these tests.

Bias error derived from maneuver accuracy data should approximate rate integrate mode spacecraft drift. Drifts were about +0.91 degree per hour in yaw and +0.50 degree per hour in pitch when the tests were run.

5.2.1.1 Inertial Reference Unit (IRU)
The IRU performed satisfactorily during the extended mission. Table 5-4 shows the results of drift measurements made during both the

Table 5-3: Extended-Mission Maneuver Accuracy

Commanded Maneuver	Actual Magnitude	Error deg	Error %	Bias Error deg	Bias Error deg/hr	Scale Factor
YAM 360	359.25 ±0.02	+0.75	0.21	+0.172	+0.88	0.99840
YAP 360	359.60 ±0.02	−0.40	0.11	+0.175	+0.88	
PIM 360	359.76 ±0.02	+0.26	0.07	+0.092	+0.48	0.99959
PIP 360	359.95 ±0.02	−0.05	0.01	+0.089	+0.48	

Table 5-4: Inertial-Hold Drift Measurements

Day(GMT)	Measured Drift (deg/hr) Roll	Pitch	Yaw	Comments
1967 214		+0.075	+0.071	NDZ before Canopus acquisition, 5 hr
214	+0.045	0.078	0.093	NDZ after Canopus acquisition, 7 hr
215	0.038	0.094	0.090	NDZ, 30-hr test
216	0.064	----	----	Pitch and yaw in CLC, NDZ
221	----	0.094	0.117	3-axis test, 4 hr, insufficient data for roll
291	----	0.53	0.24	WDZ, estimated drift during eclipse, 5 hr
325	0.68	0.33	0.61	WDZ, pitched off −53°, 6 hr
335	----	0.46	0.79	NDZ on Sun, 3 hr
1968 008	----	0.51	0.91	NDZ, on Sun, 1.5 hr
018	0.77	----	----	NDZ, on Sun, tracking Acrux 0.25 hr
021	0.52	----	----	NDZ, on Sun, tracking Canopus 0.3 hr
026	----	0.5	----	WDZ, pitched off-Sun about +54°
031	----	0.5	----	WDZ, pitched off Sun about +50°

photographic and extended missions. Drift measurements obtained while off Sun or from tests of less than about 3 hours' duration are of limited accuracy but are tabulated because no better data are available.

Figure 5-2 shows drift data plotted against time, emphasizing the increasingly positive trend of drift in all three axes.

Gyro wheel currents were well behaved throughout the mission. Start, end, and extreme values of wheel currents are shown in Table 5-5. These data indicate a slight decrease of wheel current in all three axes, which is to be expected as the bearing preloading relaxes. Comparing wheel current for Days 026 and 029, it is significant that for the same temperature, pitch current decreased three telemetry bits while yaw current increased two bits after the period when a probable power interruption was experienced.

Table 5-5: Gyro Wheel Currents

GMT Day	Current (ma)			Gyro Temperature Percent of Full Scale
	Roll	Pitch	Yaw	
242 (start)	83.5	91.0	88.3	41.2
026 (before anomaly)	83.0	90.4	87.7	50.0
029 (after anomaly)	83.5	88.8	87.8	50.0
031 (high)	85.1	92.0	88.8	88.8
291 (low bus voltage: 21.6 volts)	80.3	86.2	85.7	10.8

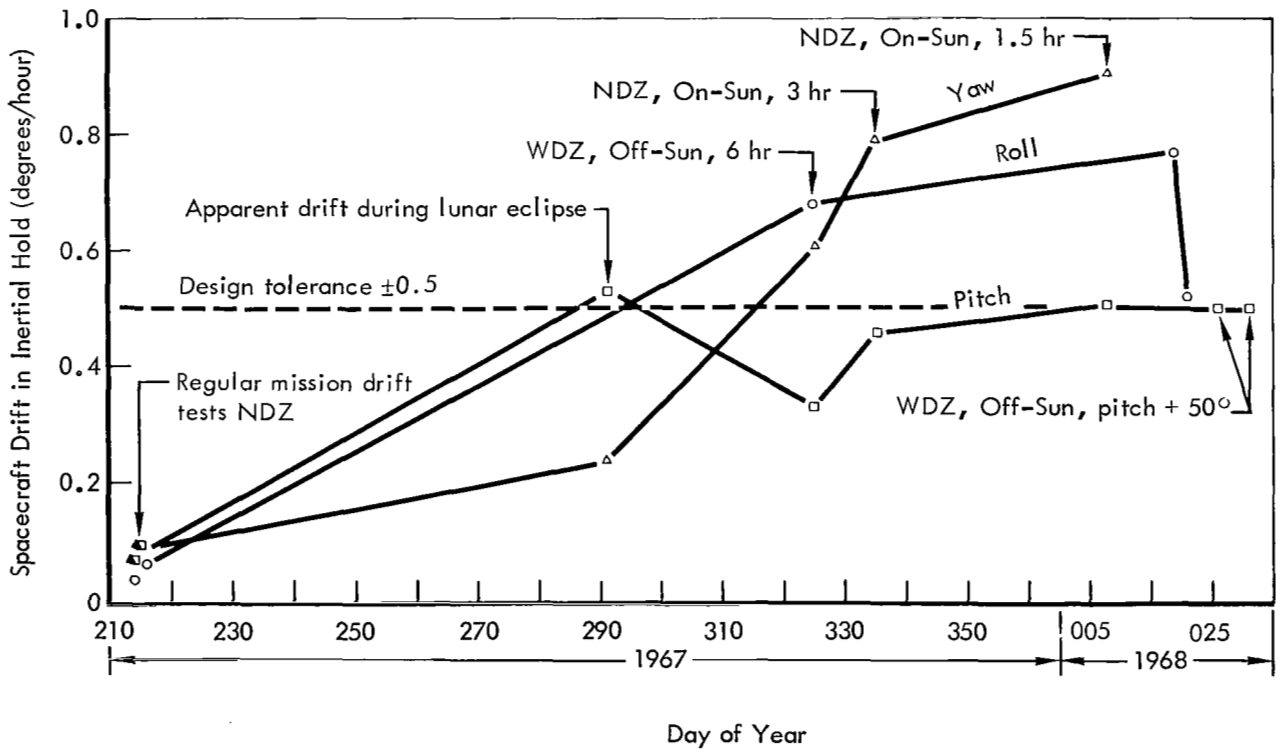

Figure 5-2: Drift Measurement History

Gyro temperature is a pseudo-temperature output signal derived from the addition of error signals in the roll, pitch, and yaw gyro heater control circuits plus the accelerometer heater circuits, and is somewhat dependent on spacecraft bus voltage. The temperature-control circuits are used to stabilize the viscosity and density of the gyro and accelerometer flotation fluid. The measurement is expressed in percentage of full scale from 0 to 100%, corresponding to the telemetry range of 0 to 5 volts. The approximate indicated IRU temperature range for 0 to 100% is 142.5 to 147.5°F. The gyro heater control circuits are normally off when the IRU temperature goes above 100% and the IRU temperature increases at a 1:1 rate, with increase in spacecraft EMD temperature.

Gyro temperature telemetry indicated that at least one gyro heater loop saturated on Day 335 and again on Day 031. On both occasions gyro temperature reached 88.8% of full scale. Temperature history for Day 031 is shown in Figure 5-3 when the EMD (ST03) reached a peak for the extended mission of about 114°F.

Gyro and EMD temperatures during the lunar eclipse are shown in Figure 5-4. As the temperature increased following the eclipse, gyro temperature was observed to oscillate in a characteristic manner observed on Lunar Orbiter IV and during IRU testing. This oscillation is shown in Figure 5-5. There was no apparent coupling into the wheel currents as observed on other IRUs, and the oscillation did

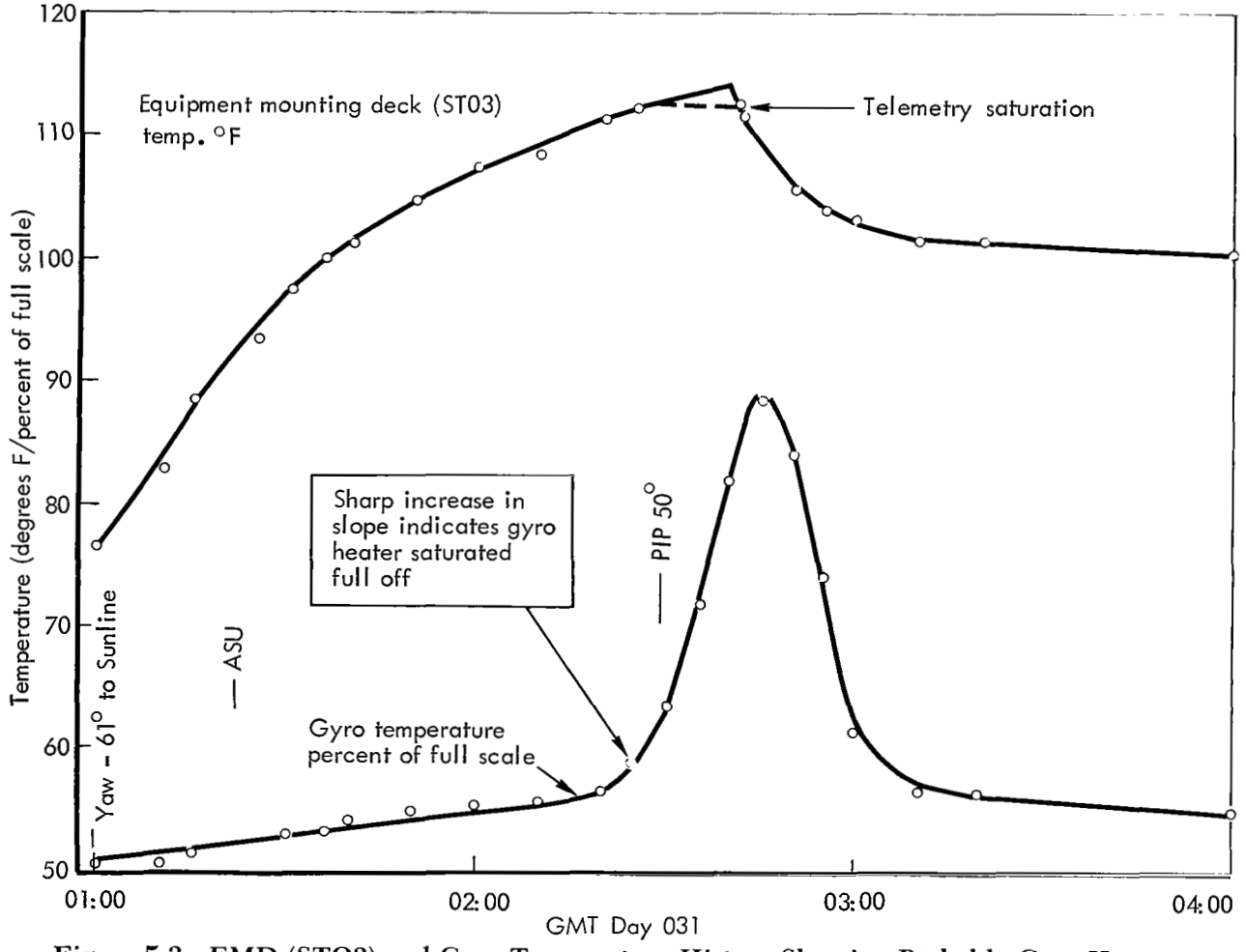

Figure 5-3: EMD (STO3) and Gyro Temperature History Showing Probable Gyro Heater Saturation

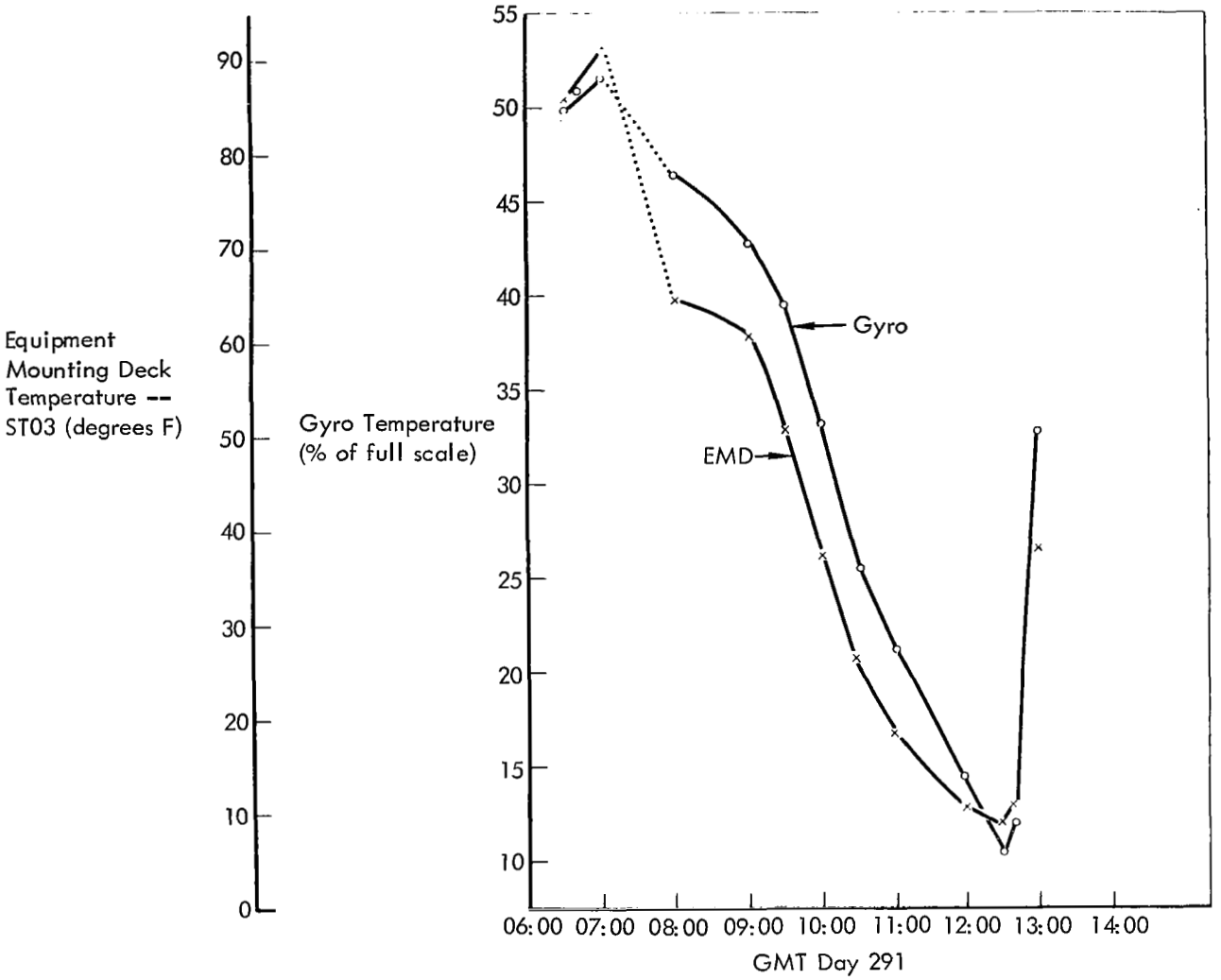

Figure 5-4: EMD (STO3) and Gyro Temperature History During Lunar Eclipse – Day 291

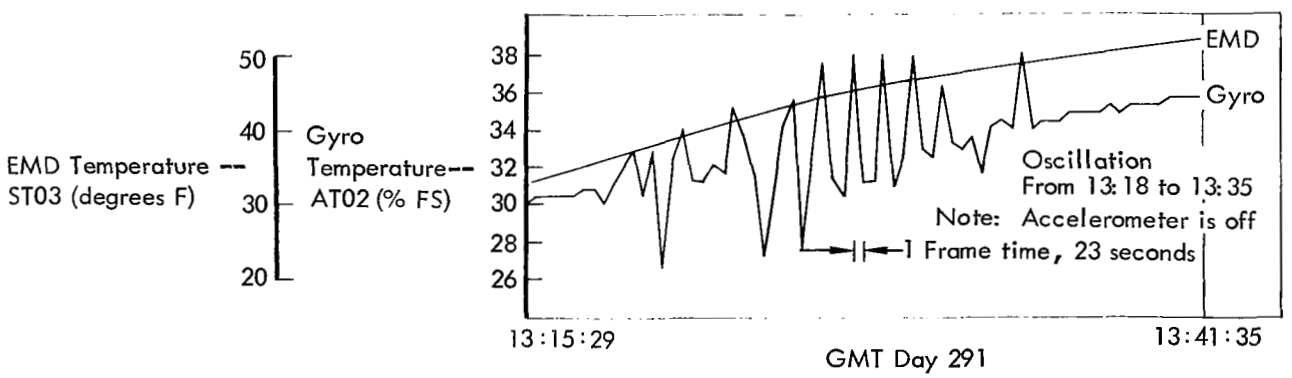

Figure 5-5: Gyro Temperature Oscillation

not occur when the gyro temperature was at a normal 40 to 60%.

5.2.1.2 Star Tracker

The star tracker, which continued to perform satisfactorily during the extended mission, was cycled on and off 31 times for a total operating time of 46 hours, 35 minutes. Including the photographic mission, the tracker was on a total of 80 hours, 45 minutes and was operated through 229 on-off cycles. Star map signal for Canopus remained at about 2 volts during the mission.

Comparison of maneuver angle and change in tracker position signal during a wide deadband roll maneuver with Canopus in the field of view demonstrated a one-to-one correspondence between these two measurements of roll displacements, within the resolution of telemetry (about 0.05 degree).

Another comparison of gyro position change with tracker position change while tracking Canopus in the inertial hold mode showed that these parameters agree within the telemetry accuracy.

The lower Canopus presence gate and the tracking mode gate continued to operate at their design points. The upper Canopus presence gate was not activated during the extended mission.

During the yaw maneuver accuracy test, the BOS closed when the tracker bore was about 80 degrees from the sunline.

Star maps were performed on Days 270, 324, and 335. Telemetry maps for these occasions are shown in Figures 5-6 to -8. Roll 360-degree antenna maps were performed on Days 018 and 031 with the tracker on; however, no stars were identified and the peak signal strength point was used as the primary reference. On Day 018 the reference obtained with the antenna was used to locate the star Acrux, which was successfully tracked.

5.2.1.3 Sun Sensors

Yaw sun sensor output voltage at a pitch angle of 30 degrees was approximately 75% of the voltage when oriented on the Sun. The values corresponded with those of previous missions; however, the predicted change was 86%. The difference of 11% was caused by a masking effect due to sensor construction and was not detrimental to the mission. The sun sensor narrow- and wide-deadband limits (see Table 5-6) are within specification, except as noted in pitch.

5.2.1.4 Closed-Loop Electronics

On Day 270 it was observed that the pitch-minus maneuver rate in wide deadband was −0.24 degree per second and that the pitch deadband limits (narrow deadband, inertial hold) were +0.115/−0.171 degree. The nominal rate is 0.05 degree per second and the deadband limits observed during the photographic mission were +0.163/−0.171 degree. Operation of the pitch axis was normal on Day 239. Short tracks between Days 239 and 270 did not provide sufficient data to evaluate the deadband; therefore, the exact time the problem began is not known. Operation of the pitch attitude control channel was consistent with the conclusion that the minus threshold detector was triggering at −1.1 volts instead of a normal −2.0 volts. Calculations show that this would result in a wide-deadband maneuver rate of −0.27 degree per second, a narrow-deadband rate of −0.53 degree per second, and a pitch deadband turnaround at about half the normal value. This condition did not impair operation of the spacecraft; however, it is estimated that about 0.25 pound of additional nitrogen was consumed as a result of the higher maneuver rate.

Except for the change in the pitch-minus threshold detector between Days 239 and 270, the operation of the closed-loop electronics was normal, and is summarized in Tables 5-6 and -7.

Star Map Tabulation
Roll Start Day 270, 12:19

T/M No.	SIDL No., Name	Clock Angle (deg) A Priori	Clock Angle (deg) Observed	Canopus Flux Ratio	Map Voltage A Priori	Map Voltage Actual
1	601, Earth	99	99/110	$5.8X10^8$	—	1.34
2	602, Moon	—	160/270	$5.8X10^3$	—	*
3	2, AL CAR, Canopus	0	Reference	1	2.5	1.75
4	52, TH SCO	84	85/90	.09	0.7	1.0
	46, KA SCO	88		.05	0.7	
	19, LA SCO, Shaula	90		.19	0.8	
5	32, EP SGR Kaus Australis	93	91	.12	0.7	0.8

* BOS Closed

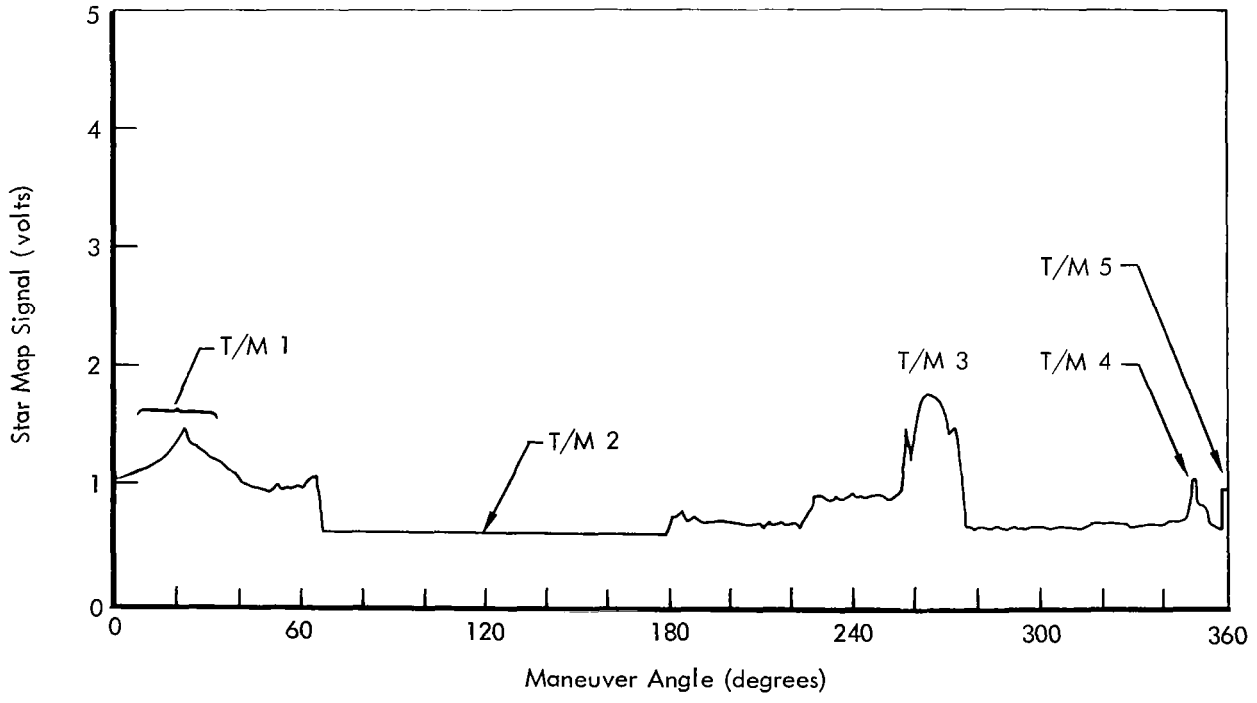

Figure 5-6: Telemetry Data Star Map – Day 270

Star Map Tabulation Roll Start Day 324, 15:06						
T/M No.	SIDL No., Name	Clock Angle (deg)		Canopus Flux Ratio	Map Voltage	
		A Priori	Observed		A Priori	Actual
1	602 Moon	—	125/220	—	—	4.3
2	132 GA LEO	271.6	272.4	0.05	0.6	0.98
3	502 Jupiter	279.4	Reference	1.36	4.1	4.56
4	23 GA VEL, Alnitak	344.9	345.0	0.10	0.6	0.94
5	40 DE VEL	348.9	348.2	0.08	0.6	0.92
6	61 IO CAR	351.7	352.3	0.06	0.6	0.90
7	131 EP CAR Avior	354.6	355.1	0.05	0.6	0.92
8	Unidentified	—	1.0	—	—	0.96

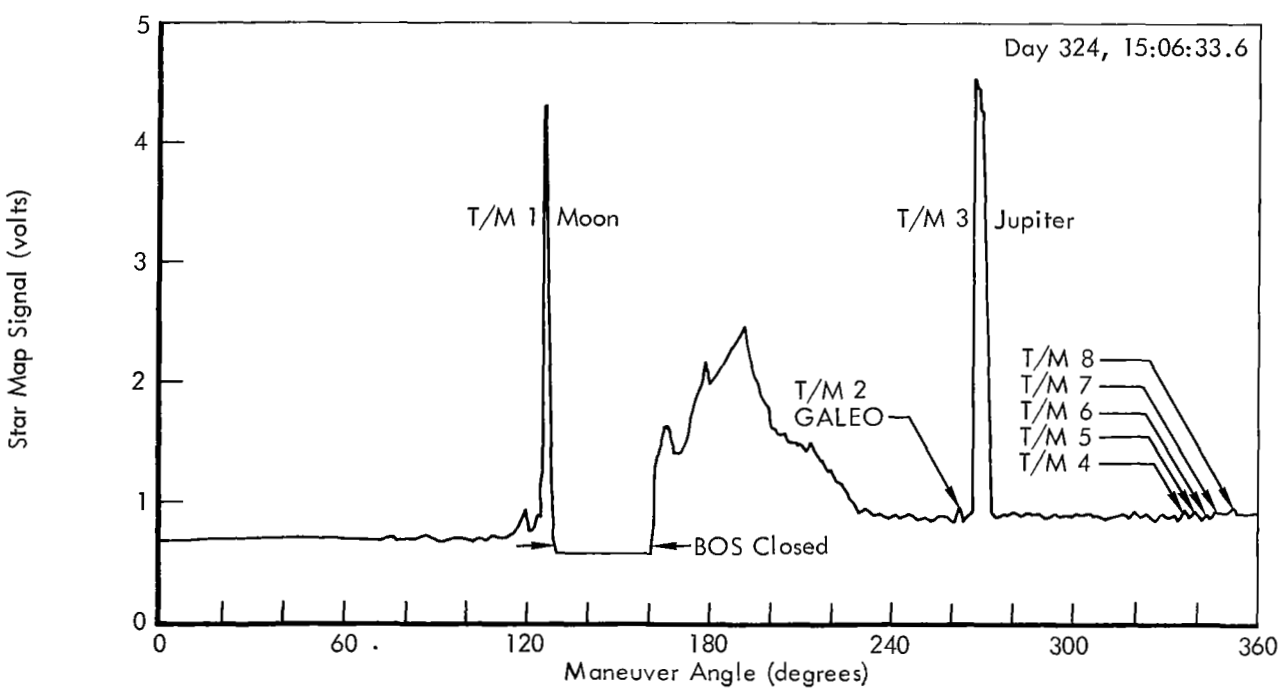

Figure 5-7: Telemetry Data Star Map – Day 324

Star Map Tabulation
Roll Start Day 335, 14:31 (Minus Roll)

T/M No.	SIDL No., Name	Clock Angle (deg) A Priori	Clock Angle (deg) Observed	Canopus Flux Ratio	Map Voltage A Priori	Map Voltage Actual
1	16 AL PSA Fomalhaut	77	Reference	0.14	0.6	0.7
2	5 AL ERI Achernar	40	42	0.43	*	0.8
3	28 BE CAR Miaplacidus	358	356	0.09	0.6	0.68
	131 EP CAR Avior	352	Not separately identified	0.05	—	—
	61 IO CAR	348		0.06	—	—
	40 DE VEL	346	346	0.08	0.6	0.72
	56 KA VEL	344	340	0.05	0.6	0.70
4	31 EP UMA Alioth	224	224	0.09	0.6	0.68
	27 ET UMA Alkaid	223		0.09		
	55 ZE UMA Mizar	222		0.06		
5	18 AL CYG Deneb	158	161	0.13	0.6	0.72

* AL ERI cone angle =93.4, predicted to be out of yaw F.O.V.

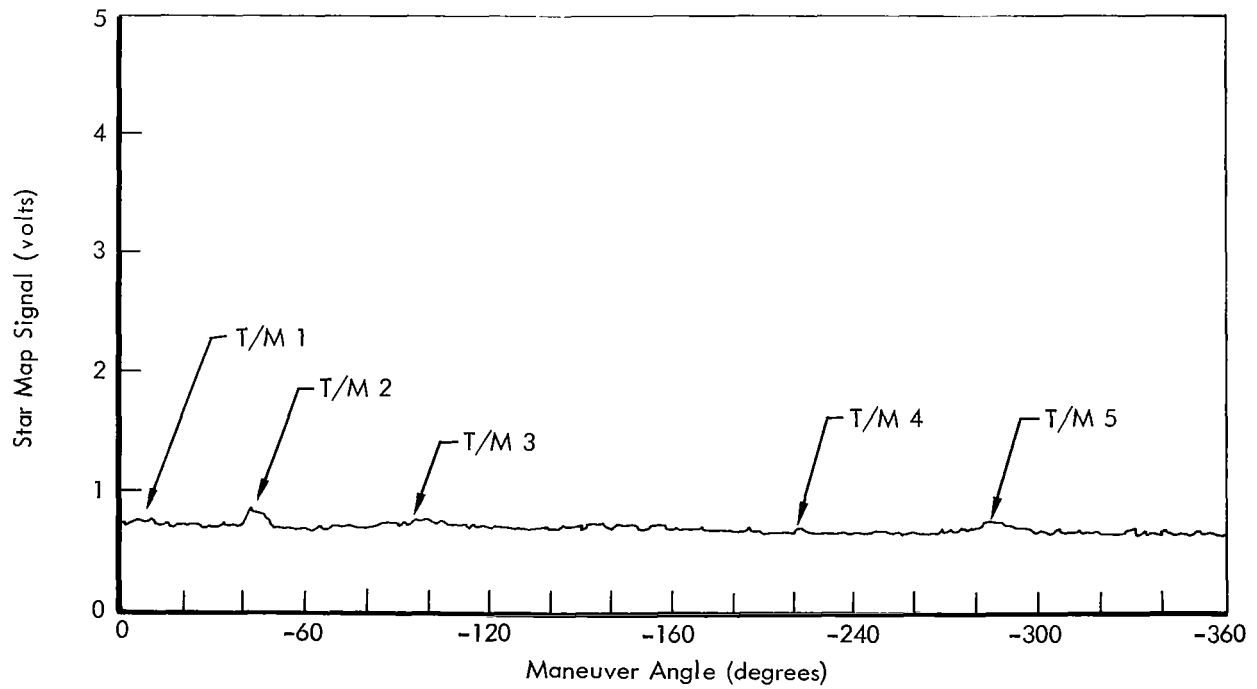

Figure 5-8: Telemetry Data Star Map – Day 335

Table 5-6: Limit Cycle Characteristics

Operational Mode	Deadband Limit (degrees) Roll Plus	Roll Minus	Pitch Plus	Pitch Minus	Yaw Plus	Yaw Minus
Inertial hold, 0.2° deadband	+0.162	−0.170	+0.068	−0.172	+0.164	−0.170
Inertial hold, 2.0° deadband	+1.893	−1.991	+1.097	−1.967	+1.957	−2.010
Conventional limit cycle, 0.2° fine sun sensor only	N.A.	N.A.	+0.074	−0.173	+0.160	−0.202
Conventional limit cycle, 0.2° fine and coarse sun sensor	N.A.	N.A.	+0.081	−0.125	−0.047	−0.263
Conventional limit cycle, 2.0° fine sun sensor only	N.A.	N.A.	*	*	+1.999	*
Conventional limit cycle, 2.0° fine and coarse sun sensor	N.A.	N.A.	+0.912	−1.582	+1.574	−1.846

*Insufficient data
Notes: 1) CLC in roll not used
2) CLC 2.0 ° and 0.2° coarse eyes not used

The maneuver rates shown in Table 5-7 represent the lower constant rate mode deadband limit since they were taken as soon after acceleration cutoff as possible.

Thrust vector control during the two velocity maneuvers is summarized in Table 5-8. Residual limit cycle rates after the burns are shown in Table 5-9.

Figure 5-9 is a plot of actuator and gyro positions during the burn of Day 283. The short duration of the burn on Day 031 does not allow a useful graphical representation.

Table 5-7: Extended-Mission Maneuver Rates
(typical rate at acceleration cutoff)

	Maneuver Rate (deg/sec) Narrow Deadzone Plus	Narrow Deadzone Minus	Wide Deadzone Plus	Wide Deadzone Minus
Roll	+0.500	−0.500	+0.0505	−0.0408
Pitch	+0.516	−0.537	+0.0673	−0.260
Yaw	+0.508	−0.513	*	−0.0560

* No data

Table 5-8: TVC Actuator Position Summary

GMT of Burn	Actuator Position (degrees) Pitch Start	Pitch Change	Pitch End	Yaw Start	Yaw Change	Yaw End
238:19:37	−0.135	−0.030/−0.170	−0.085	+0.490	+0.360/+0.440	+0.460
031:06:13	−0.085	−0.062/−0.085	−0.085	+0.428	+0.428/+0.473	+0.428

Table 5-9: Postburn Residual Rates

	Residual Rates (deg/sec)		
GMT of Burn	Roll	Pitch	Yaw
283:19:37	−0.0040	+0.077	+0.051
031:06:13	−0.0046	+0.027	+0.037

Figures 5-10 and -11 show typical limit cycle activity during the extended mission.

5.2.1.5 Reaction Control and Nitrogen Usage
Figure 5-12 shows nitrogen supply as calculated from both telemetry data and spacecraft dynamics. The dynamic calculation is based on the

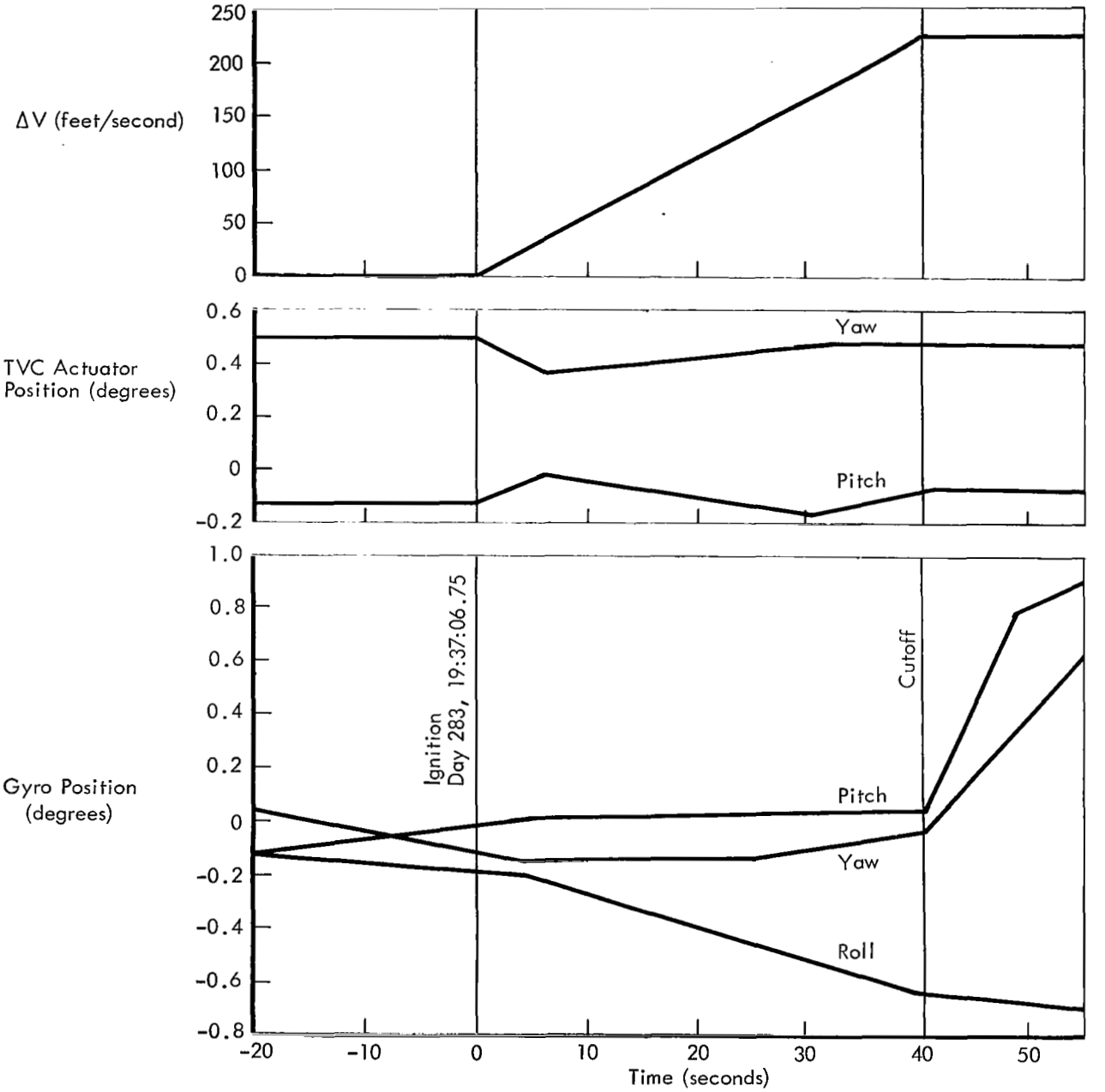

Figure 5-9: Gyro and Actuator Position During Burn — Day 283

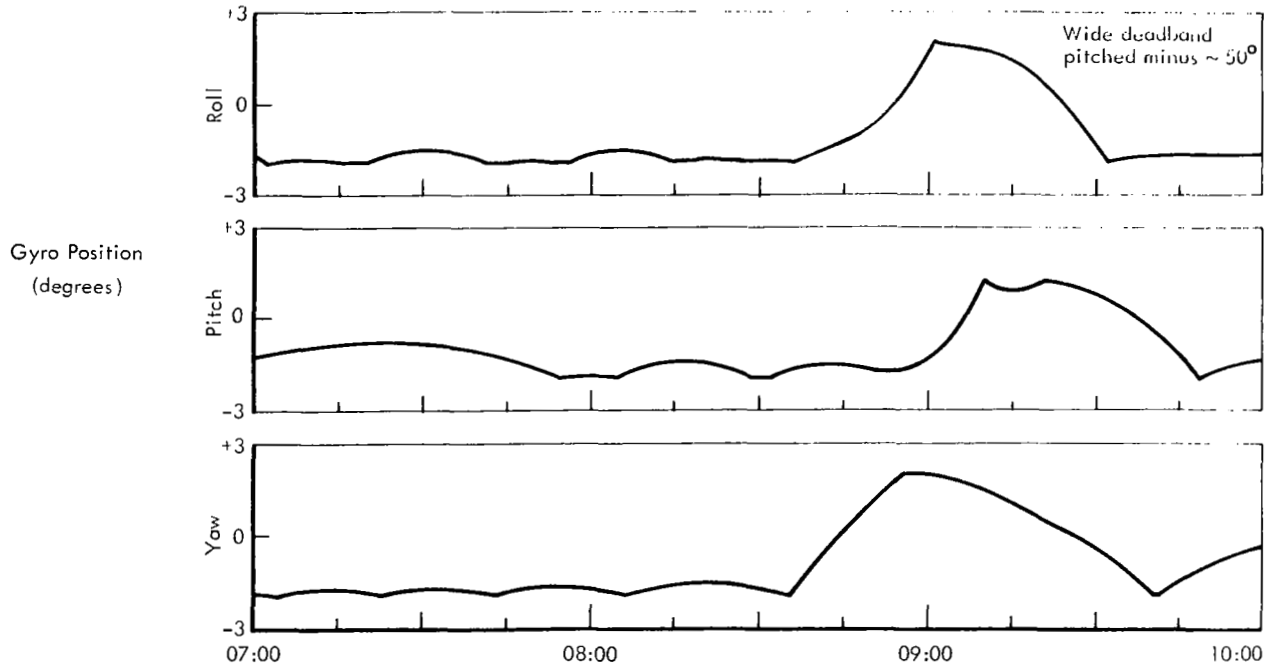

Figure 5-10: Limit Cycle – Day 331, 07:00 to 10:00

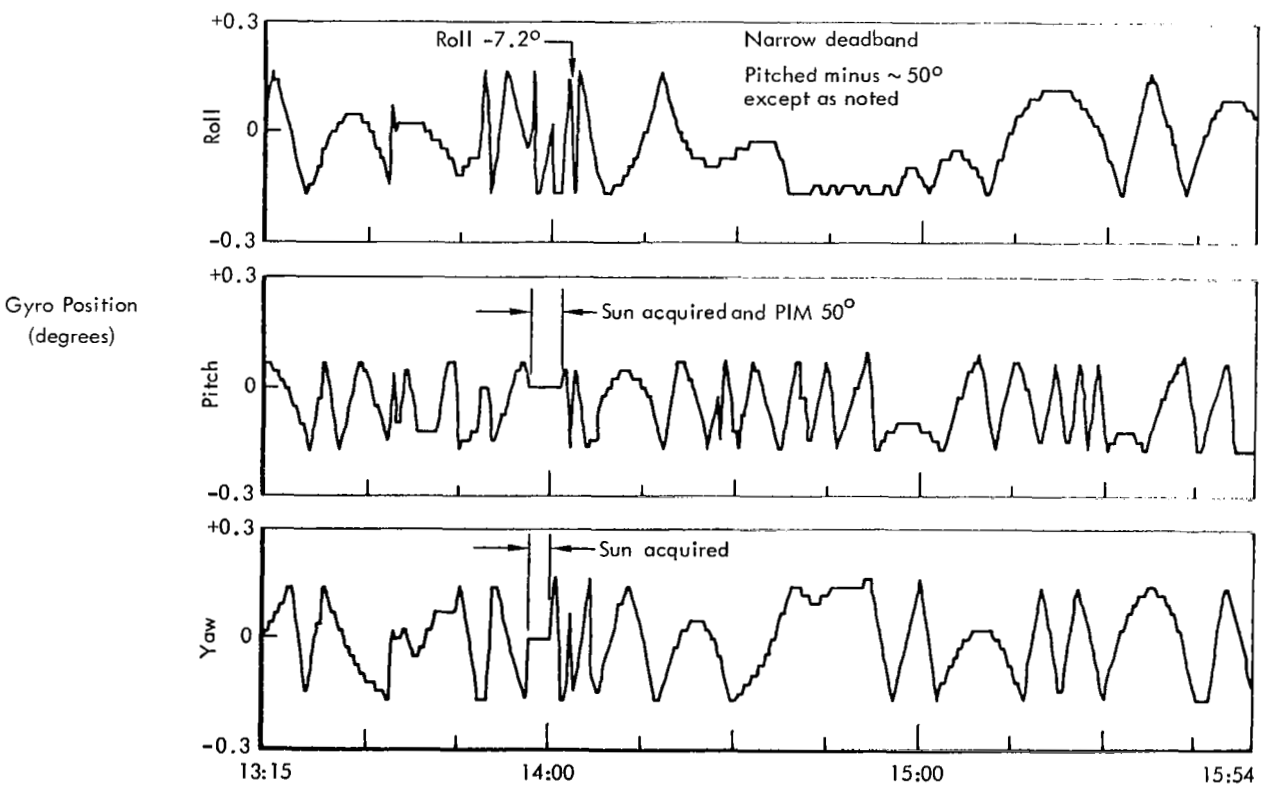

Figure 5-11: Limit Cycle – Day 024, 13:15 to 15:54

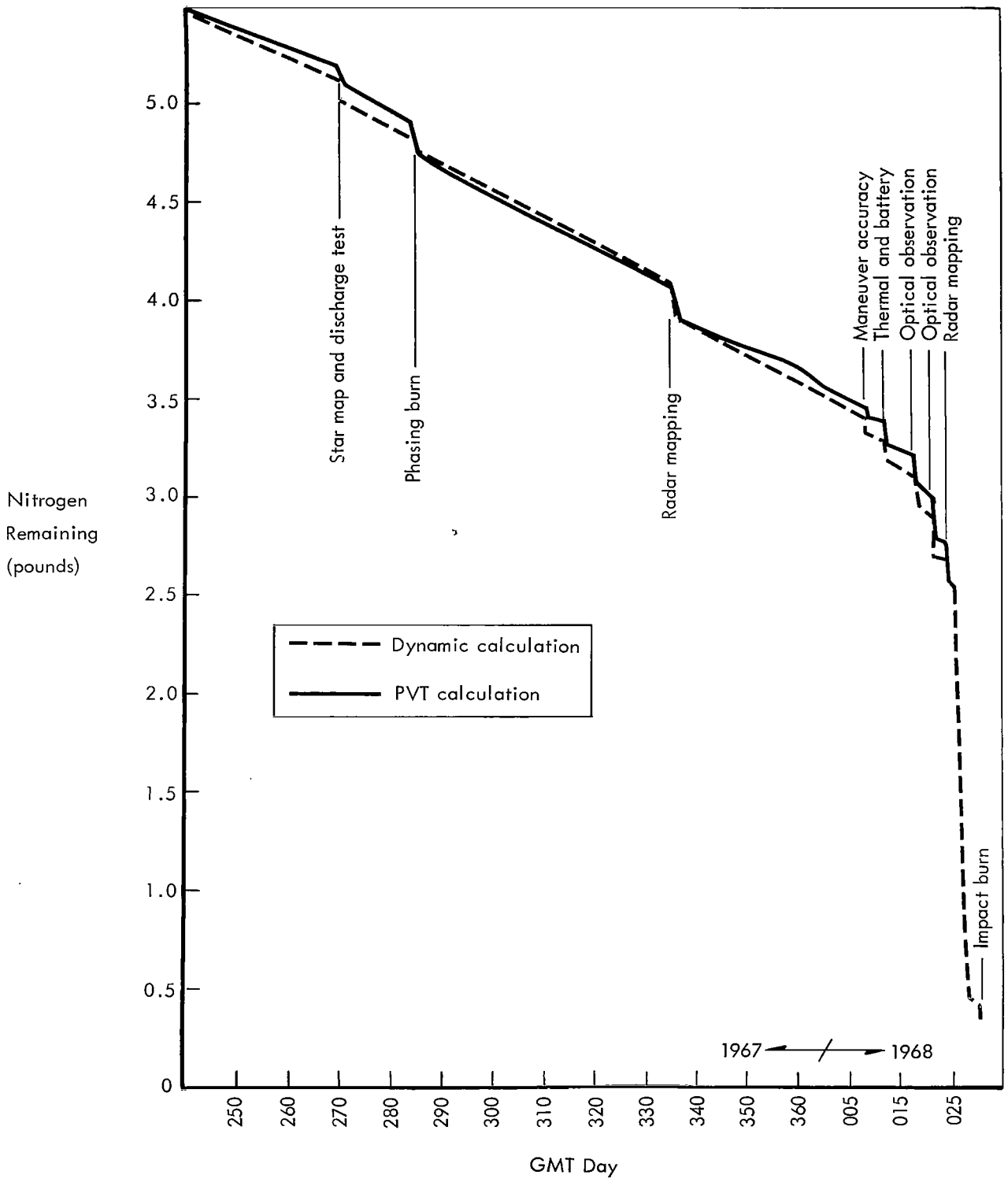

Figure 5-12: Nitrogen Supply History

maneuver rates of Table 5-7, a total spacecraft weight of 580 pounds, and actual samples of limit cycle characteristics. The dynamic calculations show a slightly higher usage than do telemetry data. There was some nitrogen leakage through the isolation squib after the burn on Day 283, as indicated by the rebound in propellant tank pressures.

Using the telemetry data, it is estimated that 5.09 pounds of nitrogen were consumed during the extended mission. Usage is broken down into various categories in Table 5-10. The slight leak into the propellant tanks is ignored.

Table 5-10: Nitrogen Usage Breakdown

A	
Limit cycle	1.25 lb
Maneuvers	1.73 lb
Anomaly (026/029)	2.11 lb
Total	5.09 lb

B	
Cruise mode	1.90 lb
Special activity	1.08 lb
Anomaly (026/029)	2.11 lb
Total	5.09 lb

At impact about 0.36 pound remained at a pressure of 77 psi. Despite the low pressure, operation appeared normal.

When possible, thruster performance was evaluated for maneuvers. The results, shown in Table 5-11, indicate that the roll thrusters were still operating at full thrust on Day 031.

In the course of performing 235 maneuvers, 119 Sun acquisitions, 154 days of wide deadzone limit cycle, and about 43 hours of narrow deadzone limit cycle, it is estimated that there were

Table 5-11: Reaction Control Thruster Performance

Axis	Direction	Thrust (lb)	Pressure (psi)	Time of Maneuver
Roll	Plus	0.0640	93	031:01:27
Roll	Plus	0.0635	613	021:13:03
Roll	Plus	0.0640	645	021:07:55
Pitch	Plus	0.061	710	012:22:30

64,100 roll, 87,600 pitch, and 62,700 yaw thruster operations.

5.2.1.6 Control Assembly

During the extended mission the control assembly responded correctly to all real-time and stored-program commands. A total of 911 commands was transmitted and executed during the extended mission.

The programmer cycled over 1.54 billion times and accumulated 154 million clock incrementations while directing spacecraft operation. The total clock error as of Day 026 was plus 4.78 seconds for a drift rate of 1.11 milliseconds per hour. This drift is within the design tolerance of 3.4 milliseconds per hour.

When possible, the programmer was configured in a nonstandard mode to permit accurate determination of Sun occultation times to be used as a data input for experimental orbit determination work. The sequence commanded was as follows:

1) All sunsensors off
2) Wait 3.2 seconds
3) Acquire Sun; acquire Canopus
4) Wait 819.2 seconds
5) Pitch plus 0.011 degree
6) Wait 51.2 seconds
7) Roll plus 0.011 degree
8) All sunsensors on

This sequence placed the flight control switching to a pseudo-sensor mode; consequently, the Sun occultation time was stored in Fixed Memory Address 6 (FMA6).

The sequence was initiated by a real-time JMP command, the timing of which ensured that Sun occultation occurred during the 819.2-second wait time. The sun sensors were disconnected from the closed-loop electronics before the acquire-Sun command in an effort to inhibit actual Sun acquisition and, consequently, nitrogen usage.

5.2.1.7 Switching Assembly

The switching assembly was not used during the extended mission except for velocity maneuvers. Performance was normal. No anomalies in the spacecraft telemetry data were observed that would indicate a switching assembly problem.

5.2.2 Communications Subsystem

The communications subsystem (see Figure 5-13) consists of the equipment which: (1) receives information from the ground via an RF link and converts this information to a form suitable for use by the spacecraft; (2) receives information from the spacecraft (telemetry and video), converts this information to modulation on an RF carrier, and transmits this modulated RF carrier to the ground; (3) receives ranging information from the ground via RF link, modulates this information on an RF carrier, and retransmits this to the ground for use in range determination; and (4) establishes a specific ratio between the received RF frequency from the ground and the spacecraft-transmitted frequency for accurate determination of the spacecraft velocity using Doppler information.

The communications subsystem operated nominally throughout the extended mission while performing the functions listed below.

Command Capability – The command loop received, verified, and executed 911 commands without error; the use of the command decoder redundant-command register was never re-

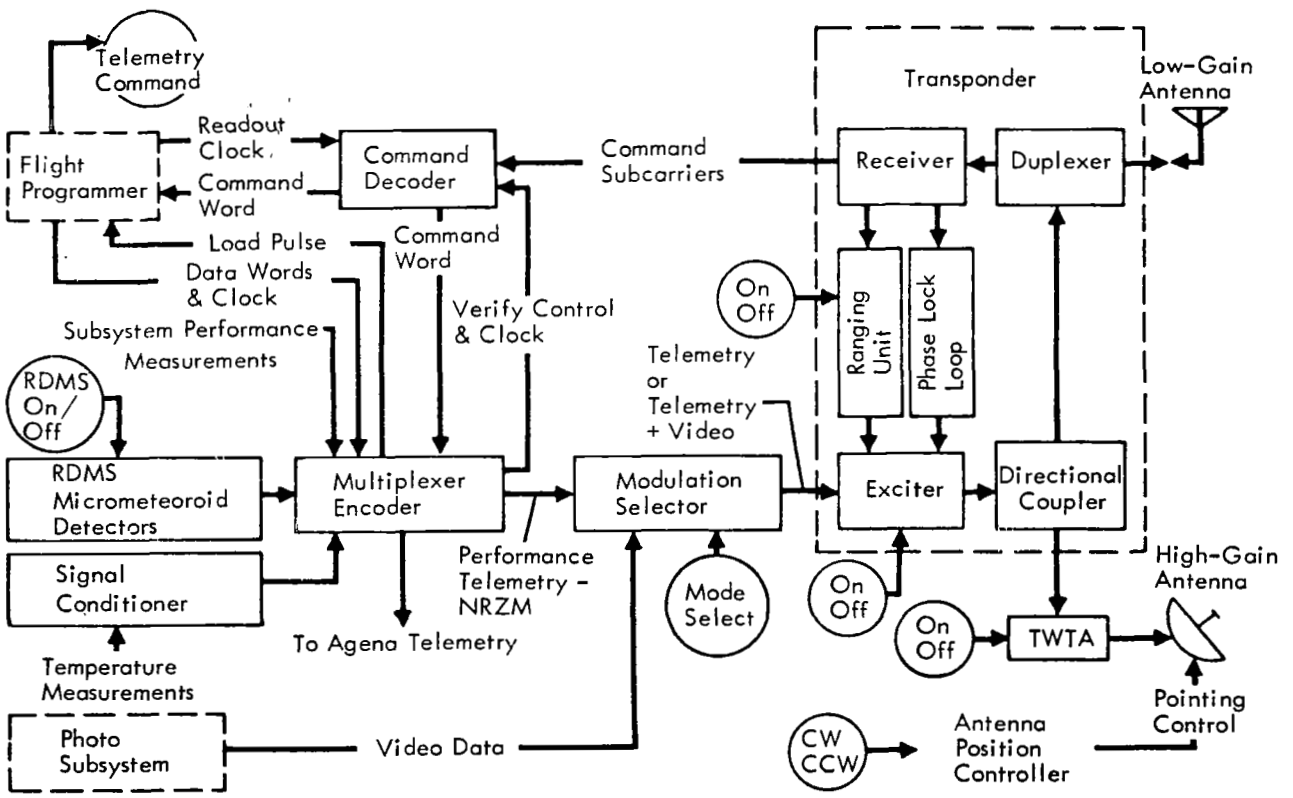

Figure 5-13: Communications Subsystem

quired. The communications subsystem responded to all operational commands as directed.

Spacecraft Performance Information – Telemetry data from all spacecraft subsystem transducers were compiled and transmitted with desired accuracy.

Lunar Environment Information – As a primary objective of the extended mission, radiation and micrometeoroid data were provided by the communications subsystem throughout the extended mission.

Photographic Information – Although the communications subsystem maintained this capability, no video data were transmitted during the extended mission.

Selenodetic Information – Ranging and coherent Doppler data using two tracking stations were successfully provided throughout the extended mission. Time correlation between tracking stations was accomplished using the ranging system.

5.2.2.1 Transponder

The transponder operated satisfactorily throughout the extended mission. Telemetry indications of transponder RF power output variations with transponder temperature are shown in Figure 5-14. The data prior to and during the lunar eclipse agree favorably with the flight acceptance test (FAT) data. After the eclipse, however, the flight data diverged from the FAT data and a noticeable discontinuity was observed when the transponder temperature was between 80 and 90°F. This discontinuity is

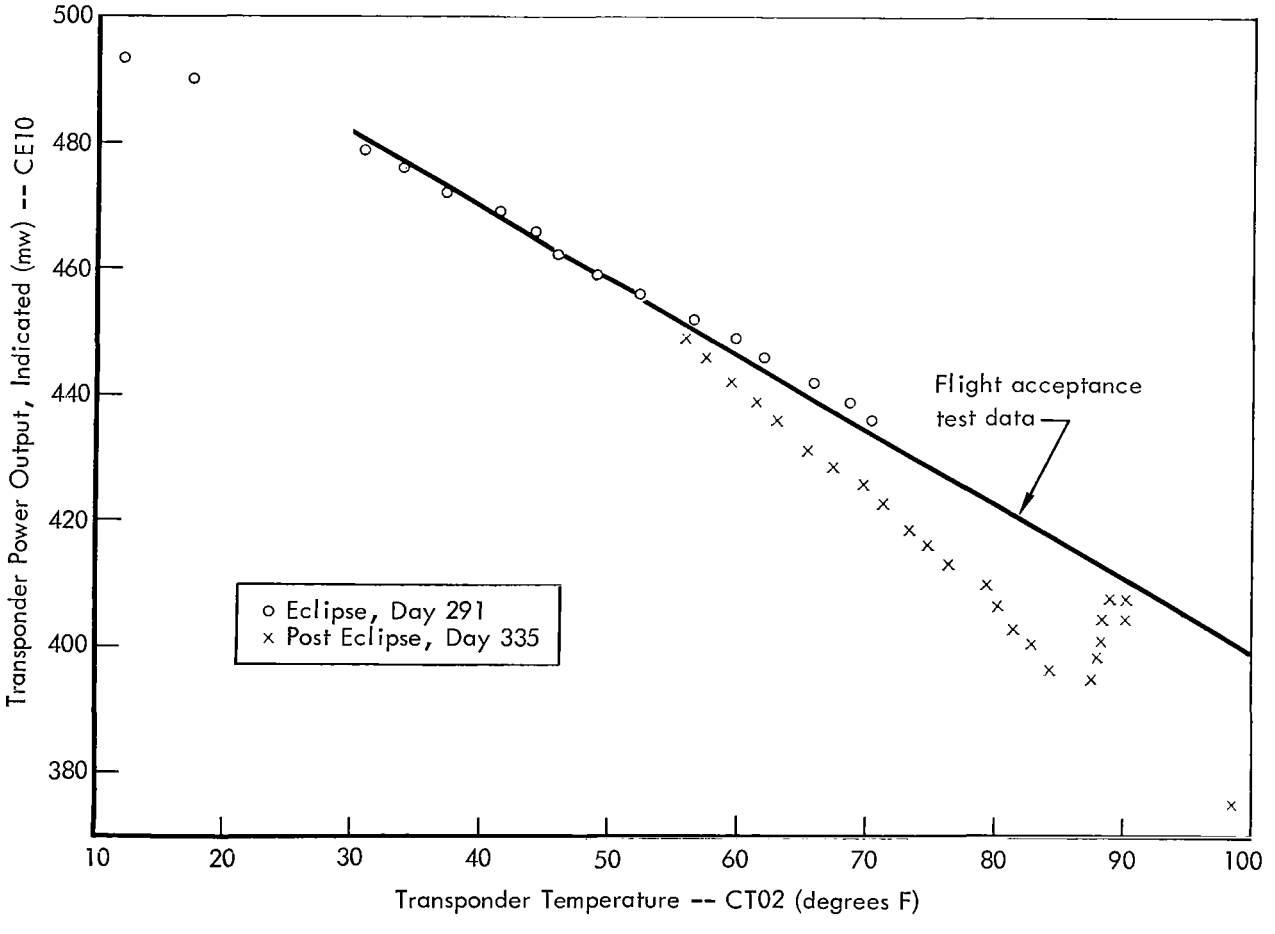

Figure 5-14: Transponder Power Output

better illustrated in Figure 5-15. The discontinuity was regularly observed later in the extended mission whenever the transponder temperature was greater than 80 to 90°F. The accuracy of the transponder RF power output telemetry measurement (CE10) is ± 20% of full scale, which would more than encompass the variations observed. Actual power output variation was only about one third to one half that indicated by telemetry because of the temperature sensitivity of the transponder power output signal sampler. Figure 5-16 illustrates the transponder temperature and indicated RF power output observed during all the extended-mission tracking periods.

The transponder ranging module was on throughout the extended mission except for a short period during the lunar eclipse. Approximately 142 hours of ranging data were obtained.

No problems were encountered with the ground-received signal strength, and the transponder fulfilled all design requirements while operating for 183 days.

5.2.2.2 Traveling-Wave-Tube Amplifier

The TWTA provided a high-power signal for extended-mission operations and for tracking by the manned spacecraft network stations. The TWTA was operated in the on state through 85 Sun occultations, the longest of which was of 36 minutes' duration.

Previous low-input voltage tests have shown that the TWTA power supply loses regulation at input voltages between 24.7 and 24.9 volts d.c. and that all TWTA telemetry values are affected. Figures 5-17 to -19 indicate typical TWTA performance during a Sun occultation (low-input voltage). It can be seen that this TWTA power supply loses regulation at an input voltage (bus) of 24.7 volts d.c. No degradation of TWTA performance was observed during the Sun occultations, and the TWTA telemetry values returned to nominal with the return of the input voltage to normal (30.56 volts d.c.).

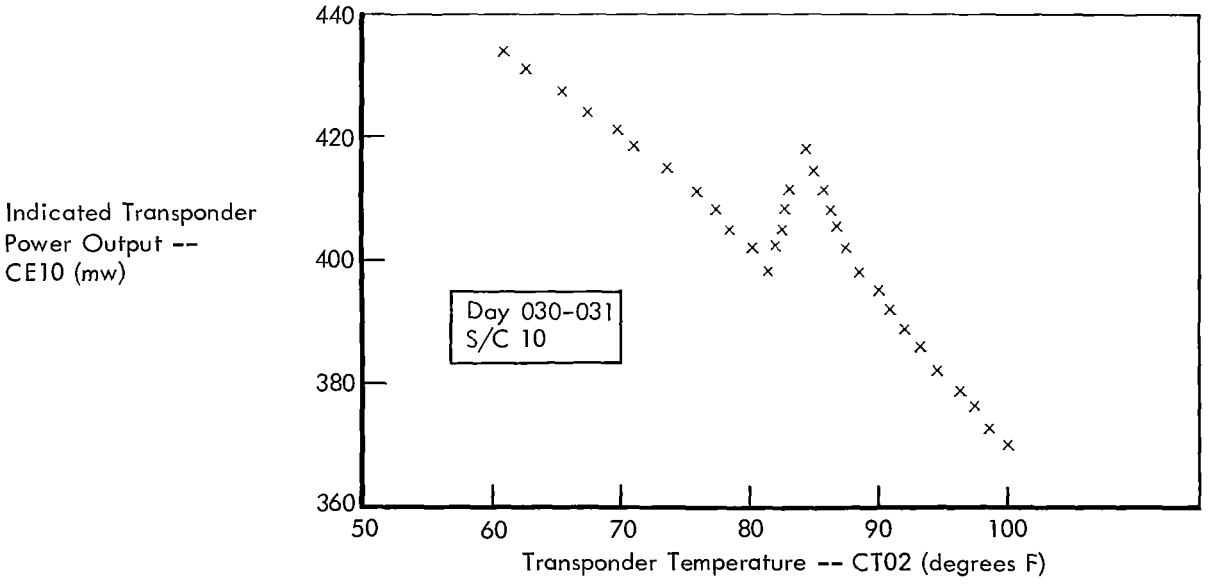

Figure 5-15: Transponder Power Output

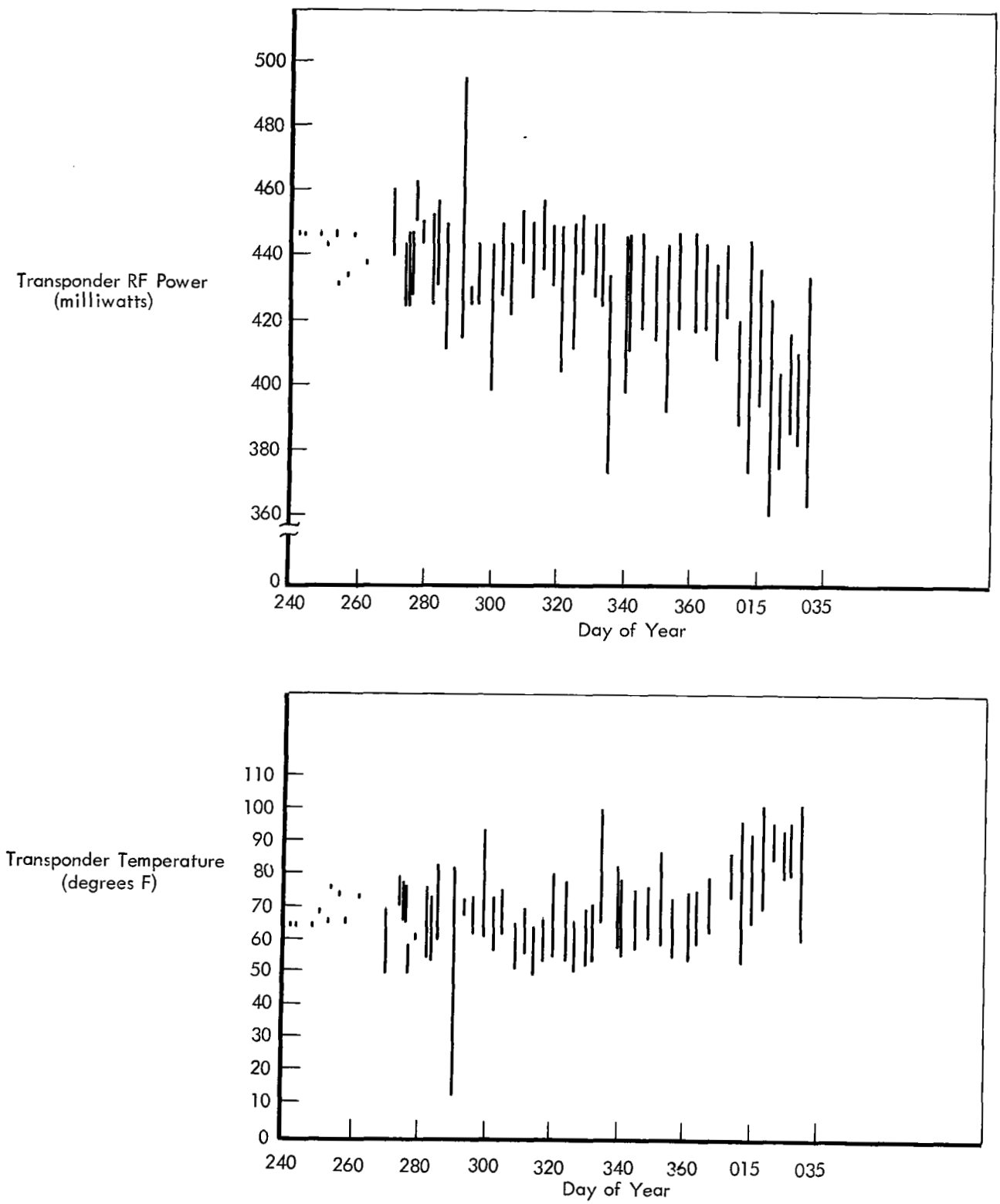

Figure 5-16: Transponder Power/Thermal History

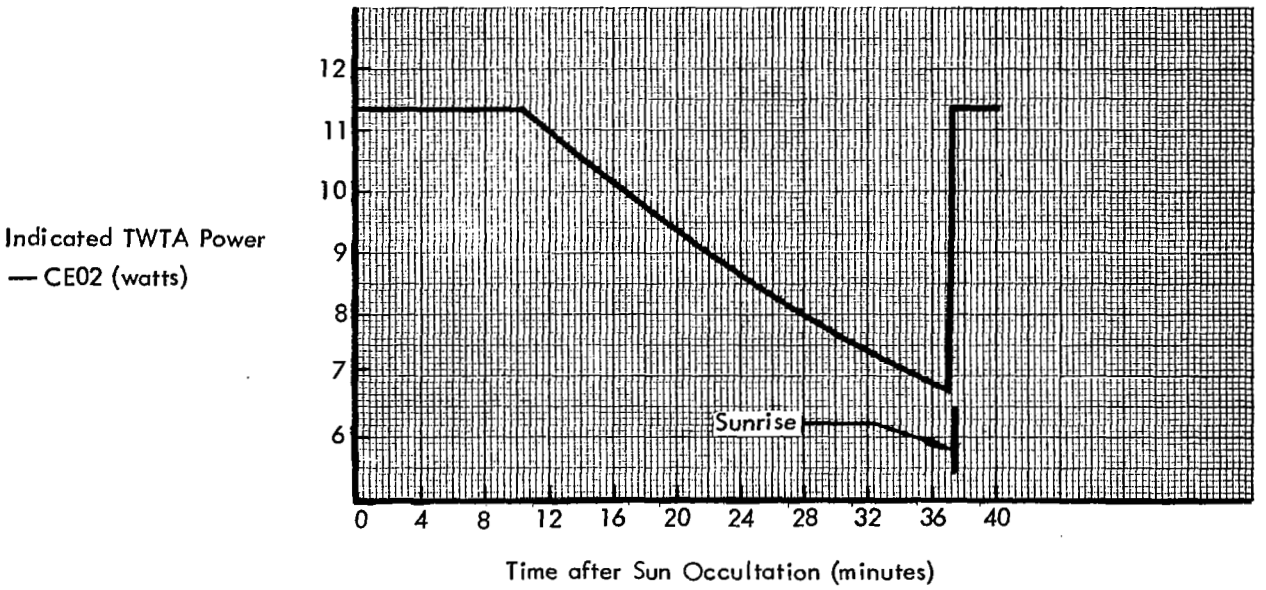

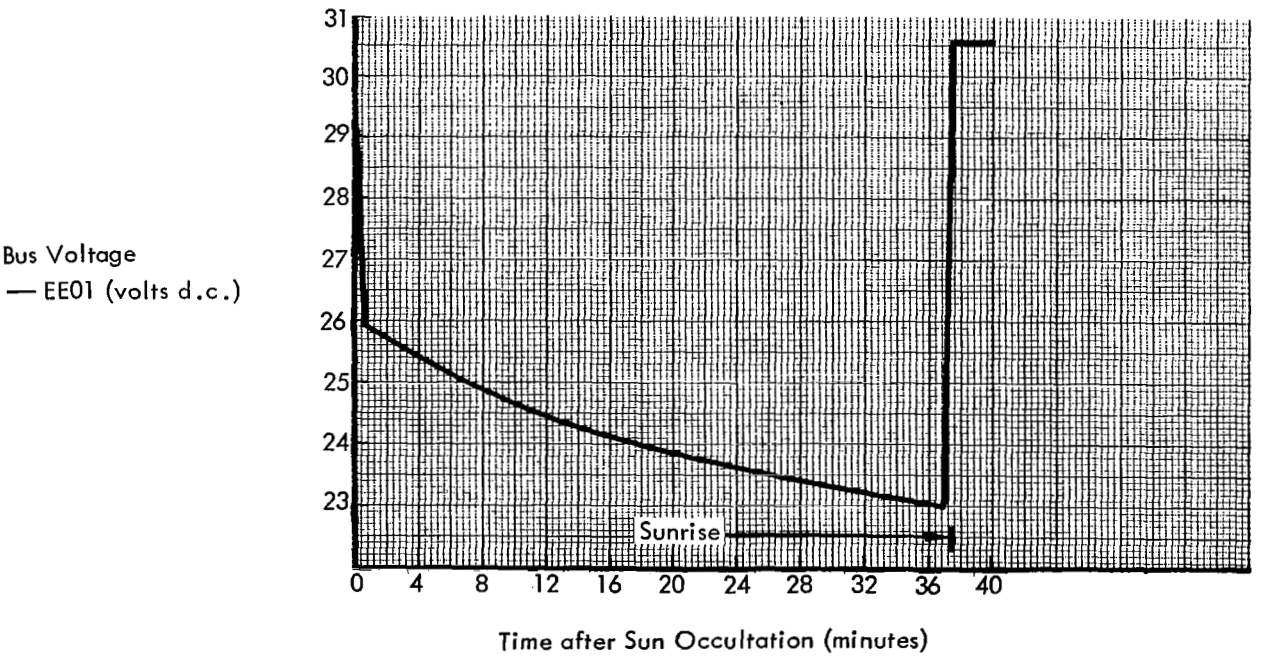

Figure 5-17: TWTA Sunset Performance

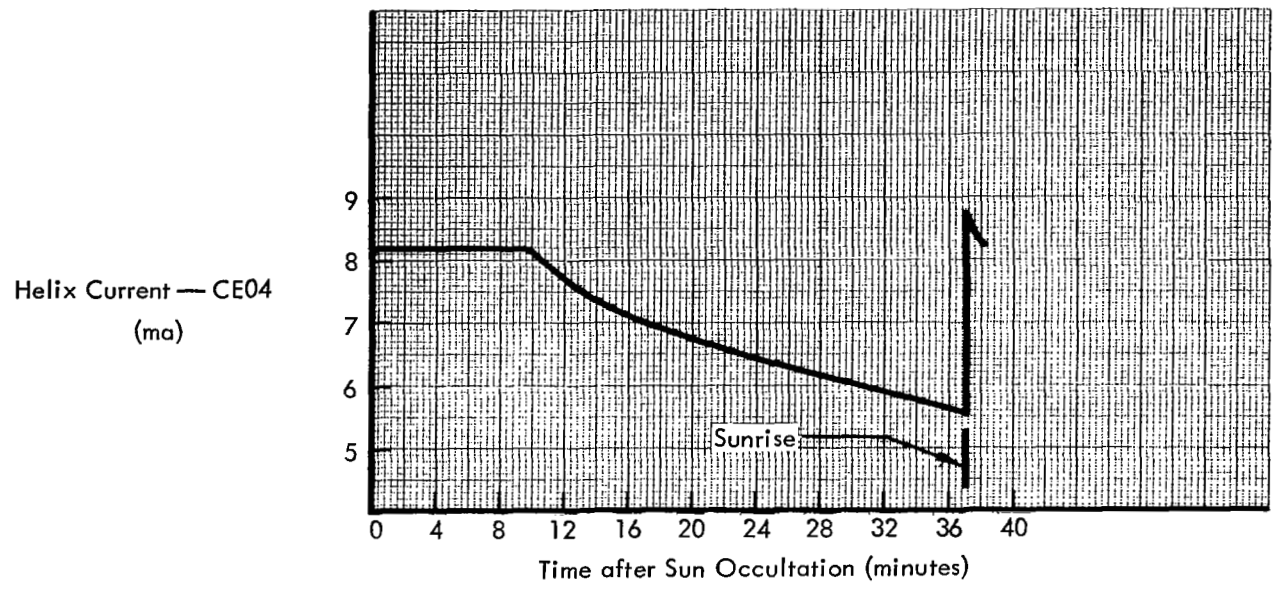

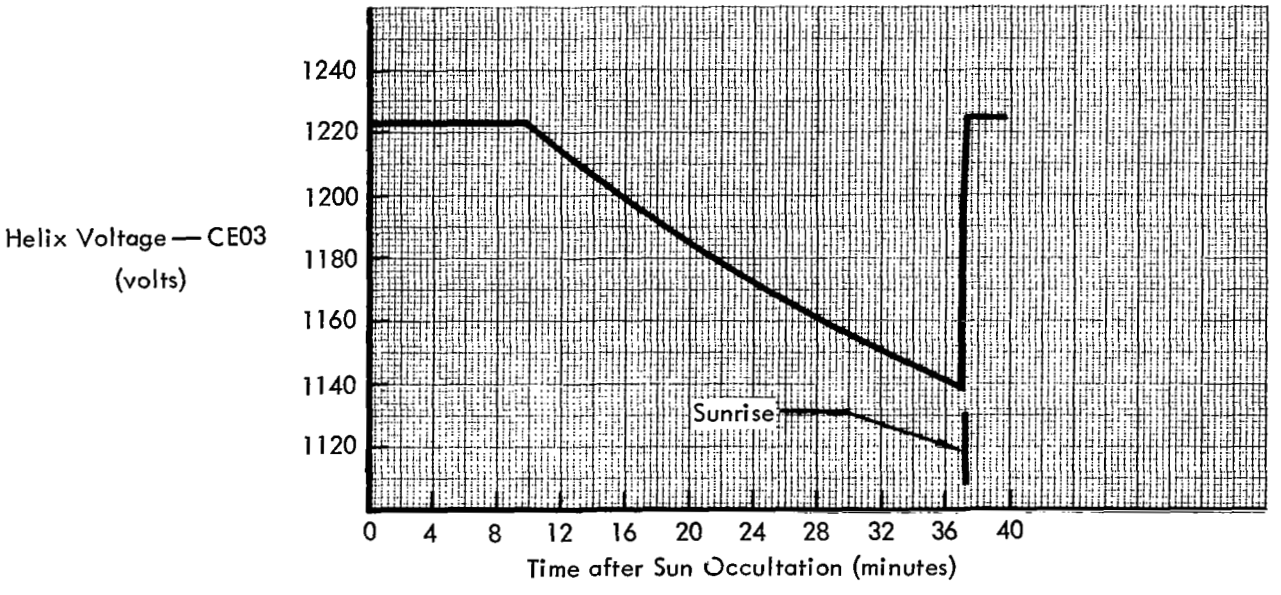

Figure 5-18: TWTA Sunset Performance

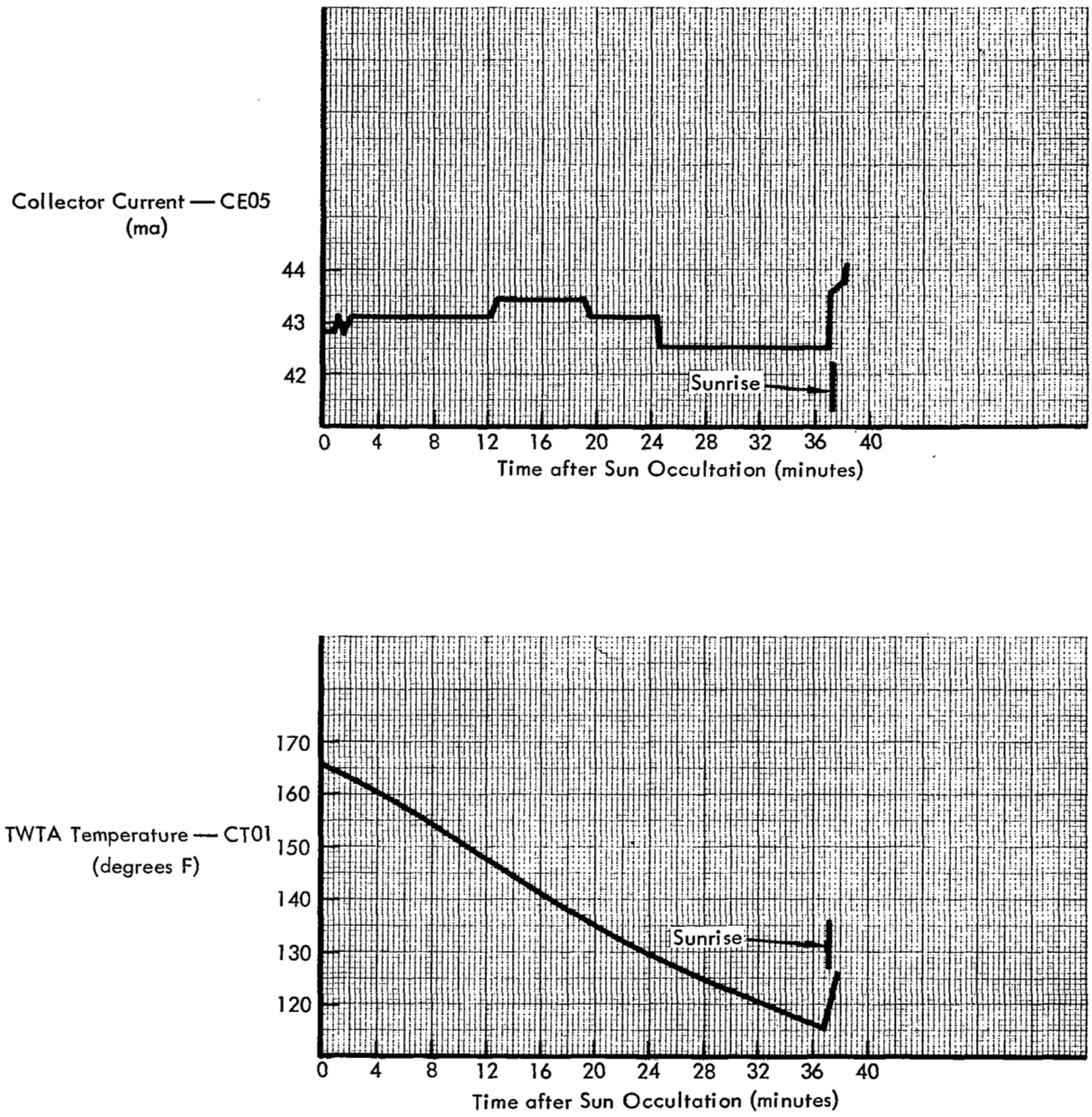

Figure 5-19: TWTA Sunset Performance

The TWTA was cycled on and off 24 times and had an accumulated operating time of 280.5 hours during the extended mission. Figures 5-20 and -21 indicate TWTA turn-on characteristics at the start and completion of the extended mission. TWTA operation throughout the extended mission was nominal as indicated by Figure 5-22 (minimum and maximum telemetry values recorded during each tracking period the TWTA was operating).

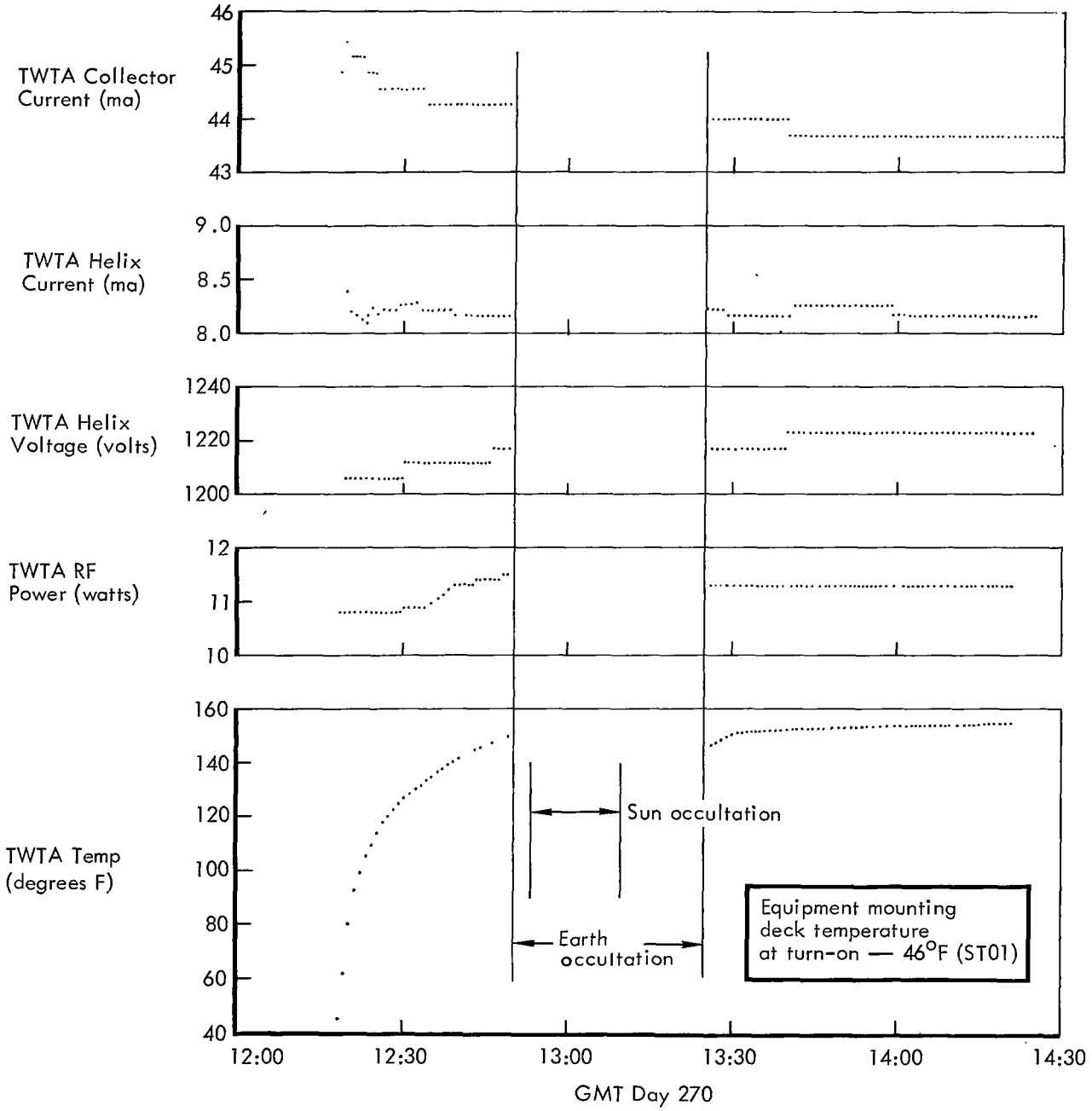

Figure 5-20: Initial TWTA Turn-On

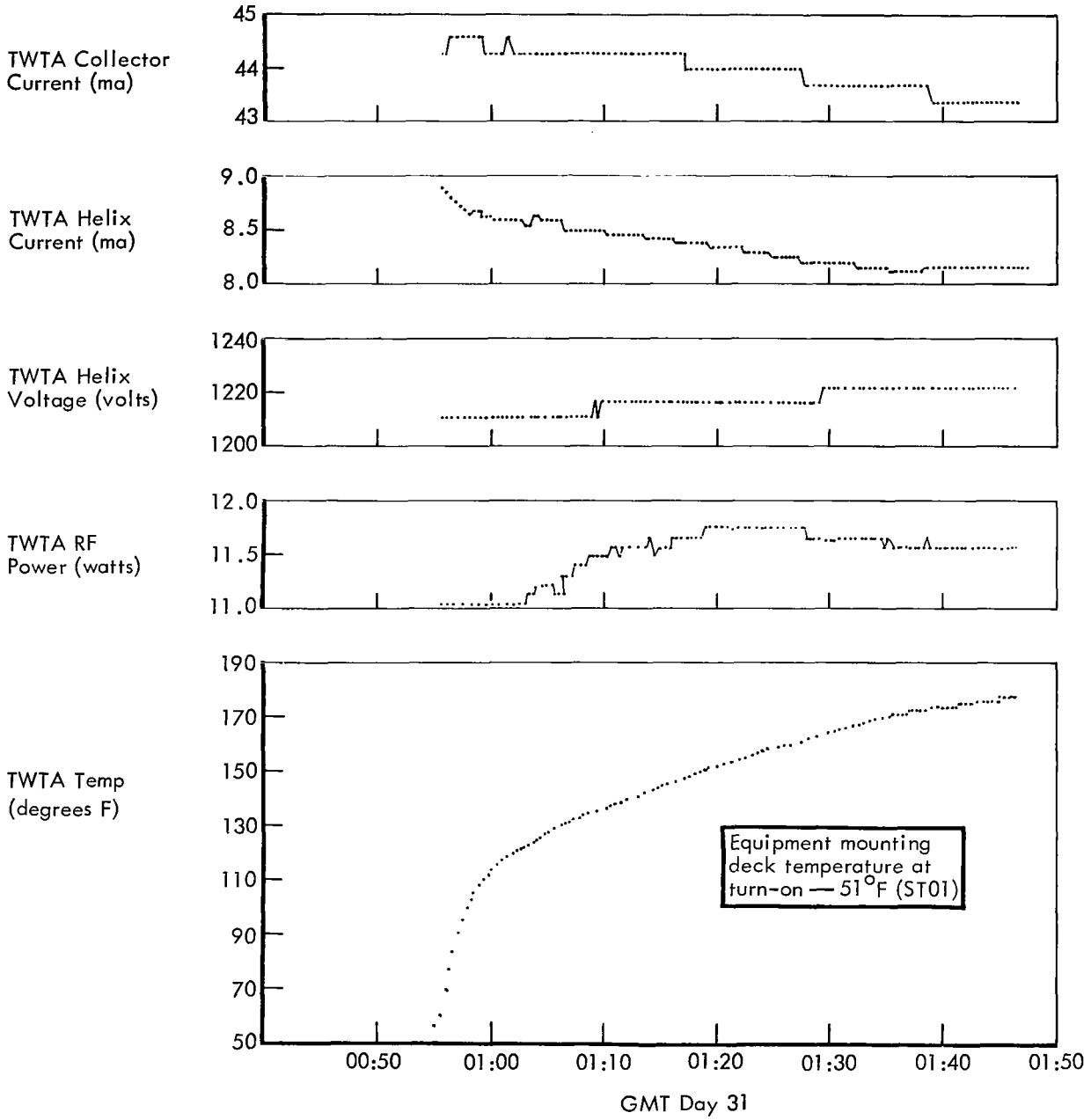

Figure 5-21: Final TWTA Turn-On

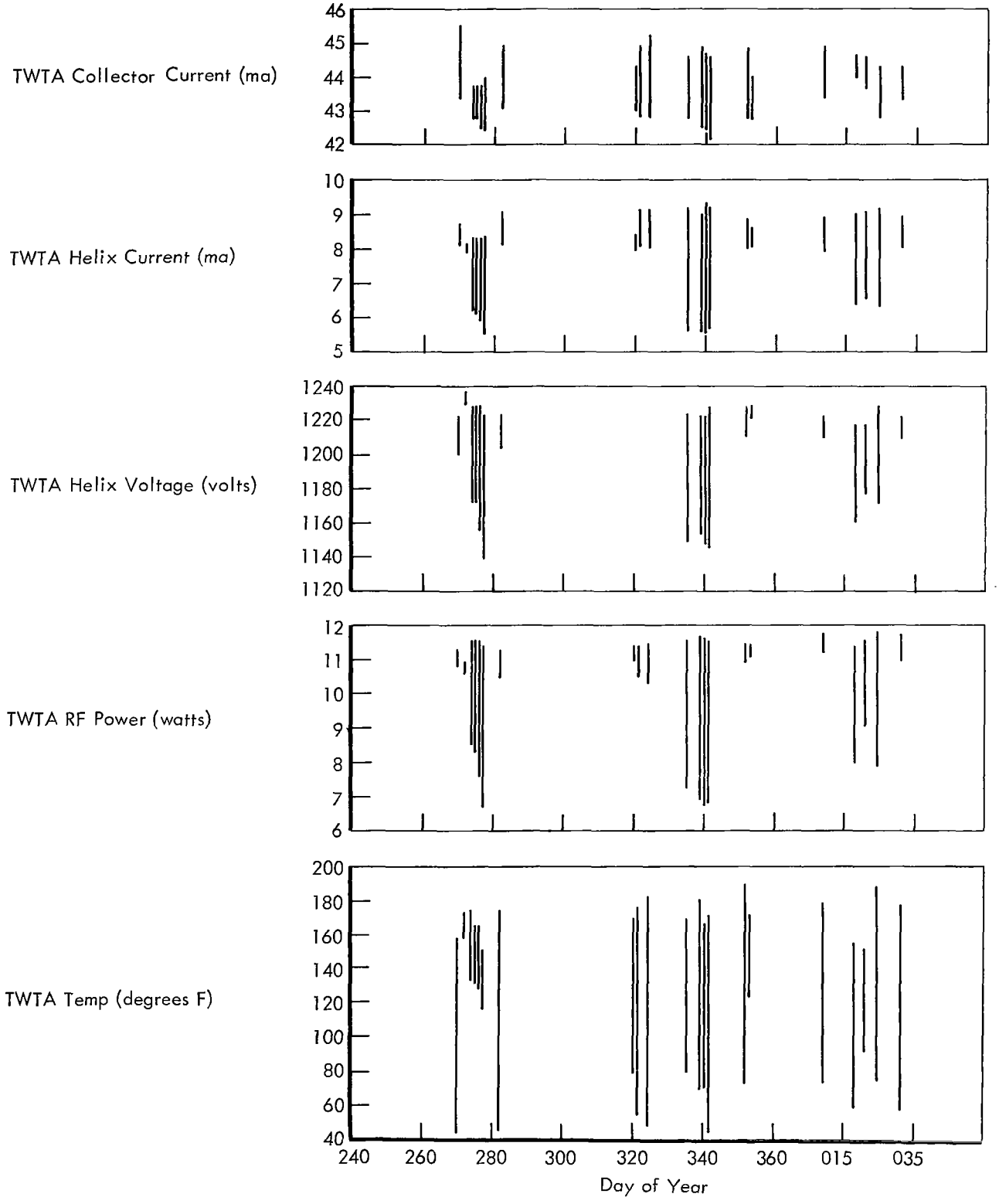

Figure 5-22: TWTA Performance History

5.2.2.3 Command Decoder
The command decoder performed as planned throughout the extended mission; there were no errors in any of the verified words that were executed into the flight programmer.

5.2.2.4 Modulation Selector
Operation of the modulation selector was very satisfactory. All design and operation requirements for the modulation selector were fulfilled.

5.2.2.5 High-Gain Antenna Position Controller
The antenna position controller responded successfully to all rotation commands, and the encoder that telemetered rotation angle functioned correctly. During exposure to outerspace environment, the antenna was rotated a total of 1,183 degrees to the left and 958 degrees to the right. The portion of this total rotation accumulated during the extended mission was 1,147 degrees left and 641 degrees right.

5.2.2.6 Radiation
The RDMS continued to function normally during the Lunar Orbiter V extended mission. Dosimeter 1 (DF04), located near the film cassette, had a sensitivity of 0.25 rad per count with a capacity of 0 to 255 counts. Dosimeter 2 (DF05), located near the camera looper, had a sensitivity of 0.5 rad per count and a similar capacity of 0 to 255 counts. Dosimeter 1 had recorded 1.50 rads at the beginning of the extended mission and increased to 5.75 rads by the end of the mission. Dosimeter 2 had recorded 1.0 rad at the beginning, and increased to 9.0 by the end of the mission. More detailed radiation information is presented in Section 4.1.1.

5.2.2.7 Micrometeoroid Hits
At the initiation of this extended mission, a hit had already been sustained on Detector 6. Five additional hits were later recorded. Additional information regarding the location and time of these hits is presented in Section 4.1.2.

5.2.3 Power Subsystem
The electrical power subsystem is the sole source of all electrical power used by the spacecraft as it performs all phases of its space mission. Radiant solar energy is collected by 2,714 N-on-P solar cells mounted on each of four solar panels and is converted into electrical energy. This energy supplies all spacecraft loads, power subsystem losses, and charging current to the nickel-cadmium battery. The shunt regulator also limits the bus voltage to less than 31 volts by dissipating excess electrical energy in power resistors mounted externally to the spacecraft thermal shield. A charge controller protects the battery from over voltage and over temperature conditions by regulating the charging current. The 12-ampere-hour battery provides electrical power to the spacecraft loads during periods of Sun occultation. Refer to Figure 5-23 for a functional schematic of the subsystem. The boost regulator provides regulated power to the photo subsystem.

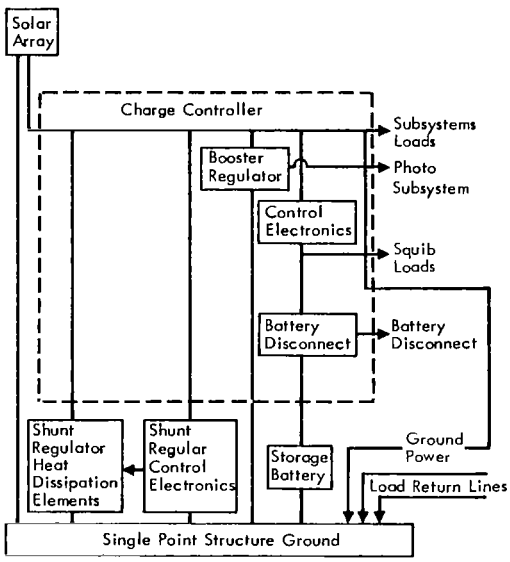

Figure 5-23: Power Subsystem

5.2.3.1 Solar Array Performance
The solar array operated normally throughout the extended mission. Sufficient power was provided to maintain a constant bus voltage of 30.56 volts when in the sunlight. Solar panel degradation was minimal. Total solar panel output power at Lunar Orbiter V launch was 12.49 amperes at 30.56 volts. As the mission progressed, the output power varied with time as a function of solar cell degradation and the changing solar constant (see Table 5-12). The figures are adjusted to an equal solar constant.

Solar panel degradation is in agreement with that measured on other Lunar Orbiter flights.

Table 5-12: Solar Panel Degradation

GMT Day	Measured Data At Solar Constant (amps)	Data Converted To Launch Day Solar Constant (amps)	Apparent Degradation (%)
213 (Launch)	12.49 at 126.1 w/sq ft	12.49	-----
300	12.73 at 131.6 w/sq ft	13.03	2.3
335	12.91 at 133.6 w/sq ft	13.23	2.4
031	12.85 at 133.9 w/sq ft	13.26	3.1

The performance of the solar array during the lunar eclipse on Day 291 (October 18) is shown in Figure 5-24. The bus voltage was maintained at 30.56 volts until 08:48GMT, at which time the array current was 6.19 amperes. The solar array performed as expected.

A special test was conducted on Day 012 to determine solar array performance at high off-Sun angles under dynamic and static maneuver conditions. The array current was monitored while the spacecraft was being pitched in a positive direction by 95 degrees, and at the three static angles of plus 70, 77 and 85 degrees. The results are shown in Section 5.3, Special Flight Tests.

5.2.3.2 Battery Performance

Battery performance was as predicted during the extended mission. The highest battery temperature recorded was 125.8°F on Day 031 at 02:53. This high temperature is due in part to changes in the thermal properties of the spacecraft that occurred after Day 002. The battery at 114°F satisfactorily sustained the spacecraft load of 4 amperes during a 27-minute solar array occultation starting at 05:54 of the same day, thereby confirming the adequacy of the design to operate at elevated temperatures.

Several extensive battery discharges occurred during the extended mission. To ascertain the capability of the battery to support the October 18, 1967 (Day 291) lunar eclipse, a planned discharge occurred on Day 270. Another planned discharge occurred on Day 012 during the solar array performance test. Both of these discharges are covered in Section 5.3, Special Flight Tests. An extensive natural discharge occurred during the lunar eclipse on October 18. The power subsystem successfully supported subsystem electrical load demands throughout the eclipse. The minimum battery voltage throughout this period was 22.24 volts and the minimum bus voltage was 21.6 volts. Figure 5-25 shows the performance of the battery. The bus voltage was maintained at 30.56 volts up until 08:48 GMT, at which time the array current was 6.19 amperes. This voltage would have been maintained for another 15 minutes but for the shunt regulator, which at that time had a fault current of 1.1 amperes at 30.56 volts.

The normal nighttime discharges were not seen, since the spacecraft was occulted from the Earth at these times, but it is estimated that the nighttime discharge immediately prior to the eclipse was 2.30 ampere-hours. It appears that 1.15 ampere-hours were returned to the battery during the initial period of the eclipse for a net loss of 1.15 ampere-hours. The battery was in the discharge mode for 217 minutes during the eclipse; thus, it is estimated 10.65 ampere-hours were taken out of the battery. The total discharge

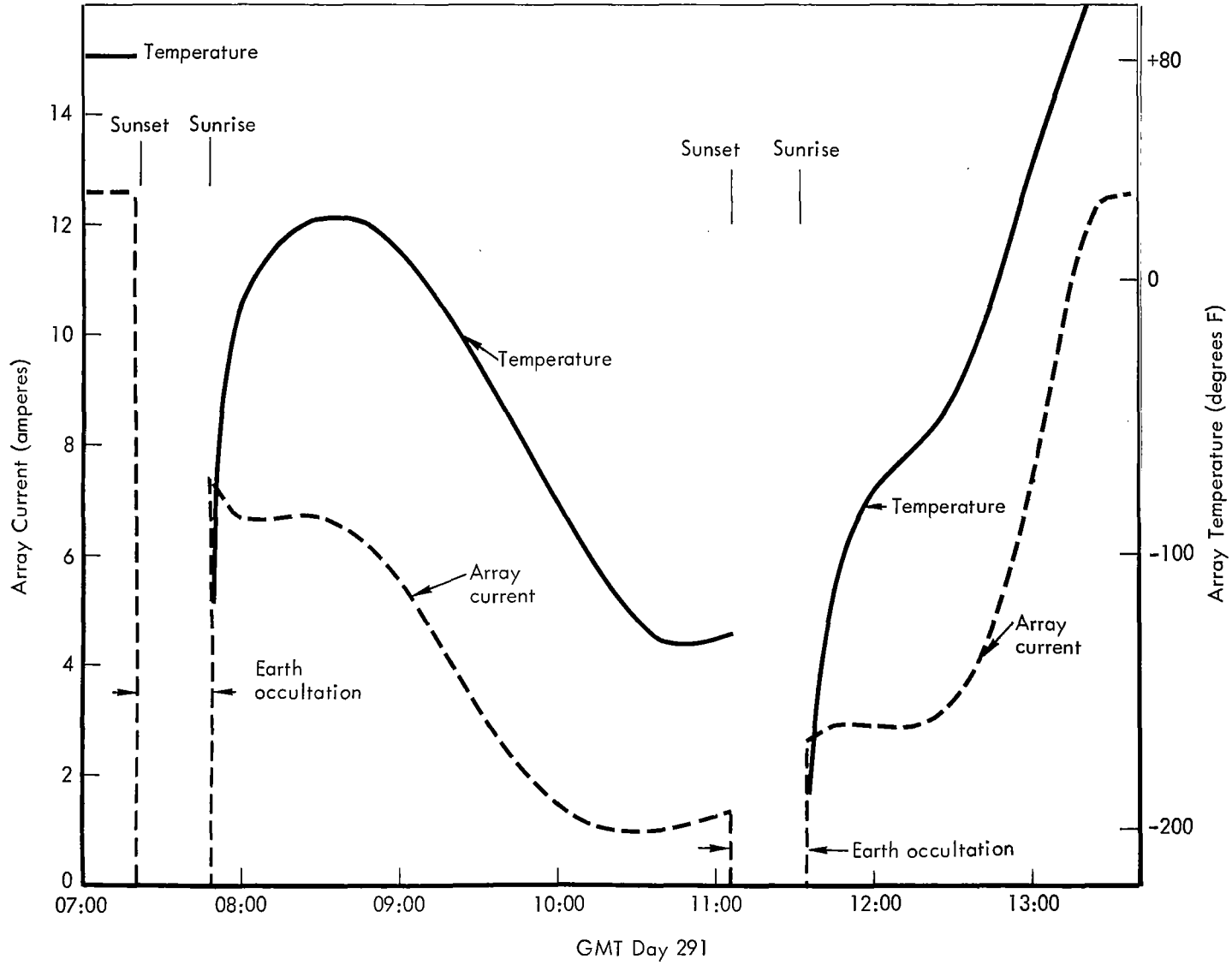

Figure 5-24: Solar Array Performance – Lunar Eclipse of Day 291

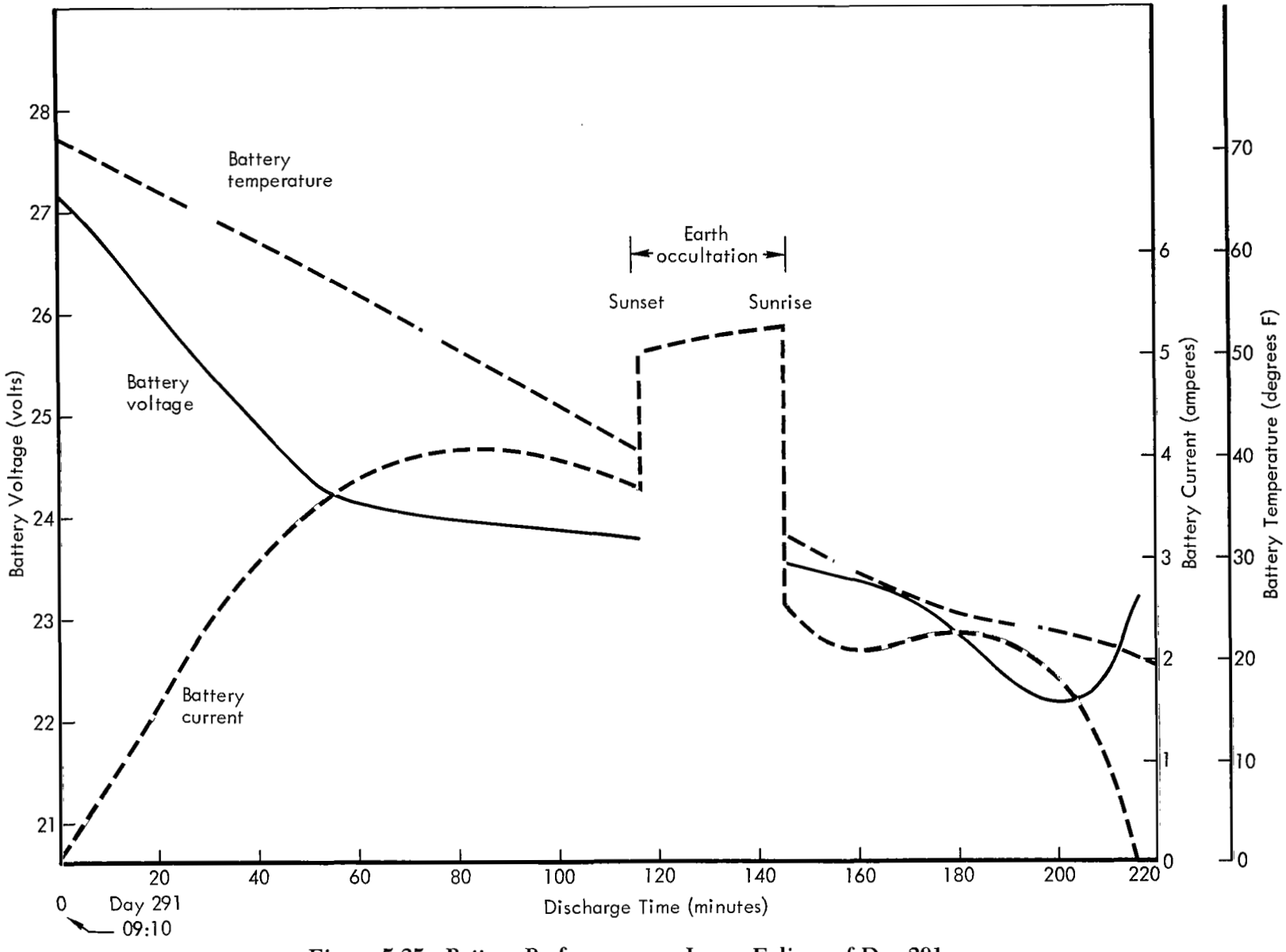

Figure 5-25: Battery Performance – Lunar Eclipse of Day 291

was therefore 11.8 ampere-hours for a 98.3% depth of discharge based on a nominal 12-ampere-hour capacity. This depth of discharge was almost equalled on the subsequent nighttime discharge; however, the battery voltage at 3 minutes after sunrise was 25.28 volts at 36.7°F, with a charge rate of 1.35 amperes.

5.2.3.3 Shunt Regulator Performance

Shunt regulator performance was satisfactory throughout the extended mission except for a short period of time when excessive nighttime current was being drawn by the unit. This anomaly started some time between GMT Day 275, 20:29 and Day 276, 12:10 and ceased some time between Day 291, 12:55 and Day 300, 16:41. Although there were intervening tracking periods, some of these did not include solar occultation periods. Therefore, it is not possible to cite exactly when the fault cleared itself. The maximum value observed was 0.70 amperes, whereas the typical value was about 0.50 amperes. Figure 5-26 shows the shunt regulator leakage current during the October 18 lunar eclipse period. The current was proportional to the spacecraft bus voltage, indicating an IR drop. The quality of the power supplied to the spacecraft was not affected. Insufficient information was available from telemetry data to develop an explanation for this phenomenon.

5.2.3.4 Charge Controller Performance

The charge controller regulated the battery charging current to a maximum of 1.350 amperes

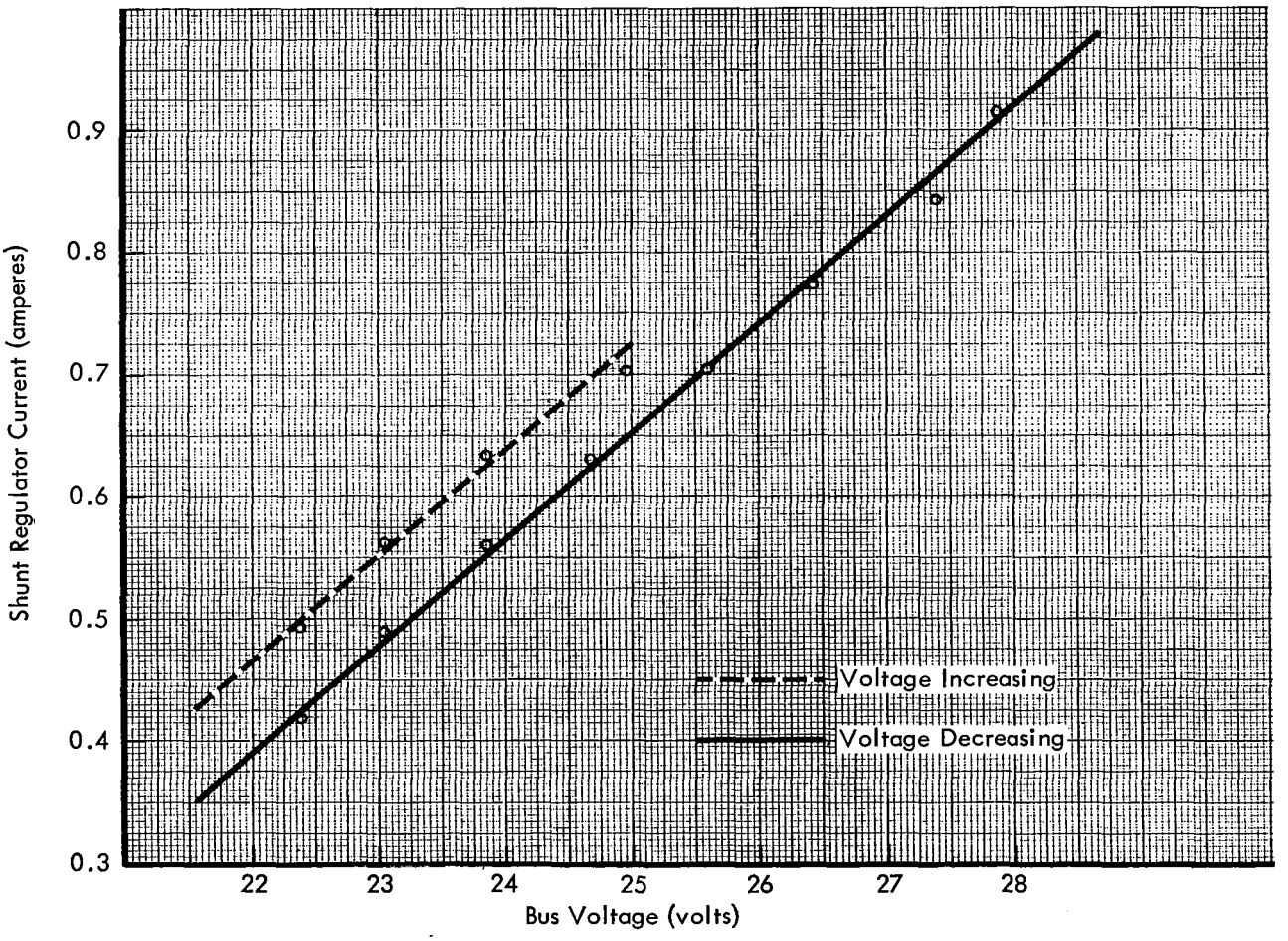

Figure 5-26: Shunt Regulator Leakage — Day 291

throughout the extended mission and performed as expected. This value of charging current, which was optimized for the photographic mission, became the limiting factor in determining extended-mission lifetime because of the light-to-dark ratio shown in Figure 5-27.

The minimum light-to-dark ratio (L/D min) indicates the ratio of the daylight time to the night-time at which the power provided by the battery is equal to the power restored to the battery. If the L/D drops below this "L/D min," energy balance will not be maintained and the battery will reach a deeper depth of discharge each orbit.

Assuming Q_{AN} (battery energy content) is unchanged at any point in the daytime-night-time cycle, the following equation is developed:

$$\text{L/D min} = \frac{(EE07)_n + 0.28}{E\,(EE04)}$$

where: L = Daylight time (hours)

D = Nighttime (hours)

$(EE07)_n$ = Nighttime load current (amperes)

0.28 amperes = Power S/S shunt loss

E = ampere-hour charge-discharge efficiency

EE04 = Battery charge current (amperes) = 1.35 max

from empirical data:

$$(EE07)_n = f(t)$$

$$\cong 3.68 + 0.013t \text{ for } t \leq 100 \text{ minutes}$$

where: t = nighttime period in minutes

Assuming E = 0.85

$$\text{L/D min} = 3.43 + 0.0113t$$

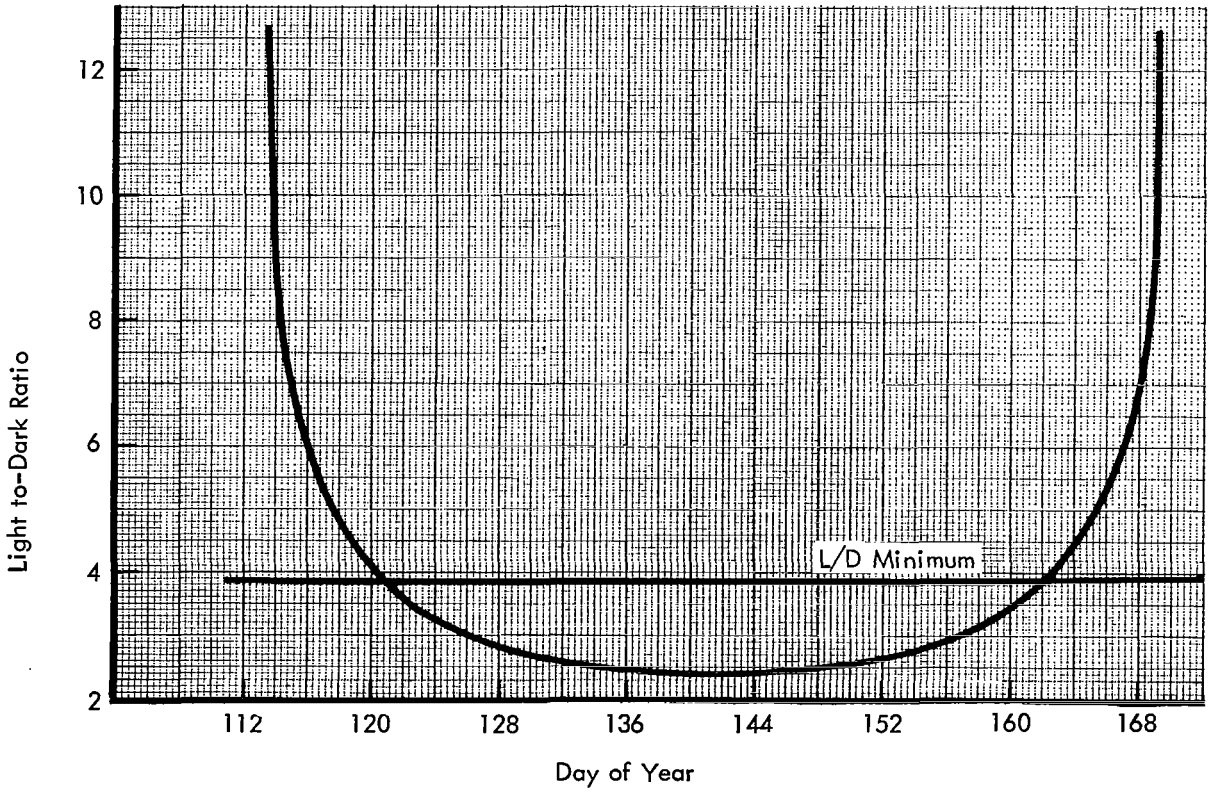

Figure 5-27: Predicted Light-to-Dark Ratio

If the actual orbit period of 225 minutes is used, the L/D min may be determined by substituting for t,

$$t = \frac{225}{1+\frac{L}{D}}$$

and by setting L/D min = L/D

the resulting L/D min = 3.94. This line is shown in Figure 5-27 and the curve predicts that this value would have been attained on Day 121. The propellant remaining at that time (Day 121) was inadequate to alter the orbital geometry and prevent the light-to-dark ratio from decreasing below this allowable minimum. The flight plan (reference paragraph 3.0) was then to impact the spacecraft at the latest opportunity and before the L/D min value was attained.

5.2.3.5 Power Subsystem Performance

A comparison of power subsystem data from the first day of the extended mission and the last available data before sunset on Day 031 is shown in Table 5-13.

Table 5-13: Power Subsystem Data

	GMT	
	242:02:55:20	031:07:51:01
Pitch off-Sun angle	54.4 degrees	54.0 degrees
Bus voltage	30.56 volts	30.56 volts
Solar array current	7.03 amps	7.46 amps
Load current	3.68 amps	3.68 amps
Shunt regulator current	1.93 amps	2.33 amps
Battery charge current	1.350 amps	1.350 amps
Battery voltage	28.64 volts	27.68 volts
Battery temperature	88.5 degrees F	91.6 degrees F
Average solar panel temperature	82.4 degrees F	38.1 degrees F
Signal conditioner supply	20.00 volts	20.00 volts

The data reveal that the power subsystem was operating normally when the spacecraft was last monitored.

5.2.4 Photo Subsystem

The photo subsystem is housed in a pressurized, thermally controlled container, and includes camera, lens, film, film handling equipment, film processor, readout equipment, and environmental controls (see Figure 5-28). The subsystem is designed to expose, develop, and read out images for transmission to Earth via the communications system.

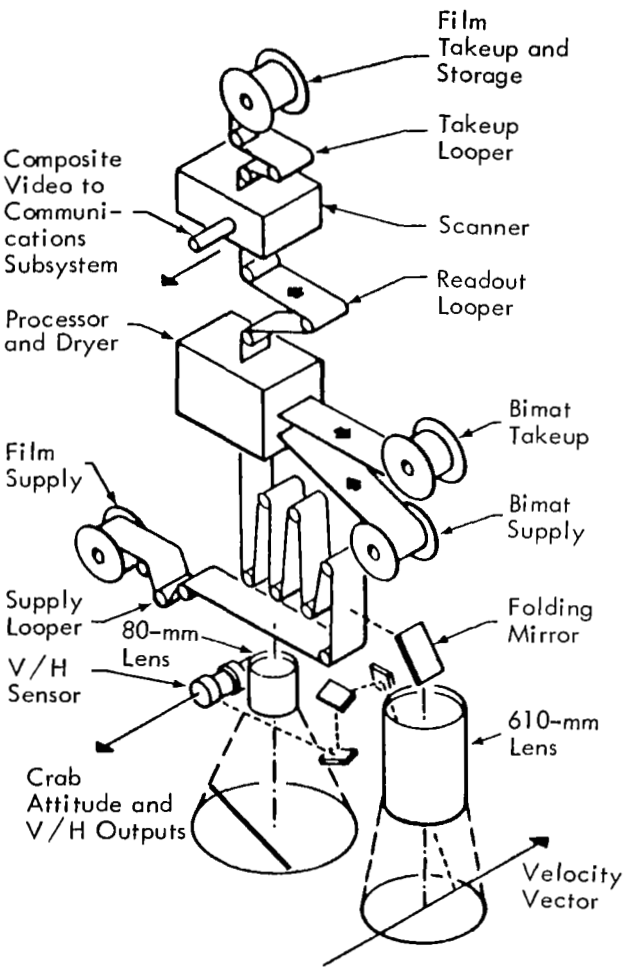

Figure 5-28: Photo Subsystem

At the end of the photographic mission, while rewinding the film, data indicated that the film had parted. The photo subsystem was placed in a safe status and remained in that condition through Day 026. There was no command activity pertaining to the subsystem during this period. Table 5-14 shows the pertinent photo subsystem temperatures and pressures during the extended mission.

Upon acquisition on Day 029, there was evidence of some logic change in that shutter operations had changed from 17 to 2 counts. No other photo subsystem logic changes were noted. (Table 5-15 shows this initial condition and subsequent activities.) This information, coupled with the anomalous state of the spacecraft, and a not-closed condition of the camera thermal door, led to the conclusion that there could have been a power interruption aboard the spacecraft. To investigate whether the power to the photo subsystem had been interrupted, two shutter-advance commands were sent to the spacecraft. A camera shutter setting of 2 indi-

Table 5-14: Photo Subsystem Temperature and Pressure History

GMT Day	Internal Pressure (psia)	Nitrogen Bottle Pressure (psi)	Readout Thermal Fin Temperature (°F)	Lower Environment Temperature (°F)	Upper Environment Temperature (°F)
242	1.39	2,002	36.5	34.7	39.3
250	1.44	2,010	46.8	45.8	47.9
254	1.39	2,092	53.9	53.6	54.7
258	1.44	2,055	47.0	48.0	50.0
265	1.28	2,025	43.3	44.1	46.9
276	1.39	2,152	53.1	58.6	63.0
284	1.16	2,062	44.3	43.6	45.5
296	1.16	2,092	55.5	54.4	53.9
306	1.16	2,122	49.3	55.5	58.7
315	1.16	2,077	46.4	46.5	46.9
327	1.16	2,092	48.3	48.6	50.8
335	1.09	2,092	63.0	56.1	55.4
345	1.16	2,137	48.9	51.5	55.6
353	1.09	2,137	60.7	56.3	61.4
364	1.09	2,107	57.3	53.6	56.1
008	1.16	2,092	70.6	64.3	64.7
018	1.16	2,152	68.3	76.8	77.8
026	1.32	2,197	80.8	80.5	81.1
029	1.16	1,972	56.6	55.5	57.4
031	1.24	2,032	60.6	65.9	66.9

Table 5-15: Summary of Photo Subsystem Responses

Measurement	1	2	3	4	5	6
PB01 takeup contents (feet)	29.3	29.3	29.3	29.3	38.1	40.6
PB02 camera looper (inches)	232.2	232.2	232.2	232.2	106.2	220.6
PB03 readout looper (inches)	54.29	54.29	54.29	54.29	54.29	54.29
PB04 shutter operations (counts)	17	2	2	2	1	23
PB05 platen operations (counts)	16	16	16	16	16	16
PC01 V/H on/off (state)	1	1	1	1	1	1
PC02 camera on/off (state)	1	1	1	1	0,1	0,1,0
PC03 camera program setting (counts)	3	3	3	3	0	5,0
PC04 camera shutter setting (counts)	2	2	1,2	2	2	2
PC07 Bimat clear (state)	0	0	0	0	0	0
PC08 Bimat takeup (state)	0	0	0	0	0	0
PC09 cut Bimat (state)	0	0	0	0	1	1
PC10 readout electronics (state)	1	1	1	1	1	1
PC11 readout drive on/off (state)	1	1	1	1	1	1
PC12 Line scan tube focus or gain (state)	1	1	1	1	1	1
PC15 shutter setting or camera rate (state)	0	0	1,0	0	1	0,1
PC16 solar eclipse on/off (state)	1	1	1	1	0,1,0	1,0,1,0
PC18 camera thermal door open (state)	0	0	0	0	0	0
PC19 camera thermal door closed (state)	1	0	0	1	1	1
PC20 heaters enabled (state)	0	0	0	0	0	0
PE01 +10-volt output (volts)	9.90	9.90	9.90	9.90	9.90	9.90
PE03 LST cathode current (μ amps)	0	0	0	0	0	0
PE04 video output voltage (volts)	0	0	0	0	0	0
PE05 high voltage (K volts)	0	0	0	0	0	0
PE06 photo multiplier voltage (volts)	0	0	0	0	0	0

Notes:

1. Condition until spacecraft anomaly (Day 028)
2. Condition at acquisition (Day 029)
3. Change shutter speed twice to verify preset pulse signal occurrence (Day 029, 21:33)
4. Closed camera thermal door (Day 029, 21:39)
5. Reset camera logic to final readout standby (Day 029, 22:41)
6. Condition prior to crash after camera storage looper refill sequence (Day 030, 21:30)

cates a shutter speed of 1/25 second, whereas a 1 indicates a 1/50 and a 3 indicates a 1/100 second. The shutter speed setting cycles in the following pattern: 1/25, 1/50, 1/100, 1/50, and back to 1/25 second as commanded by each "change shutter speed" command (or, in terms of telemetry: 2, 1, 3, 1, and back to 2). If the power to the photo subsystem has been interrupted, upon the return of power a preset pulse signal is generated, setting, among other things, the shutter speed memory to 1/100 second. However, the telemetry indication will remain as it was prior to the preset pulse signal. The first shutter setting advance command resulted in a telemetry indication of 1. However, this is ambiguous since it is not known whether the 1/50-second shutter speed setting is the one before or after the 1/25-second setting. The second command resulted in a telemetry indication of 2. This pattern shows that the preset pulse signal had been initiated in the photo subsystem.

Prior to Day 029, after Bimat-cut, the photo subsystem was in a standby mode with solar eclipse on. If a preset pulse signal is received by the command control programmer while the photo subsystem is in this mode, it is required to reset the logic to a known condition by an appropriate command sequence. This was accomplished on Day 029 at 22:41 GMT. As a part of the logic reset command sequence, the camera looper decreased from 232.2 to 106.2 inches. Since it was desirable to have minimum tension on the film in the camera looper, a stored-program sequence was employed to change the camera logic and take eight fast frames and two single frames. This action increased the looper contents to 220.6 inches, which placed near-minimum tension on the film. It was noted that the takeup contents increased during the logic reset and camera looper refill sequences. This is due to the film separation which allows the takeup reel to rotate during these sequences.

No additional photo subsystem activity was attempted during the remainder of the extended mission.

5.2.5 Structures and Mechanisms Subsystem

The structures and mechanisms subsystem consists of the support structure, thermal control coatings, thermal barrier, engine deck heat shield, solar panel and antenna deployment mechanisms, camera thermal door, rocket engine gimbal, bipropellant tank heaters, and the interconnecting electrical wiring.

With the exception of the camera thermal door (CTD) and the rocket engine gimbal, this subsystem is in a passive state during the extended mission. Only the EMD thermal coating and thermal coating paint experiment are discussed, since the remainder of the subsystem elements performed as anticipated.

5.2.5.1 EMD Thermal Control Coating

The Mission V EMD thermal control coating was the same as that of Mission IV (20% OSR mirrors by area on 2 mils of S13G over 8 mils of B1056), except that a concentration of 30% OSR mirrors was used in the areas adjacent to the photo subsystem and TWTA. This modification was required to counteract the increased infrared radiation that would be absorbed from the lunar surface during the Mission V low-orbit mission.

The rate of temperature rise due to EMD thermal coating degradation was as expected during the extended-mission period. The spacecraft was oriented approximately 50% off-Sun throughout the extended-mission period for thermal control. Thermal and off-Sun attitude histories for the spacecraft are shown in Figures 5-29 to -31 and indicate the effect of continued EMD thermal coating degradation over the extended-mission period.

5.2.5.2 Thermal Control Coating Coupons

The Mission V spacecraft was instrumented with a paint coupon assembly to provide flight data on selected thermal control coatings by measuring the temperature of the individual coupons. The following paint coupons were used.

Paint Coupon	Paint Description
• S13G over B1056 (ST09B)	S13G is zinc oxide with a potassium-silicate treatment, RTV-602 binder, and SRC05 catalyst. B1056 is zinc oxide with RTV-602 binder and SRC05 catalyst.
• Hughes Organic White (ST15)	Calcined china clay dispersed in GE RTV-602 silicone resin.
• Silicone on aluminum foil (ST16)	One-quarter-mil 1145-0 aluminum foil with 3.8 mils RTV-602 silicone catalyzed with 0.15% TMB.
• Z93 (ST17)	SP-500 zinc oxide dispersed in Sylvania PS-7 potassium silicate.

Performance of the thermal control paints is reported in 5.3.2.

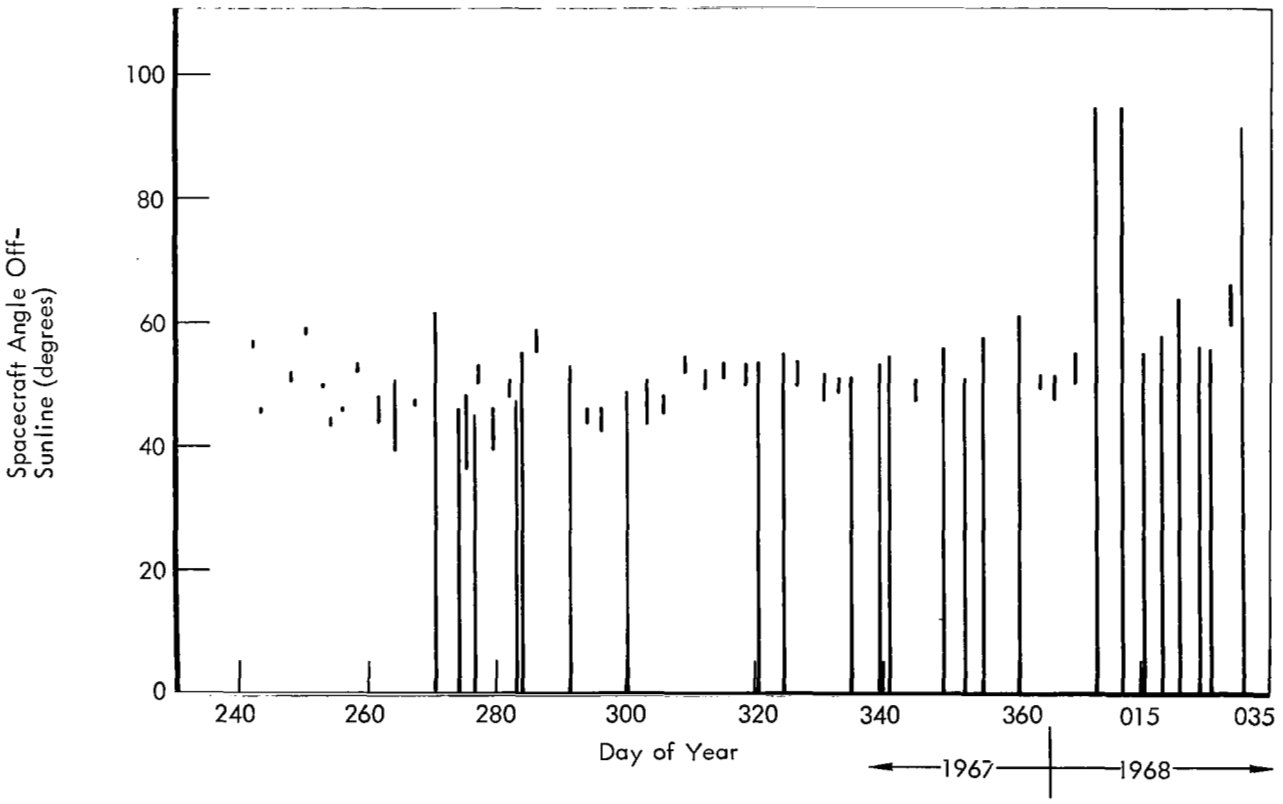

Figure 5-29: Spacecraft Off-Sunline Angle History

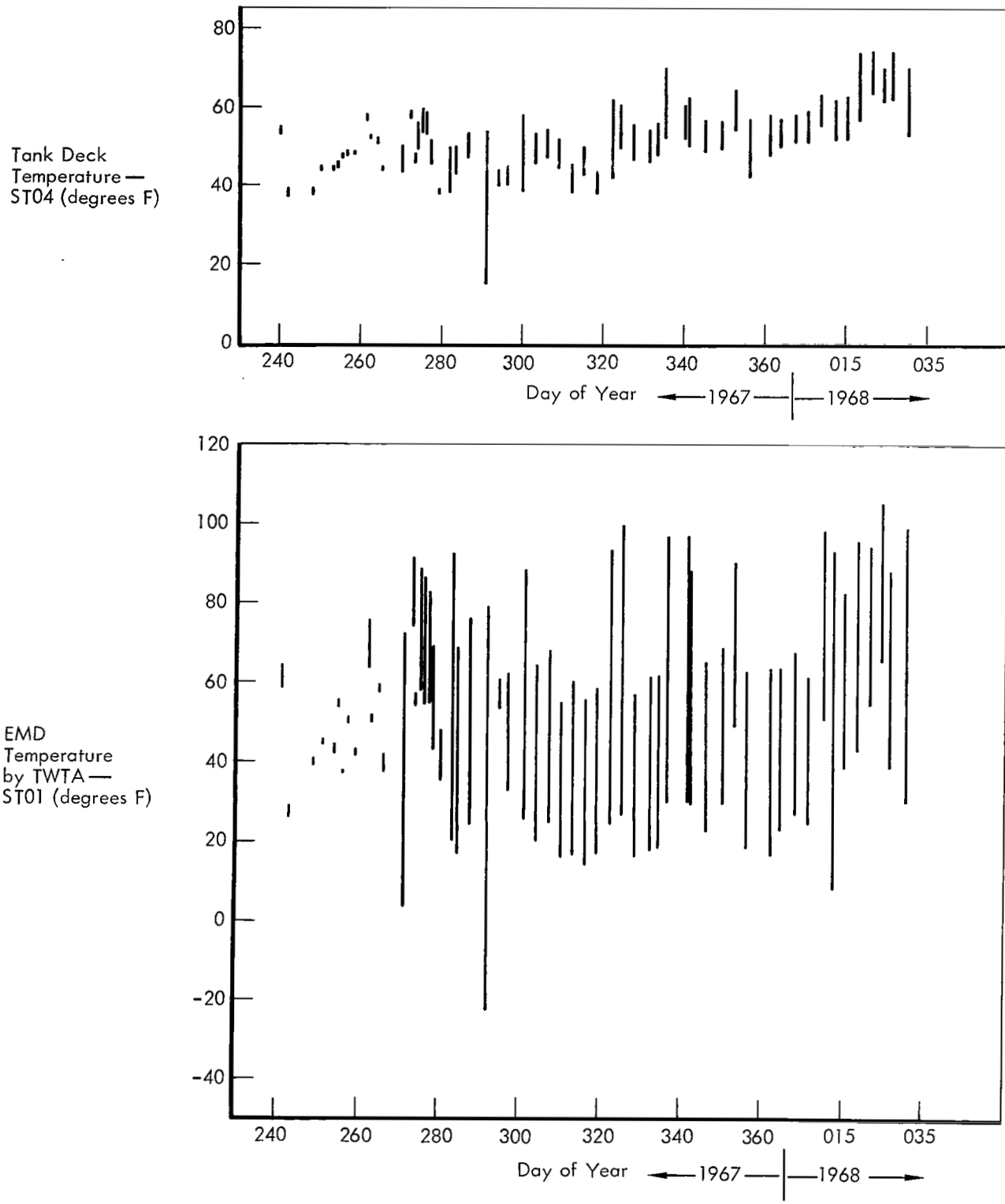

Figure 5-30: EMD Temperature History

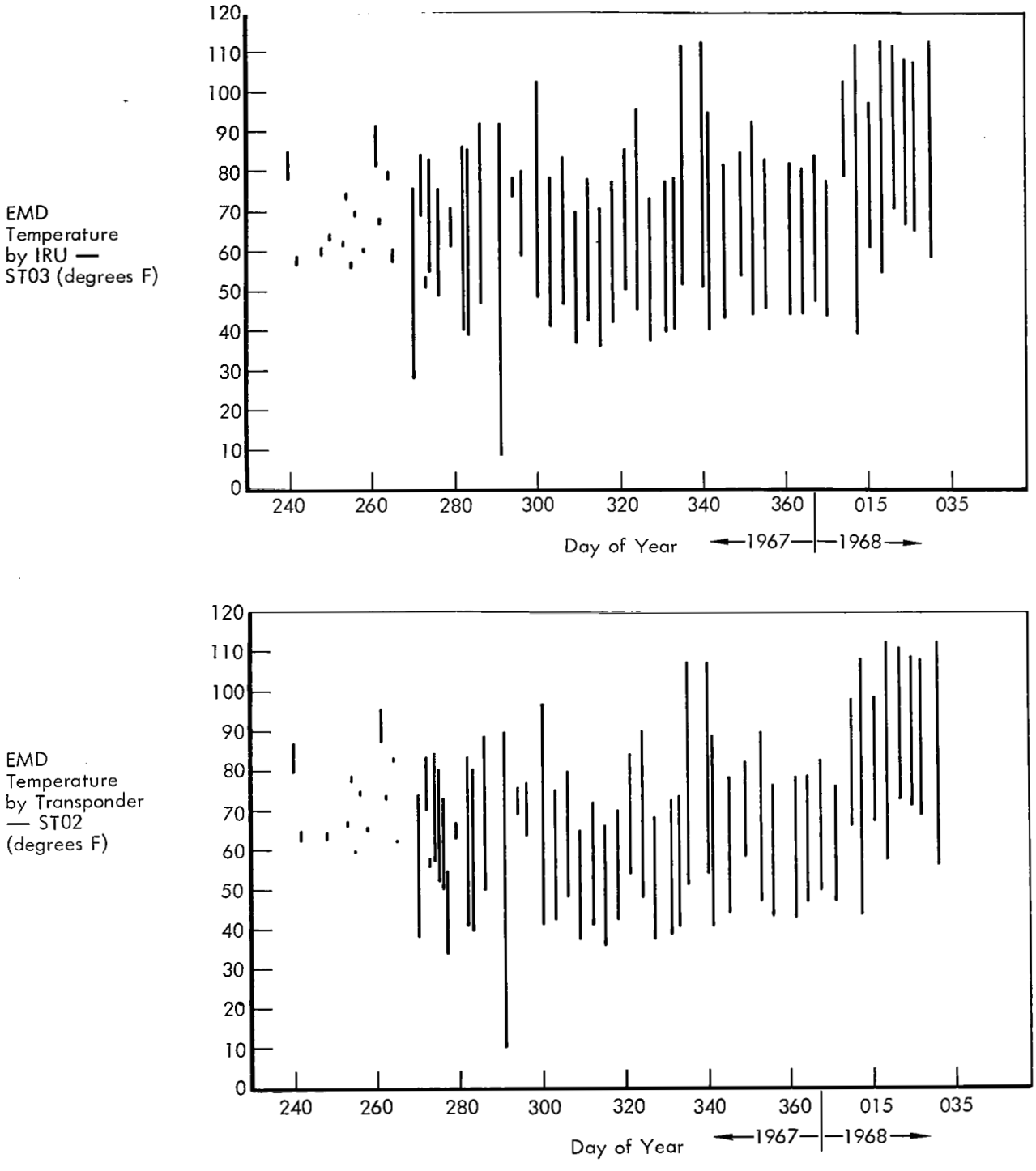

Figure 5-31: EMD Temperature History

5.2.6 Velocity and Reaction Control Subsystems

The velocity control subsystem consists of the propellant pressurization equipment, propellant storage tanks and feed system, bipropellant rocket engine, and thrust vector control actuators. The reaction control subsystem (Figure 5-32) includes the nitrogen storage tank, which is common to the velocity control subsystem, thrusters and interconnecting plumbing, filter, and regulator, and provides the impulsive force to maintain attitude control and perform attitude maneuvers about the pitch, roll, and yaw axes of the spacecraft.

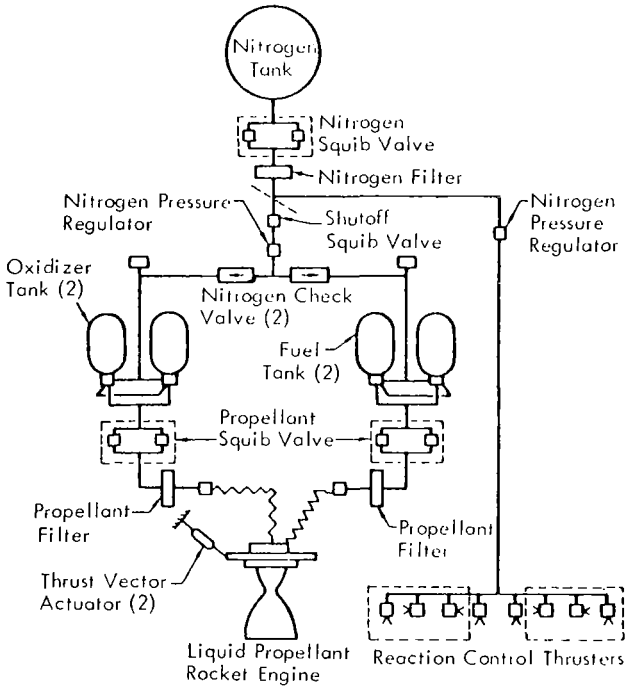

Figure 5-32: Velocity and Reaction Control Subsystem

5.2.6.1 Reaction Control Subsystem Performance

The reaction control subsystem performed satisfactorily throughout the extended mission. The subsystem maintained spacecraft attitude control in wide (2-degree) deadband while in inertial hold in all three axes during the major part of the extended mission. Maneuvers were generally limited to those required for updating of the spacecraft attitude for thermal control and for special tests. To minimize nitrogen consumption, most maneuvers were performed with the attitude control subsystem operating in wide deadband. The time histories of nitrogen tank pressure and temperature are shown in Figure 5-33. Table 5-16 shows the events that caused higher-than-cruise-mode usage.

Subsystem performance was evaluated on the basis of nitrogen gas consumption for attitude control and thruster performance. It was concluded that reaction control subsystem performance was nominal throughout the extended mission; there was no evidence of degradation in performance from that of the photo mission while the spacecraft was being monitored.

5.2.6.2 Velocity Control Subsystem Performance

Performance of the velocity control subsystem was analyzed on the basis of telemetered propellant tank pressures, actuator position, and incremental velocity change. The results compared favorably with the results of independently obtained Doppler tracking data analysis. The velocity control system was operated two times during the extended mission with no evidence of degradation.

As the nitrogen shutoff squib, which isolates the propellant tanks from the nitrogen gas supply, had been actuated prior to the extended mission, the two propulsive maneuvers performed were accomplished in "blowdown" mode of operation. Figure 5-34 shows the history of the propellant tank ullage pressures and tank deck temperature throughout the extended mission. The increase in tank pressures following the first maneuver is attributed to leakage across the shutoff squib valve. The rate of pressure rise indicated a leakage rate of approximately 530 standard cubic centimeters per hour. Although this value is larger than those observed on previous extended missions, the rate was not detrimental to the mission. It is also significant to note that the propellant temperature recorded a minimum value of 15 degrees during the lunar eclipse. This value is below the Aerozine 50 freezing temperature of 18 degrees (the Hydrazine component of the blend freezes at 35 degrees). The low temperature that should cause the blend to separate had no apparent effect on subsystem performance during the final impact burn.

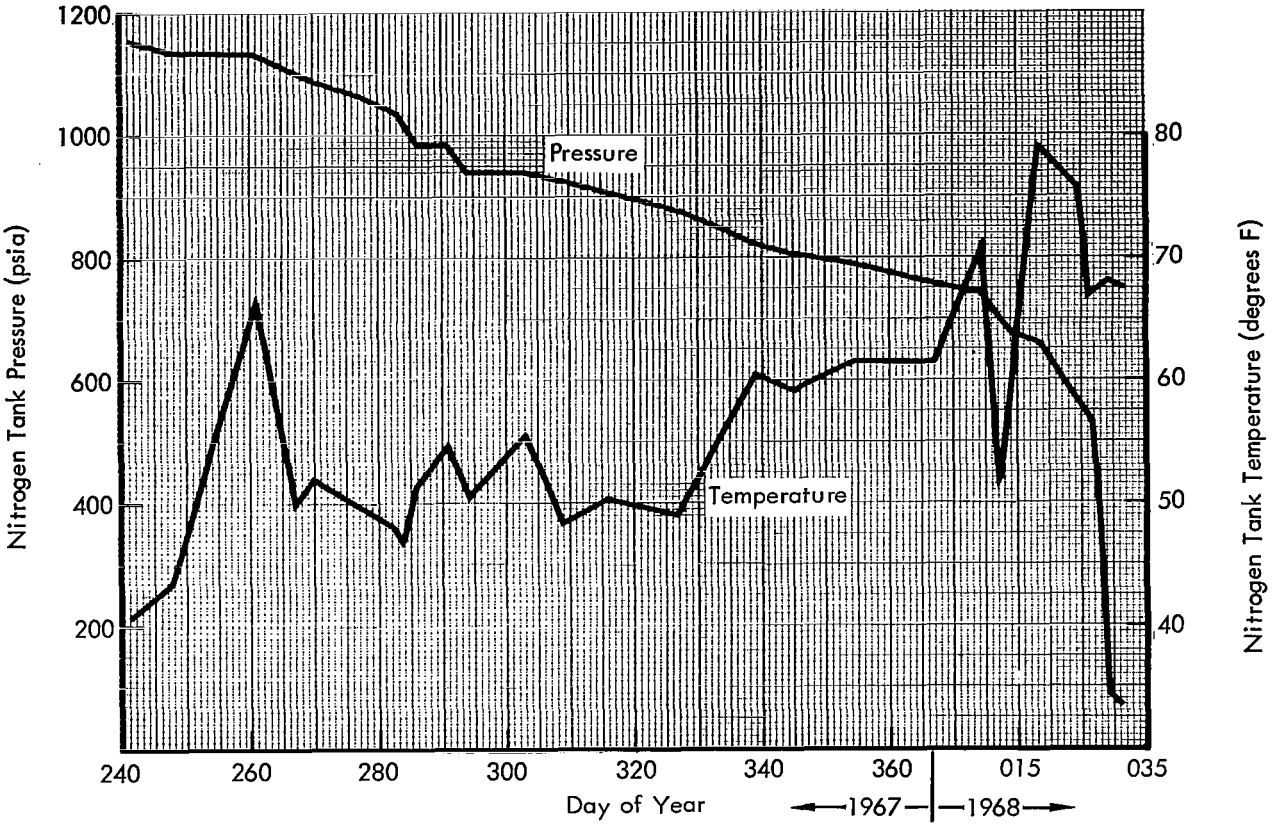

Figure 5-33: Nitrogen Tank History

Table 5-16: Major Events Using Nitrogen Gas

GMT Day	Event
270	Battery discharge test and voice relay experiment
283	Lunar eclipse phasing maneuver
335	Bistatic radar experiment
008	Maneuver accuracy test
012	Solar array and battery discharge tests
018	Visual observation experiment
021	Visual observation experiment
024	Bistatic radar experiment
026-029	Spacecraft anomaly
031	Impact maneuver

The details of the velocity maneuvers are discussed below.

Phasing Maneuver for the October 1967 Eclipse— On Day 283 at 19:37:06 GMT, a 67.5 m/sec velocity maneuver was performed to phase the spacecraft for the Day 291 lunar eclipse.

The operation was satisfactory and the programmed velocity impulse was achieved with an engine operating time of 40.8 seconds. The average thrust level during the burn was 101.2 pounds as computed from spacecraft weight and acceleration data. The thrust vector control actuators cycled from -0.177 to -0.039 degrees in pitch and from 0.359 to 0.496 degrees yaw, which indicates stable performance. The maneuver was confirmed by tracking data to be nominal. During soak-back, the engine valves reached a maximum temperature of 100.8

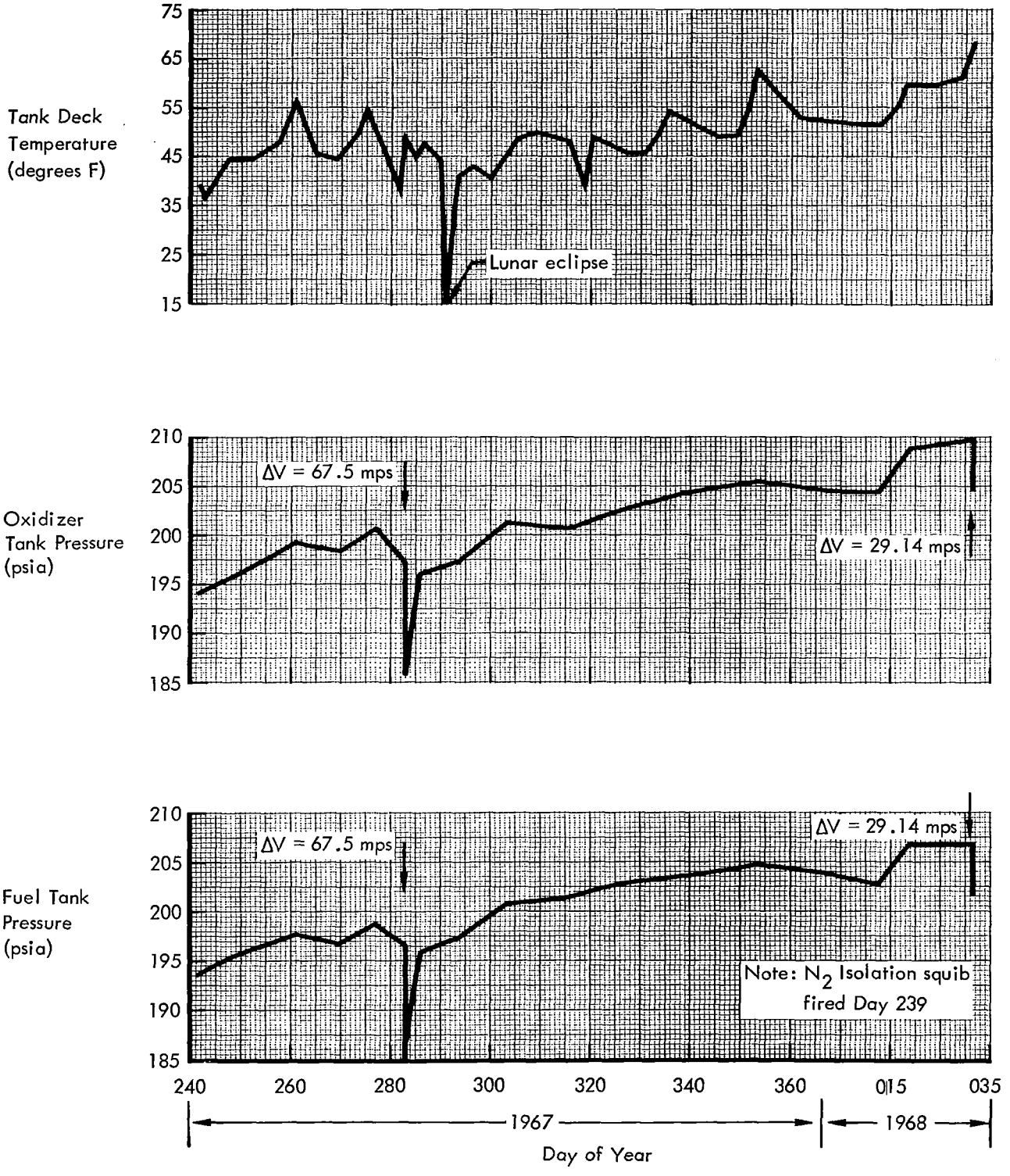

Figure 5-34: Propellant Tankage History

degrees. The decrease in tank pressures shown in Figure 5-35 was as expected for blowdown operation. The tanks recovered 7 psia in the next 93 hours, which indicated leakage through the nitrogen shutoff squib valve.

Terminal Transfer Maneuver — On Day 031 at 06:13:03 GMT, a velocity maneuver was performed to place the spacecraft in an orbit that would impact the lunar surface. It was anticipated that a portion of the commanded 29.14 m/sec impulse would be provided by fuel expulsion after oxidizer exhaustion. Within the resolution of the telemetry data (the last point was recorded 0.1 second prior to engine cutoff), oxidizer exhaustion did not occur during the 16.41-second burn. Examination of the error factors shown in Table 5-17 shows that there was a 10.1-m/sec uncertainty in Delta V remaining. Thus, the available Delta V was 25.6 ± 10.1 m/sec at the time of the terminal transfer. In addition, there were approximately 10 m/sec obtainable from the expulsion of 2.8 pounds of residual fuel.

The average thrust during the burn was 106.0 pounds, as computed from spacecraft weight and acceleration data. Propellant system pres-

Table 5-17: Delta V Error Factors

	Tolerance	Equivalent ΔV
Propellant loading	± 0.75 lb	± 3.6 m/sec
Specific impulse	± 2 sec	± 7.0 m/sec
Expulsion efficiency	± 0.5 %	± 6.4 m/sec
RSS Total		± 10.1 m/sec

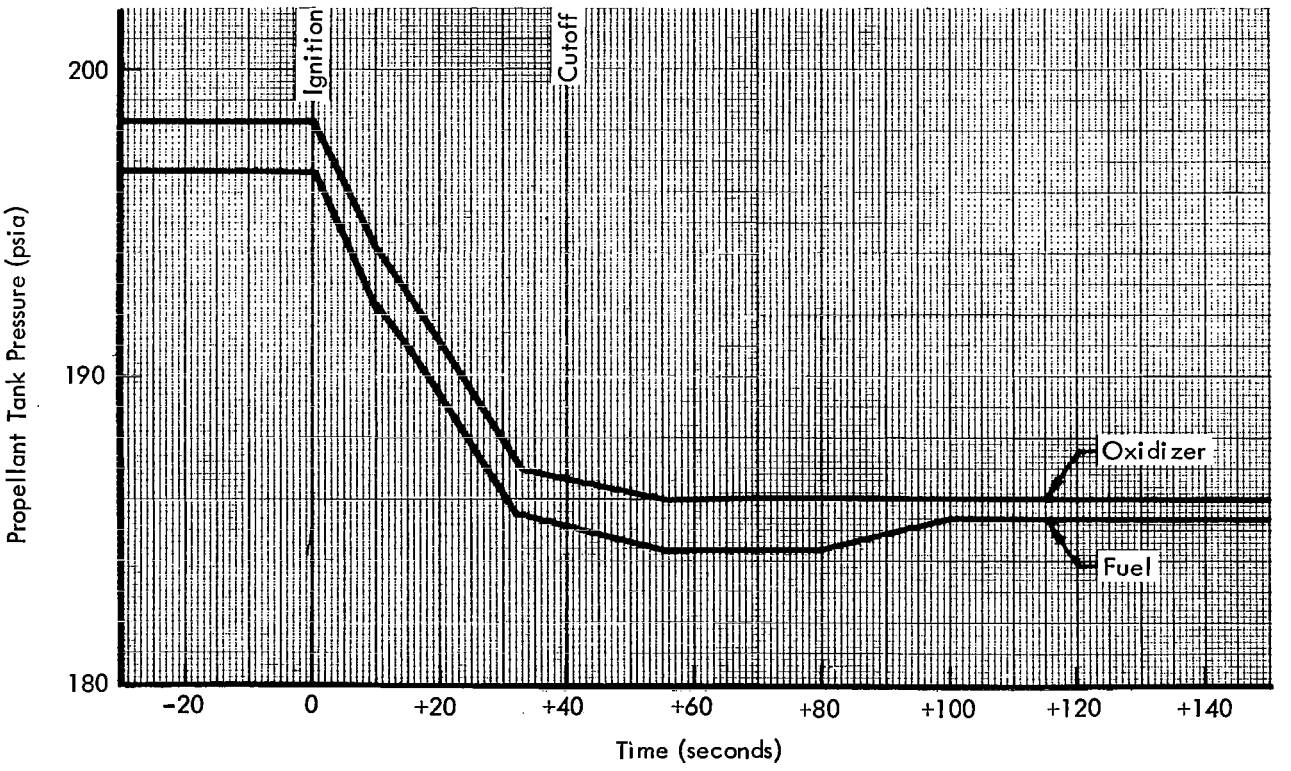

Figure 5-35: Propellant Pressures — Phasing Maneuver

sures shown in Figure 5-36 are consistent with predicted values when operating in a blowdown mode. The thrust vector control actuators cycled from -0.085 to -0.062 in pitch and from 0.428 to 0.473 in yaw, which is indicative of normal performance. The engine valve temperature reached a maximum of 109.8 degrees during soak-back, which is consistent with previous flight data.

Overall Subsystem Performance — During the photographic and extended mission, six velocity maneuvers were performed. An analysis of system performance during each burn confirmed that the engine specific impulse averaged 276 seconds. The velocity control subsystem imparted a total velocity change of 1,019.05 m/sec using 270.85 pounds of propellant, based on a specific impulse of 276. The total burn time was 745 seconds, which yields a total impulse of 74,699 pound-seconds.

5.3 SPECIAL FLIGHT TESTS

Special tests performed during the extended mission fall into two categories: (1) special experiments using the Lunar Orbiter spacecraft as a tool to obtain scientific data, and (2) special exercises that are tests of the spacecraft or equipment on board. Only the latter are reported herein; special experiments are to be reported by the particular agency requesting the experiment.

5.3.1 Battery Discharge Tests

Objective — The purpose of the discharge tests was to check battery characteristics after a prolonged period of overcharge and after sunset discharge cycling.

Data and Discussion — The first test, on Day 270, was initiated by pitching the spacecraft 95 degrees off the Sun to place the battery in the discharge mode. A total of 7.05 ampere-hours was removed from the battery in 74 minutes using the propellant heaters to increase the base spacecraft load. This value represents a 58.7% depth of discharge based on a nominal 12 ampere-hour capacity. The end-of-discharge voltages were 23.84 volts (battery) and 23.04

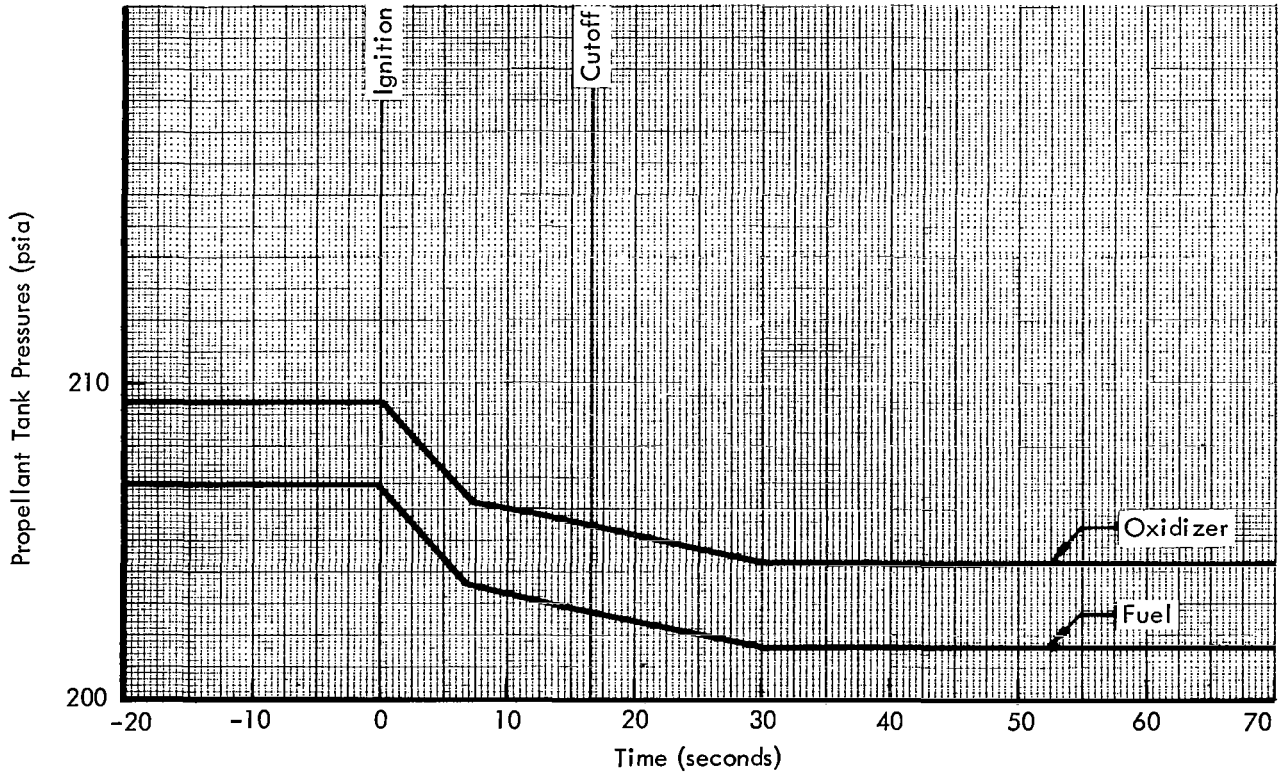

Figure 5-36: Propellant Pressures — Terminal Transfer Burn

volts (bus). The battery temperature dropped from 83 to 68°F during the discharge period.

The second test was performed on Day 012 concurrently with the test of solar array performance at high off-Sun angles. The test was again initiated by pitching 95 degrees from the sunline. After 83 minutes the spacecraft was returned to the sunline and then pitched to plus 70, 77, and 85 degrees. At these angles, the battery was used to partially support the spacecraft loads. The total discharge during the test was calculated to be 8.0 ampere-hours (a 67% depth of discharge). The end-of-discharge voltages were 22.88 volts (bus) and 23.52 volts (battery). The battery temperature varied from 111 to 69°F during the discharge. Figures 5-37 and -38 are graphical representa-

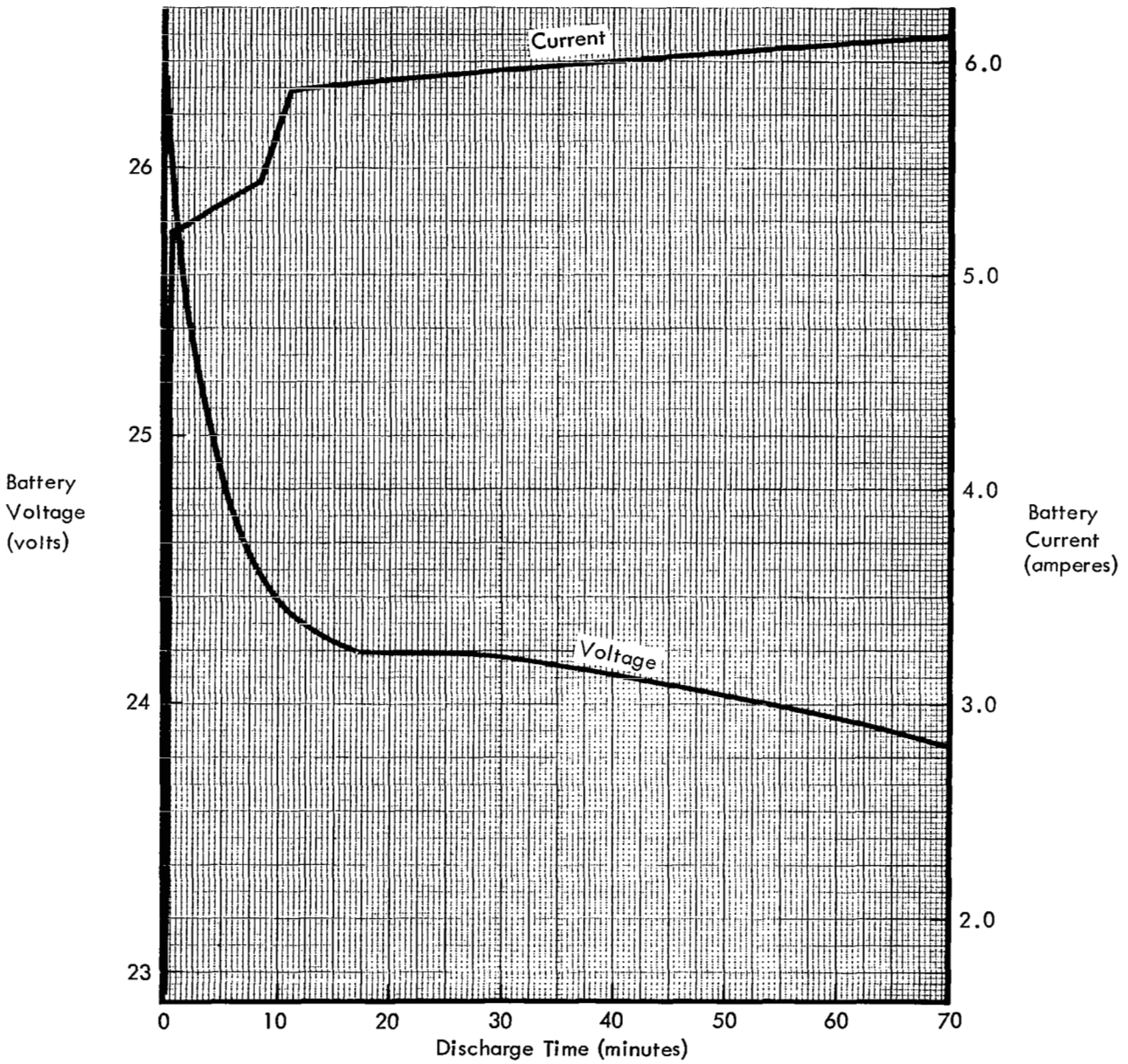

Figure 5-37: Battery Discharge Test — Day 270

Sequence of Events

GMT	Event	GMT	Event
19:30:00	PIP 95°	21:38:33	PIP 70°
20:12:00	Command decoder on	22:15:18	PIP 7°
20:14:12	Command decoder and star tracker off	22:30:00	PIP 8°
21:17:00	PIM 95°	22:52:42	PIM 110°

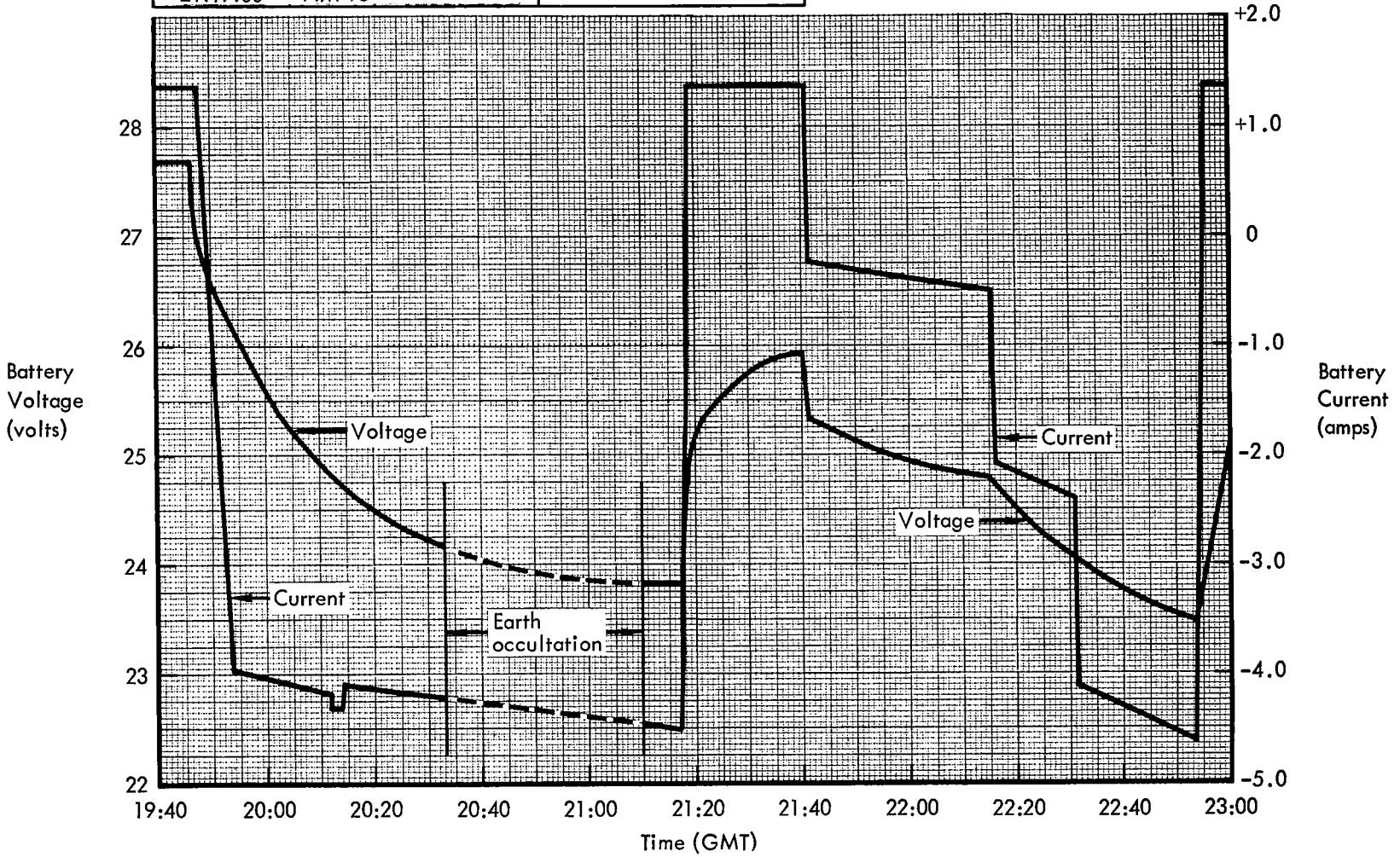

Figure 5-38: Battery Discharge Test — Day 012

tions of the battery characteristics recorded during the discharge tests.

Conclusion – The tests demonstrated that 51 days of constant overcharge and approximately 750 discharge cycles did not detrimentally affect normal battery characteristics.

5.3.2 Paint Degradation Test

Objective – The objective of this test was to obtain temperature data on four thermal control paint coupons to evaluate degradation characteristics as a function of time.

Description – The test, which was conducted on Days 271, 300, 335, and 012, consisted of orienting the spacecraft on the sunline 1.5 hours prior to apolune for a period of 2 hours.

Data and Discussion – The data points acquired at thermal equilibrium with no lunar infrared energy are shown in Table 5-18. Data from the prime mission are included to establish the starting reference and show the overall trend. The data from Day 012 were not incorporated because of lunar thermal radiation effects that could not be corrected with sufficient accuracy. The temperature correction was applied to account for solar constant changes and spacecraft heat sources.

Conclusion – During 122 days of exposure to the cislunar and lunar environments, the paint coupons degraded as follows:

S13G over B1056	final absorptance (α) = 2.420 times initial α
Hughes Organic	final α = 2.345 times initial α
Silicone on aluminum	final α = 1.622 times initial α
Z93	final α = 1.481 times initial α

Table 5-18: Thermal Coating Experiment Data

	GMT Day								
	213	218	224	230	236	244	271	300	335
ST09 (S13G over B1056)									
Telemetry, (°F)	17.3	31.6	44.3	55.0	62.5	68.7	90.2	115.2	135
Temperature corrected (°F)	8.0	23.0	37.4	48.2	56.5	62.6	82.1	106.3	125.4
α_s	.189	.214	.240	.261	.278	.292	.339	.403	.458
ST15 (Hughes Organic)									
Telemetry (°F)	4.3	19.5	30.8	39.8	46.8	52.7	71.0	94.8	111.5
Temperature corrected (°F)	−9.5	6.5	18.5	28.2	36.0	42.2	60.5	82.7	97.8
α_s	.162	.186	.206	.223	.237	.249	.287	.341	.380
ST 16 (Silicone on Aluminum)									
Telemetry (°F)	47.3	56.3	64.0	69.8	73.7	76.6	84.6	104.0	115.8
Temperature corrected (°F)	37.4	47.5	56.0	61.5	65.2	68.0	74.2	92.3	102.1
α_s	.240	.259	.277	.289	.298	.305	.320	.365	.389
ST17 (Z93)									
Telemetry (°F)	16.5	23.3	18.7	32.4	35.2	37.0	41.0	58.0	68.3
Temperature corrected (°F)	5.7	13.5	18.5	22.5	25.0	26.5	29.5	45.6	54.5
α_s	.185	.197	.206	.213	.217	.220	.225	.256	.274

5.3.3 Solar Array Performance at High Off-Sun Angles Test

Objective — The objective of this test was to establish solar panel performance at high angles of incident illumination.

Description — The solar array current was monitored while the spacecraft was pitched plus 95 degrees and at three static pitch angles of plus 70, 77, and 85 degrees. The spacecraft was rolled minus 45 degrees while at $\theta = 85°$, to verify whether partial shading of a lower solar panel by an upper one affected the data.

Data and Discussion — The test was performed concurrently with the battery discharge test on Day 012. The results are shown in Figure 5-39. The curve and the three static points are annotated with the average solar panel temperature, so that the array current output varies as a function.

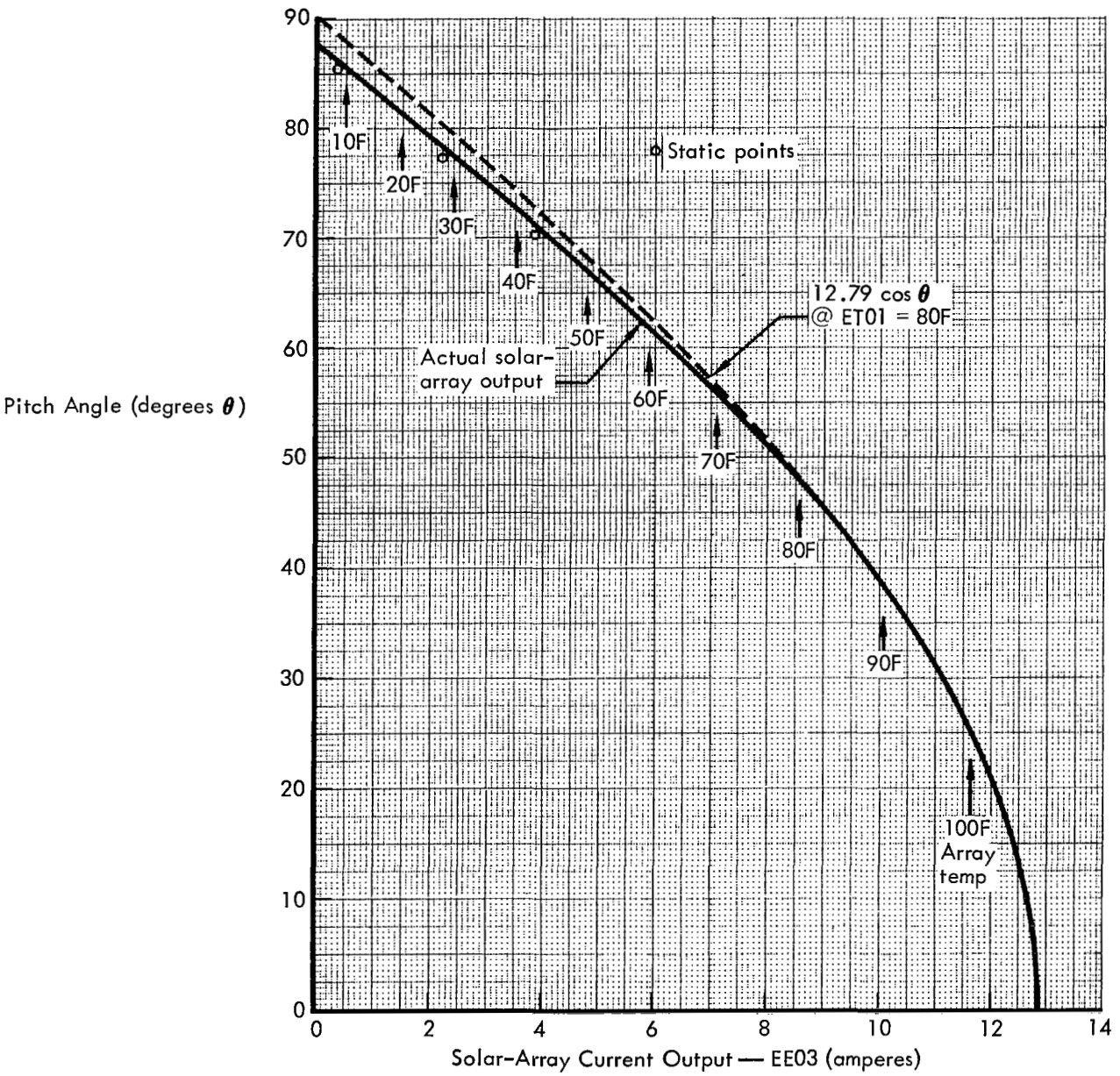

Figure 5-39: High Off-Sun Angle Solar Array Performance

of the temperature. The dashed curve shows the output if it varied as the cosine of the off-Sun angle.

Conclusion — The actual array current output as anticipated did not follow the cosine curve, as shown on the figure. This divergence can be accounted for in several ways. First, the reflection of the incident light from the glass cover plate over the solar cells becomes higher at high pitch angles, thereby allowing less incident light to fall on the cells. Second, the efficiency of the solar cells decreases at lower illuminations encountered at high off-Sun angles. Third, the array current output is a function of the solar panel temperature. The dashed curve assumes a constant temperature of 80°F, whereas the solid curve shows the indicated panel temperature. No correction for the dynamic lag of the temperature sensor was taken into account.

The data obtained during static and dynamic conditions are not in exact agreement. To some extent this may be accounted for by the difference in panel temperatures. However, most of the difference may be attributed to quantization uncertainty of ± 0.03 amperes, and to positional accuracy. Solar panel shading was not a factor.

5.3.4 Maneuver Accuracy, Pitch and Yaw

The purpose of the experiment was to determine spacecraft maneuver accuracy in pitch and yaw as an aid in postphotographic mission error analysis.

The collective system accuracy for a particular axis was measured by commanding a 360-degree maneuver and noting the actual maneuver magnitude as indicated by the initial and final fine sun sensor position outputs. Maneuver accuracy data determined in this manner are shown in Table 5-3.

5.4 SPACECRAFT ANOMALY

When the spacecraft was acquired by DSS-12 on Day 029, it was immediately apparent that a major anomaly had occurred since the last tracking period (Day 026). Table 5-19 shows the significant changes in spacecraft parameters. After the programmer was placed in infinite jump and the deadzone opened, the contents of the memory were telemetered. Analysis of the telemetered programmer data indicates that the spacecraft sustained an apparent power loss or losses for a total aggregate time of approximately 1 hour and 12 minutes as determined by the clock error. On regaining power the programmer was initialized, which would account for the following anomalous conditions:

- Programmer in halt mode;
- Camera thermal door partially open and door stepping motor off;
- Attitude control subsystem in ± 0.2 degree deadband;
- All sun sensors on.

The programmer-integrated maneuver data (AB05-D9) still showed the minimum maneuver value performed during the occultation time sequence, which was initiated at Day 026:19:04 GMT by an RTC JMP-030. This indicated that the programmed PIM 60-degree maneuver had not occurred. When the programmer memory was subsequently read out, the EMM for the maneuver had not incremented, confirming that the maneuver had not been performed. Therefore, it appears that the operation of the programmer was normal until the anomaly occurred.

Using this assumption, and the fact that the programmer was in Memory Location 022 and in the halt mode (which prevented further execution of stored-program commands), it can be concluded that the wait time in Memory Location 022 could not have been executed. The anomalous condition, therefore, must have occurred prior to Day 028:14:16 GMT, which was the programmed end-of-the-wait time in Memory Location 022.

A cycle through the camera shutter-speed settings after the anomaly indicated that the photo subsystem had sustained a preset pulse. This was also indicated by the change in shutter operations observed. The photo subsystem generates a preset pulse when it is initialized by regaining power, either from a momentary or long-term excursion below approximately 20 volts d.c.

Operation of the attitude control subsystem at low voltages can be accurately determined only

Table 5-19: Subsystem Status

Parameter	Day 026	Day 029
Attitude control		
Pitch Sun sensor	Saturated plus	-13.22 degrees
Yaw Sunsensor	-1.29 degrees	Saturated plus
Deadzone	2.0 degrees	0.2 degrees
Gyro wheel currents		
Roll	83.0 ma	83.5 ma
Pitch	89.9 ma	88.8 ma
Yaw	86.7 ma	87.8 ma
Gyro temperature	48.8%	50.4%
Velocity control		
Nitrogen pressure	556 psia (2.55 lb)	93 psia (.45 lb)
Nitrogen temperature	66.4 degrees	60.9 degrees
Fuel pressure	206.8 psia	201.7 psia
Oxidizer pressure	209.5 psia	204.4 psia
Tank deck temperature	62.2 degrees	61.3 degrees
Photo		
Telemetry logic indication	Unchanged	Unchanged
Temperature		
Upper environmental	66.3	55.5
Lower environmental	70.6	57.7
Window	75.5	Off scale — low
Shutter operations	17	2
Camera thermal door	Closed	Not closed
Flight programmer		
Clock error	+4.78 seconds	−4320 seconds
Halt mode indication	Operating-location 16	Halt-location 22
Last maneuver magnitude	0.0 degrees	0.0 degrees
SPA location	SPA 160	SPA operation code garbled
Power		
Off-Sun angle	53.7 degrees	59.1 degrees
Battery temperature	96.8 degrees	98.2 degrees
Load current	3.56 amps	3.56 amps
Shunt regulator leakage	0	0

from fairly comprehensive laboratory tests, which were not conducted. The operation of certain components at low voltages is known to varying degrees, however, from preflight development and other ground tests. A test was run of the control and switching assemblies with input voltages from 32.0 down to 0 volts d.c. It was shown that while no permanent degradation to the control and switching assemblies resulted from reduction in input voltage, the output voltage, which is used to bias the differential amplifiers, did vary at voltages below 19.7 volts d.c. At 19.7 volts d.c. input, the −15 volts d.c. output to the differential amplifier began to degrade linearly at 0.82 volts per volt-drop. At 18.2 volts d.c. input, the +15 volts d.c. output to the differential amplifier began to degrade linearly at 1.06 volts per volt-drop. Thus, at 18.0 volts d.c. input to the control and switching assembly, the output to the differential amplifier's biasing network is −13.6 and +14.8 volts d.c. instead of the ±15 volts d.c. required for the differential amplifier to have zero output for zero input. Under these conditions, jet actuation can occur. As long as the input voltage to the control and switching assembly remains at a low level, the jet will remain open. The thruster actuation time required to dissipate the nitrogen gas under this condition can be calculated at follows:

$$Q = \frac{t \cdot T}{I_s}$$

where: $Q = N_2$ gas consumed (pounds)

t = time that one jet is open (seconds)

T = Thrust (pounds) − 0.064 pounds for yaw jets

I_s = Specific impulse (seconds) − 68 seconds for N_2

Therefore: $t = \frac{Q \cdot I_s}{T} = \frac{2.1\,(68)}{0.064} = 2{,}231$ seconds

Thus, a pitch or yaw jet being open 2,231 seconds would account for the lost N_2 gas. It is likely that several jets fired, over a shorter period of time, and that this activity occurred during the approximately 1 hour and 12 minutes that the programmer clock was inoperative.

Figure 5-40 shows the off-Sun angle calculated from known gyro drift rates of 0.7 degree per hour in roll, 0.5 degree per hour in pitch, and 1.0 degree per hour in yaw, positive in all axes. Telemetry data were available until Day 026, 20:50 GMT, to establish the initial part of the curve. The off-Sun angle at that time was approximately 53 degrees. The nominal curve corresponds to the gyro null. Maximum and minimum curves correspond to limit cycling within the 2-degree deadband, which is +1 degree, −2 degrees, for this spacecraft for the pitch axis, and ±2 degrees for the other two axes. As noted, solar pressure will tend to hold the vehicle between the nominal and maximum curves.

Case 1 − To calculate solar array performance, data on solar array output versus off-Sun angle from a test conducted on Day 012 were used. A curve midway between the nominal and maximum curves of Figure 5-40 was used (Curve 1), as a best approximation of the off-Sun angle produced by gyro drift rates. Spacecraft subsystem load current during the period of interest was taken from data during the October 18, 1967 lunar eclipse. During the eclipse, the spacecraft was on sunline. To approximate the thermal and battery voltage conditions encountered by a spacecraft drifting out from the sunline, the start of discharge current was taken when the solar array current during the eclipse was approximately equal to an off-Sun angle of 70 degrees. This value was 3.81 amperes, and increased to 4.68 amperes when the battery voltage was 22.0 volts, representing an approximately 100% discharge condition.

Referring to Figure 5-41, it is seen that the continuous battery discharge begins on Day 028 at approximately 09:30 GMT. The ampere-hour demand from the battery subsequent to this time is made up of (1) the ampere-hours represented by the area between the array current curve and the load line, (2) the additional battery discharge during the Sun occultations, and (3) a small amount of capacity to supply the power subsystem losses.

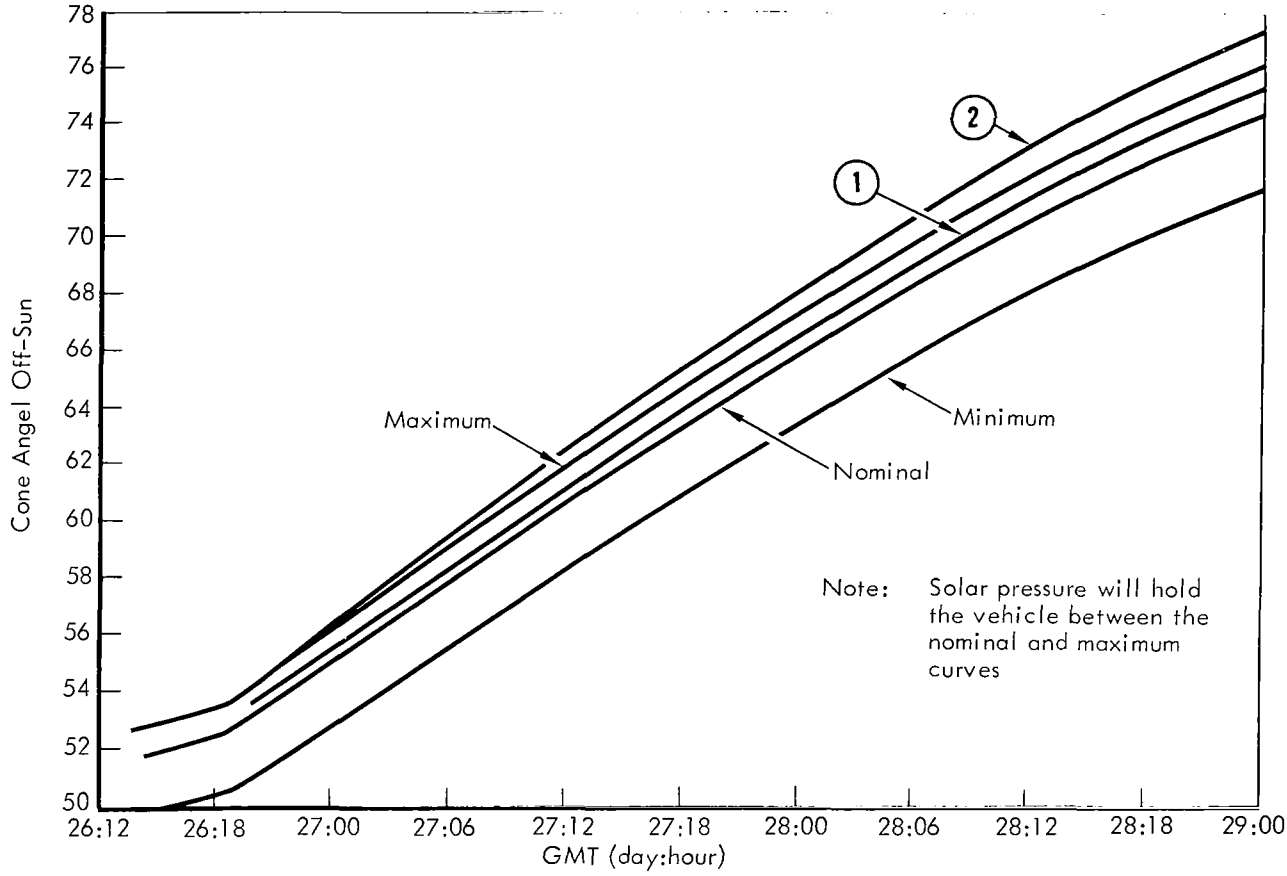

Figure 5-40: Off-Sun Angle

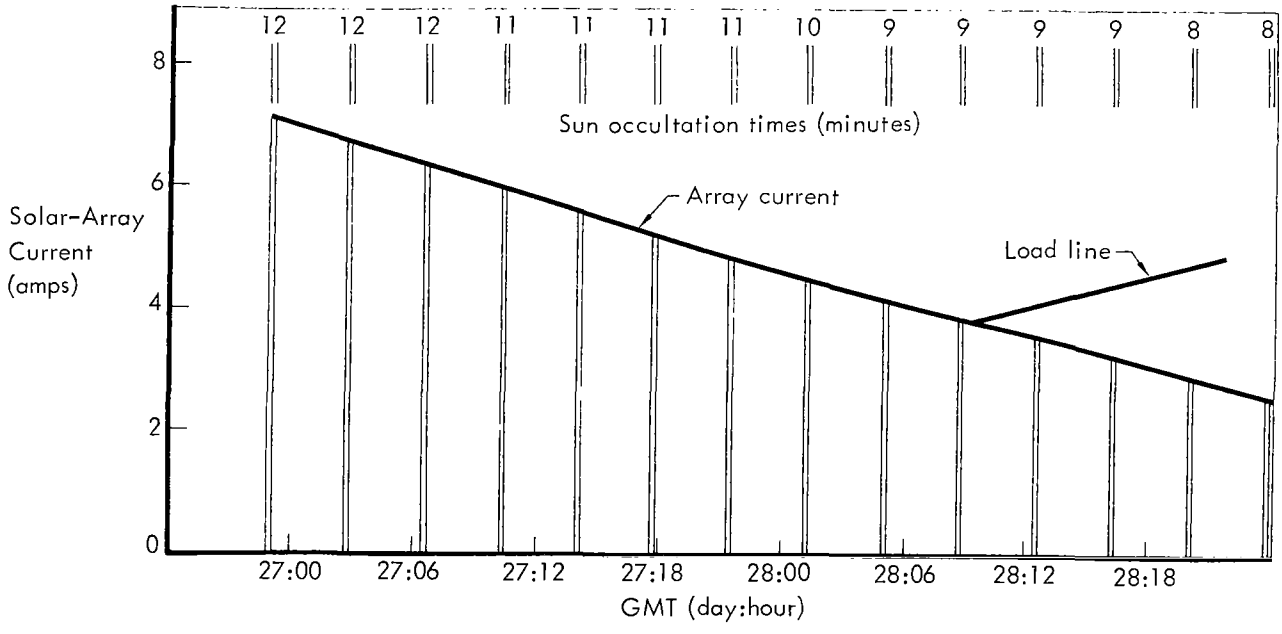

Figure 5-41: Case I Estimated Array Current versus Mission Time

On Day 028,19:47 GMT (the time programmed for the spacecraft to re-establish celestial reference by acquiring Sun), the battery discharge would be as follows.

(1) From Figure 5-41 (area between curves): 8.95 ampere-hours

(2) The additional energy to be supplied during three Sun occultation periods would be:

Sunset GMT	Average Discharge Current (amperes)		Occultation Time (minutes)	Discharge Capacity (amp-hr)
028:08:40	4.00	x	9	0.6
028:12:26	3.55	x	9	0.53
028:16:11	3.25	x	9	0.49
	Total additional energy to be supplied during occultations:			1.62

(3) The discharge attributable to power subsystem losses is 4 ampere-minutes per hour times 10.28 hours or 0.68 ampere-hours.

The total discharge capacity is then:

$8.95 + 0.68 + 1.62 = 11.25$ ampere-hours

During the October 18, 1967 eclipse, the battery was discharged 11.8 ampere-hours with an end-of-discharge voltage of 22.24 volts. From a test run on January 12, 1968, the discharge was 8.0 ampere-hours with an end-of-discharge voltage of 23.5 volts, which did not indicate any appreciable degradation of battery performance.

The conclusion that can be drawn from this analysis is that if the gyro drift rates were those that have been assumed, and if the October 18, 1967 lunar eclipse load currents were equal to the load currents encountered as the spacecraft drifted off the sunline, the anomaly was caused by something other than drift off the sunline. If the drift rates are less than the values used, the conclusion again is that drift off the sunline could not have caused the anomaly.

Case 2 – If, however, the 3-sigma dispersion in the accuracy of gyro drift rates, ± 8%, is applied in the positive direction, the power balance can be calculated as follows.

The solar array off-Sun angle is as shown by Curve 2 of Figure 5-40. Referring to Figure 5-42, it is seen that battery discharge starts on

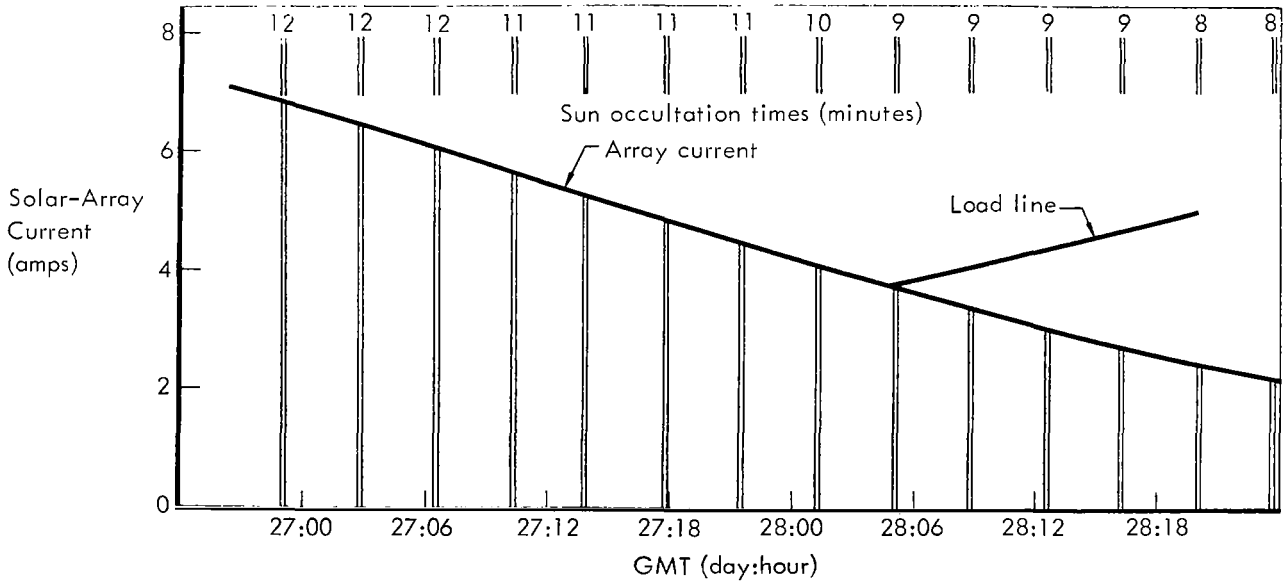

Figure 5-42: Case II Estimated Array Current versus Mission Time

Day 028 at approximately 04:45 GMT. The ampere-hour demand from the battery subsequent to this time will comprise (1) the ampere-hours represented by the area between the array current curve and the load line, (2) the additional battery discharge during the three Sun occultations, and (3) a small amount to supply the power subsystem losses. On Day 028 at 15:30 GMT the battery discharge would be as follows.

(1) From Figure 5-42 (area between curves): 9.88 ampere-hours.

(2) The additional energy to be supplied during occultations periods is therefore:

Sunset GMT	Average Discharge Current (amperes)		Occultation Time (minutes)	Discharge Capacity (amp-hr)
028:04:55	3.75	x	9	0.56
028:08:40	3.40	x	9	0.51
028:12:26	3.10	x	9	0.47
Total additional energy to be supplied during occultations:				1.54

(3) The discharge attributable to power subsystem losses is 4 ampere-minutes per hour times 10.75 or 0.72 ampere-hours.

Total battery discharge is then:

$$9.88 + 0.72 + 1.54 = 12.14 \text{ ampere-hours}$$

Under these conditions the battery would probably become fully discharged on Day 028 at approximately 15:30 hours or greater than one hour beyond the programmed end-of-the-wait time in Memory Location 22.

Conclusions – No definite conclusion can be drawn as to the cause of the anomaly. Some of the more probable of a number of possible causes are listed below.

(1) *Gyro drift off sunline causing battery discharge and a low voltage condition that resulted in the anomaly.* From the preceding analysis, this conclusion could only be arrived at if the load current profile was greater than that encountered during the lunar eclipse and if the 3-sigma gyro drift dispersion was actually followed.

(2) *A temporary increase in gyro drift rates, or a gyro gimbal hang up.* No indication of either of these conditions was noted after the anomaly and this spacecraft had no history of either of these malfunctions.

(3) *A "stuck" attitude control subsystem thruster.* Again, there was no history of this, either before or after the anomaly.

(4) *A power transient that halted the programmer and allowed the spacecraft to drift off sun.* A power transient did occur on Lunar Orbiter III, and is a possible cause, although there is no history of this type of anomaly on Lunar Orbiter V.

(5) *A programmer error that caused it to go to the halt mode.* There has been no history of this ever occurring except under low-voltage conditions.

Because of the small amount of nitrogen gas remaining, preparations for a terminal maneuver were initiated shortly after the anomaly was discovered. The terminal maneuver was conducted on January 31, 1968, and resulted in a lunar nearside impact.

6.0 Extended-Mission Program Summary

Active tracking of the five Lunar Orbiter extended-mission spacecraft, as shown in Figure 6-1, spanned a period of over 16 months from Day 260 (September 14), 1966 to Day 031 (January 31), 1968. The level of activity over this period varied from short tracking periods to monitor spacecraft performance (quick look), to continuous tracks of several days' duration during critical periods. Quick-look was also used to monitor extended-mission spacecraft while the main level of activity was focused on a primary mission spacecraft. Of primary interest was the detection of detrimental spurious commands that may have been received during command transmissions to another spacecraft.

The extended missions of Lunar Orbiters I, II, III, and V were terminated by planned lunar-impact velocity maneuvers after the attitude control subsystem nitrogen gas had been depleted to a value at or near the minimum accepted value for spacecraft control. This value decreased throughout the program as experience in ACS performance at low nitrogen pressure was gained. The terminal velocity maneuver of Lunar Orbiter V was successfully performed at the lowest nitrogen pressure reached during the extended missions – 77 psia, indicating approximately 0.4 pounds of nitrogen remaining.

On July 21, 1967 Lunar Orbiter IV could not be contacted. Repeated attempts to locate and acquire the spacecraft were officially terminated on August 16 and lunar impact was predicted to have occurred by October 31. Analysis of all information failed to reveal the reason for loss of contact.

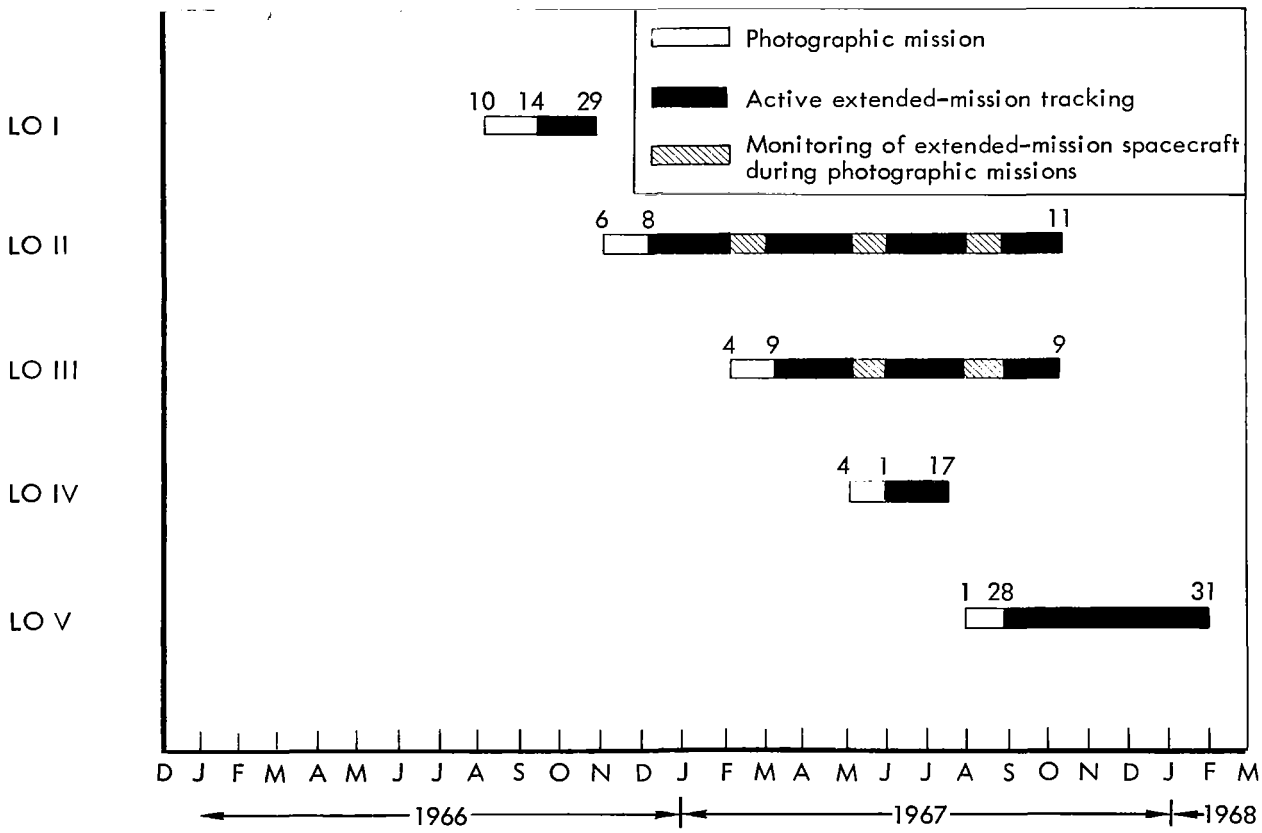

Figure 6-1: Extended-Mission Tracking Summary

6.1 EXTENDED-MISSION OBJECTIVES

Extended-mission objectives are summarized in Table 6-1. The primary objective was to secure information that could be used to define the size and shape of the Moon and the properties of its gravitational field, and to study its environment.

Secondary objectives were to develop standard operating procedures, conduct special experiments and exercises, and explore the use of Lunar Orbiter subsystems for other applications. Secondary objectives have been divided into two general categories: special experiments or tests in which the spacecraft is used as a tool, and special exercises or tests of the spacecraft or on-board equipment.

6.2 EXTENDED-MISSION ACCOMPLISHMENTS

The primary objective of the extended mission was accomplished successfully. Selenodetic data acquisition from the five spacecraft added considerably to the fund of information concerning the size and shape of the Moon, and the properties of its gravitational field. The spectrum of information obtained was due in part to orbital geometry variations between the spacecraft, which included near-polar and low-inclination orbits as well as highly elliptical and nearly circular orbits. It was also due to the fact that selenodetic data were provided over a long period of time during the extended missions, i.e., approximately 11 months in the case of Lunar Orbiter II. These data were intended to provide information on long-term orbital parameter effects, which also added significantly to lunar selenodetic knowledge. During the photographic mission there was time to perform only the calculations and analyses made necessary by the requirements of the mission. It was left until the extended mission to reflect on problems arising from the selenodetic data obtained and initiate new analysis or experiments to resolve them. An example of such an experiment was the perilune residual experiment conducted shortly before the end of the Lunar Orbiter V extended mission. The need for this experiment became apparent only after many months of study of selenodetic data; the results are providing useful new knowledge in the field.

Lunar environment monitoring was accomplished by recording galactic-cosmic radiation and micrometeoroid hits on each of the five spacecraft.

All secondary objectives (Table 6-1) of the extended mission were accomplished by one or more of the five Lunar Orbiter spacecraft. The data from the special experiments were forwarded to the requesting agency. Quantitative analysis of these data was the responsibility of the requesting agency.

The special exercises conducted provided the information summarized below.

- Tests of the star tracker provided engineering data essential to formulation of plans for later Lunar Orbiter missions. These data included the effects of glint, tracker degradation, and operation of the bright object sensor on tracker operation.
- Tests of the IRU were performed to determine maneuver accuracy, gyro drift characteristics, and IRU turn-off/turn-on effects. These data were used to assist in planning later Lunar Orbiter missions and for accuracy studies.
- Power subsystem tests provided engineering data for future missions. Battery deep discharge tests were performed to help erase memory effects and thus recondition the batteries.
- Communications subsystem tests provided engineering data that were used to develop operational procedures for multiple-spacecraft operation, to perform TWTA failure analysis, and to conduct low-voltage operation tests.
- Camera thermal door tests provided engineering data on thermal conditions with the thermal door open, as well as failure analysis data.
- Photo subsystem tests provided data useful to later Lunar Orbiter missions and system failure analysis.
- The squib-firing interaction test provided data concerning its influence on star tracker operation.
- Paint degradation tests were performed to study absorptivity-emmissivity characteristics of several types of paint after prolonged exposure to deep space.

Table 6-1: Extended-Mission Objectives
Lunar Orbiters I Through V

Objectives	LO I	LO II	LO III	LO IV	LO V
The primary extended-mission objective was to secure information that may be used to increase the scientific knowledge of the size and shape of the Moon, the properties of its gravitational field, and the lunar environment.	X	X	X	X	X
Secondary Objectives:					
A. Special Experiments:					
• Investigations of Doppler residuals near perilune.					X
• V/H mapping to obtain lunar profile data.	X	X			
• Radar mapping, RF occult determination, and lunar surface conductivity experiments.	X		X	X	X
• Ionosphere effects experiment.		X	X	X	
• Doppler ranging calibration experiment to check out Mark II ranging system at DSS 14.		X			
• MSFN Apollo GOSS Navigational Support.		X	X	X	X
• Multiple-spacecraft operations tests.		X	X		
• Voice relay experiment.				X	X
• Convolutional coding/sequential decoding experiment.					X
• Optical observation experiment.					X
B. Special Exercises:					
• Canopus tracker tests: star maps, glint tests, bright object sensor tests, map voltage tests, and tracker degradation tests.	X	X	X	X	X
• Maneuver accuracy tests, gyro drift tests, and IRU turn-off/turn-on tests.		X	X	X	X

Table 6-1 (Continued)

Objectives	LO I	LO II	LO III	LO IV	LO V
• Battery discharge tests, solar panel degradation tests, and solar panel performance at high off-Sun angles.	X	X	X	X	X
• Communications tests: downlink modulation index, transponder and command threshold tests, command address test, transponder oscillator drift test, TWTA cycling and low-voltage tests, and high-gain antenna 360-degree rotation test.	X	X	X	X	
• Photo subsystem tests: focus adjustment, V/H tests, and readouts.	X	X	X	X	
• Camera thermal door tests.		X		X	
• Squib-firing interaction test.			X		
• Paint degradation tests.	X	X		X	X

6.3 FLIGHT OPERATIONS SUMMARY

Table 6-2 provides a profile of flight operations activity. Overall activities for the extended mission of each spacecraft were developed and defined in their respective flight operations plans. In general, each plan provided broad requirements for tracking coverage, data acquisition, and performance of special activities. However, these plans underwent evolutionary changes throughout the program as experience and knowledge accumulated. A good example is the increase in spacecraft life made possible by a reduction in the gas reserve found necessary to permit spacecraft orientation for the terminal burn (0.8 pound for Mission I versus 0.4 pound for Mission V).

To implement flight plans, pass plans were promulgated that defined support requirements and the sequence of events for each pass. Criteria on which operating procedures were based included:

- The effect on flight endurance of gas consumption and gas remaining;
- Thermal history and trend;
- Electrical load and off-Sun solar array capability;
- Subsystem operating constraints;
- Maintenance of ability to control the spacecraft through the terminal transfer maneuver at the end of its useful life.

Table 6-2: Extended-Mission Summary

Mission	Length (days)	Commands (RTC&SPC)	Passes Tracked	Guidance Maneuvers	Telemetry Data (hours)
I	42	1,192	27	1	432
II	307	4,096	195	4	542.6
III	214	2,553	170	4	665.6
IV	50	656	24	2	288.6
V	156	911	65	2	471.6

Prior to the start of the extended mission, the spacecraft were placed in an extended-mission mode. This mode consisted of maneuvering the spacecraft to an off-Sun attitude for thermal relief, commanding the attitude control subsystem to wide deadzone operation to conserve gas, and configuring the programmer to provide periodic Sun acquisition to update spacecraft attitude.

Table 6-3 shows the pitch angles and thermal relief periods that were stored in the programmer.

Table 6-3: Extended-Mission Flight Plans

Spacecraft	Period Off-Sun (hours)	Pitch Angle (deg)
LO I	25.5	+25 to +30
LO II	75 to 21	+56 to +62
LO III	60	−50 to −60
LO IV	72	+40
LO V	72 to 49	+53 and −53

Tracking periods served a number of purposes. Generally, these included selenodesy, spacecraft exercises, special experiments, and development of plans or lunar harmonics for the next mission.

A history of the tracking schedule for all spacecraft is shown in Figure 6-2. A total of 13 velocity control maneuvers was executed during extended-mission operations. Table 6-4 contains a description of each maneuver, the execution date, and the velocity change involved. A summary of orbital elements for each phase of the five extended missions is presented in Table 6-5.

A variety of lunar harmonic models were used to process tracking data and generate tracking station predicts during the extended missions. The following list indicates which model was used during each extended mission.

LO I	LRC 9/4
LO II	LRC 9/4 and LRC 11/11
LO III	LRC 11/11
LO IV	LRC 11/11
LO V	LRC 7/28B

It was determined that LRC 11/11 model (released during the Lunar Orbiter II photographic mission) was the most acceptable for the low-inclination orbits (Lunar Orbiters I, II, and III), while the LRC 7/28B model (released after loss of contact with Lunar Orbiter IV) was best for the high-inclination orbits (LO IV and V).

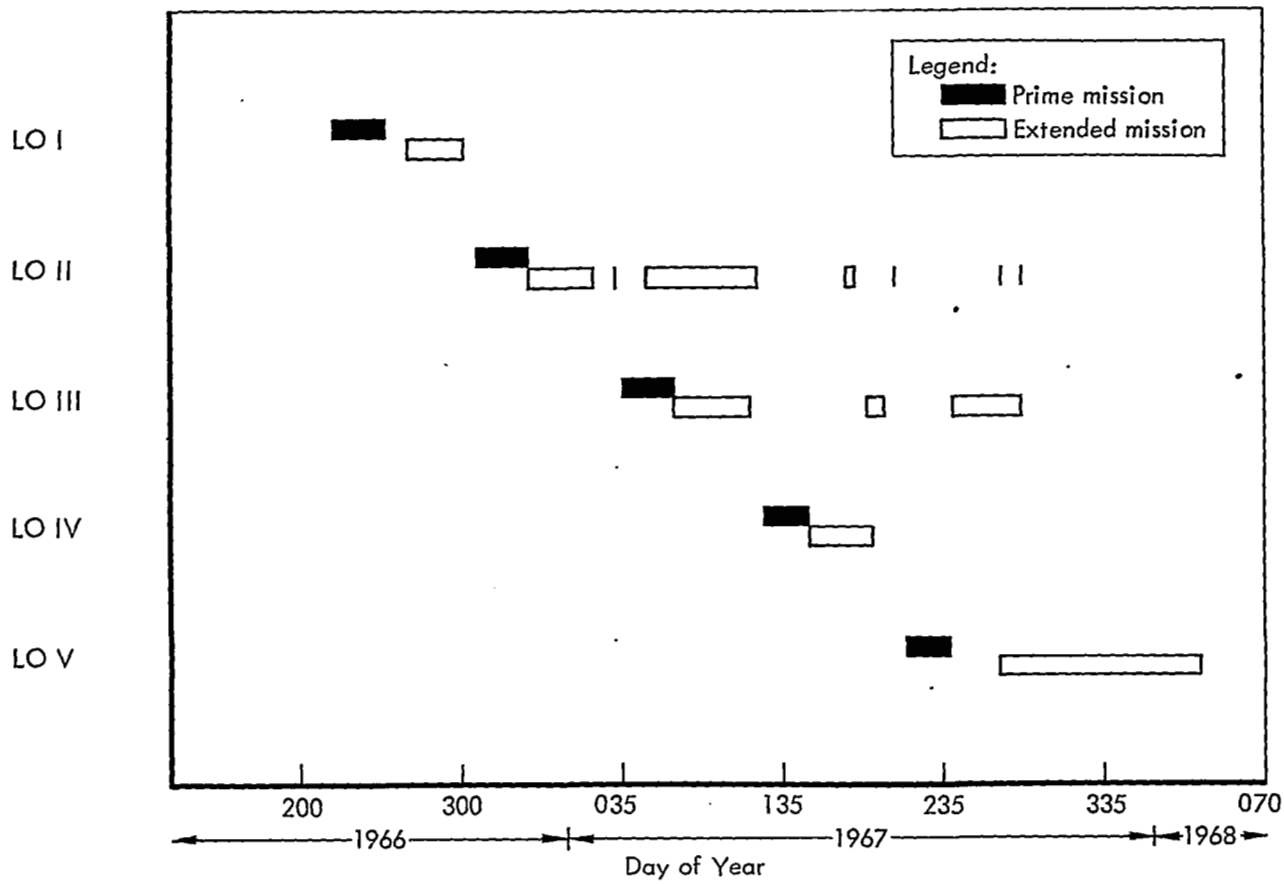

Figure 6-2: Tracking Schedule for Lunar Orbiter Spacecraft

6.4 ENVIRONMENTAL DATA

A primary objective of the extended missions was the collection of lunar environmental data over long periods of flight. Spacecraft telemetry was monitored during each tracking period to determine if there had been an increase in radiation flux or micrometeoroid activity.

6.4.1 Radiation

The solar flares that occurred on September 2, 1966, January 28, 1967, and May 24, 1967, caused sharp increases in radiation recorded by the spacecrafts. The solar proton event of September 2, 1966 resulted in an increase in recorded dosage of 8 rads at the film cassette location (DF04) and 135 rads at the camera looper location (DF05). Between January 27 and January 30, 1967 spacecraft dosimeters increased 10 rads (DF04) and 39 rads (DF05). Between May 24 and 25, 1967, spacecraft camera looper counters increased 34 rads with a negligible increase in the film cassette counters.

The Lunar Orbiter III data suggested that the looper scintillation counter of that spacecraft experienced a change in the background level after May 30, 1967, possibly due to a leak in the structure of the counter. This change in background level was not observed on either the Lunar Orbiter II or IV spacecraft.

6.4.2 Micrometeoroids

Spacecraft detectors recorded 16 micrometeoroid hits during the extended-mission periods. These hits were recorded during the period January 6, 1967 to January 21, 1968 by Lunar Orbiters II, III, and V.

6.5 SPACECRAFT SUBSYSTEM PERFORMANCE

Periodic monitoring of spacecraft telemetry

Table 6-4: Velocity Maneuvers

Event	Attitude Maneuvers	Attitude Reference	Ignition Time (GMT)	Velocity Change (mps)	Remarks
LO I					
			10/29/66	178.0	
Impact maneuver	None	Sun	12:25:49.5	Nominal burn 168.8	Impact at 10/29/66, 13:29:6.3 GMT: 6.35°N lat.
				Fuel expulsion 6.4	160.71°E long.
			12:46:25.8	Second engine on 2.8	
LO II					
Inclination change	HRoll 17.0°	Sun	12/08/66	100.0	Inclination increased from 11.9° to 17.5°.
	Yaw −72.5°	Canopus	20:36:28.7		
Orbit phasing	HRoll 89.94°	Sun	04/14/67	5.5	S/C phased in orbit to survive lunar eclipse of 4/24/67.
	Pitch 88.30°	Jupiter	09:01:15.3		Orbital period change of −64.8 sec.
Orbit transfer	HRoll 10.82°	Sun	06/27/67	8.0	Perilune altitude raised from 67.1 km to 112.9 km to pre-
	Pitch −74.69°	Achernar	07:00:45.3		vent natural impact in July 1967.
Impact maneuver	Pitch 180.00°	Sun	10/11/67	71.6	Impact at 10/11/67, 07:12:54 GMT: 3.0° N lat.
			05:55:00.0	Nominal burn 61.5	119.1°E long.
				Fuel expulsion 10.1	
LO III					
Orbit phasing	HRoll 101.63°	Sun	04/12/67	5.5	S/C phased in orbit to survive lunar eclipse of 4/24/67.
	Pitch −113.84°	Vega	17:40:28.2		Orbital period change of −58.5 sec.
Orbit transfer	HRoll −48.59°	Sun	07/17/67	14.4	Perilune altitude raised from 57.5 km to 140.3 km to pre-
	Pitch −108.0°	Acrux	01:21:46.3		vent natural impact in September 1967.
Orbit transfer	HRoll −176.10°	Sun	08/30/67	198.3	Apolune altitude lowered to 316 km for simulation of
	Pitch −78.31°	Vega	19:39:19.6		Apollo-type orbit.
Impact maneuver	HRoll 35.74°	Sun	10/09/67	52.6	Impact at 10/9/67, 10:27:11: 14.3°N lat,
	Pitch 31.83°	Canopus	09:33:05.9		92.7°W long.
LO IV					
Orbit transfer	HRoll 5.72°	Sun	06/05/67	186.7	Perilune altitude lowered from 2,588 km to 74 km and
	Yaw −83.78°	Canopus	23:16:16.8		changed argument of perilune from 9.8° to −5°.
Orbit transfer	HRoll −88.80°	Sun	06/08/67	70.5	Lower apolune altitude from 6085 km to 3953 km to
	Pitch −91.79°	Canopus	22:39:02.7		simulate Mission V orbit.
Impact					Spacecraft computed to impact Moon no later than 10/31/67 due to natural decay of orbit.
LO V					
Orbit phasing	HRoll 31.33°	Sun	10/10/67	67.5	Orbit adjusted to survive the lunar eclipse of 10/18/67.
	Pitch −50.96°	Canopus	19:37:06.7		
Impact maneuver	HRoll −88.84°	Sun	01/31/68	29.1	Impact at 1/31/68, 07:58:08.27:2.79°S lat. 83.04°W long.
	Pitch 93.61°	Canopus	06:13:03.0		Radius = 1,736.8 km

Table 6-5: Average Orbital Elements*

Mission	Time Period		Semimajor Axis (km)	Inclination (deg)	Perilune Altitude Range (km)		Period (min)
I	09/14/66	10/24/66	2,669.8	12.1	31.0	60.7	206.3
II	12/09/66	04/14/67	2,701.6	17.5	39.0	73.0	210.0
	04/14/67	06/27/67	2,692.1	17.0	60.0	71.0	208.9
	06/27/67	10/11/67	2,715.5	16.2	68.5	114.6	211.6
III	02/24/67	04/12/67	2,688.2	21.0	39.0	65.0	208.5
	04/12/67	07/17/67	2,680.0	21.0	53.0	64.0	207.5
	07/17/67	08/30/67	2,721.7	21.0	143.5	148.7	212.3
	08/30/67	10/09/67	1,967.8	21.1	108.0	139.0	130.5
IV	06/02/67	06/05/67	6,150.0	85.0	2,590.0	2,596.0	721.3
	06/05/67	06/08/67	4,820.6	85.0	74.9	77.2	500.6
	06/08/67	07/10/67	3,752.5	85.0	63.9	76.6	343.8
V	09/27/67	10/10/67	2,534.5	85.0	105.2	111.2	190.8
	10/10/67	01/31/68	2,831.7	85.0	160.0	200.0	225.4

*All values have been averaged over all orbit determination results available.

data provided information that was used to determine subsystem performance. The data were analyzed to show trends in performance in an attempt to establish detrimental effects on components or subsystems after exposure to space environment. A tabulation of anomalous subsystem performance during the extended-mission periods is contained in Table 6-6. Most of these anomalies occurred initially during the prime missions but continued into the extended-mission periods. They are briefly discussed in the following paragraphs. Detailed analysis is contained in the applicable final report for each mission or extended mission.

Individual subsystem performance was generally within design requirements; there was very little evidence of serious subsystem or component degradation. The attitude control subsystems of Lunar Orbiters I, III, and IV performed nominally during the extended mission. Lunar Orbiter II experienced an intermittent roll gyro gimbal hangup, and an apparent anomaly in the closed-loop electronics. Lunar Orbiter V experienced excessive gyro drift rates and a deadband anomaly. While these anomalies presented operational difficulties, they did not prevent the spacecraft from accomplishing any of the extended-mission objectives.

The star trackers of Lunar Orbiters II, III, IV, and V operated satisfactorily throughout their extended missions. The Lunar Orbiter III and IV

Table 6-6: Subsystem Performance

Subsystem	Mission I	II	III	IV	V
Attitude control	Performance nominal (high operating temperature). Severe star tracker glint.	Intermittent roll gyro gimbal hangup. Roll deadband shift (one time). High roll drift.	Star map signal degradation.	Performance nominal. Star map signal degradation.	Gyro drift rates (roll and yaw) exceeded design limit. Pitch-plus threshold detector triggered below spec level.
Communications	Fluctuating helix current in TWTA.	Surious-command reception. TWTA failure during prime mission prevented extended-mission video.	Nominal. Spurious command.	Nominal.	Nominal performance. Transponder rf power variation within 80 to 90°F temperature range noticed after lunar eclipse. Spurious command.
Power	Shunt regulator failure (occurred during prime mission).	Shunt regulator current leak.	Shunt regulator current leak.	Nominal.	Shunt regulator current leak.
Photo	Nominal.	Internal pressurization lost.	High-voltage power transformer failure.	Intermittent malfunction of readout looper prevented film advance — abnormal encoder operation.	Film parted at film to leader splice during prime mission.
Structures and mechanisms	Thermal control coating degradation. Camera thermal door motor failed.	Thermal control coating degradation. Camera thermal door failed.	Thermal control coating degradation	Improved thermal control due to use of optical solar reflectors.	Improved thermal control due to use of optical solar reflectors.
Velocity & reaction control	Nominal.	Nitrogen leakage across shutoff squib valve.	Nitrogen leakage across shutoff squib valve.	Nitrogen leakage across shutoff squib valve.	Nitrogen leakage across shutoff squib valve.

trackers experienced star-map signal degradation, although not sufficient to affect their missions. The star tracker of Lunar Orbiter I continued to experience severe glint during the extended mission. The star trackers of Lunar Orbiters II, III, IV, and V also continued to experience glint, but to a lesser degree, during their extended missions. The operational procedures developed during the primary missions were successfully used to minimize the problem.

The communications subsystem of Lunar Orbiter I met all mission requirements during the extended mission, in spite of continued fluctuating helix current in the TWTA and a temporary drop in bus voltage causing the transponder either to cease operation or to output a very low power signal. Data indicated that the performance of Lunar Orbiter I's communications subsystem was normal down to 17.6 volts, which is 3.8 volts below the component-specification minimum requirement. The communications subsystems of Lunar Orbiters III, IV, and V operated nominally throughout the extended missions of those spacecraft. Multispacecraft control procedures were developed to minimize reception of spurious commands by passive spacecraft such as occurred with Lunar Orbiter II. These procedures consisted primarily of a judicious selection, based on the current orbital geometry, of (1) the track synthesizer frequency (TRACK SYNFRQ), (2) the DSS transmitter power, and (3) the DSS transmitter tuning rate, such that uplink lock would not be acquired on the secondary spacecraft.

Power subsystem performance was generally normal during the extended-mission periods, with adequate electrical power being provided to the spacecraft during all maneuvers and Sun occult periods. However, the power subsystem of Lunar Orbiter I began the extended mission operating with an excessive nighttime load caused by a fault in a shunt regulator transistor during the primary mission. In addition, the battery temperature was higher than desired due to the high operating temperature of the equipment-mounting deck. Under these conditions the early decay of the battery was a normal characteristic and was one of the factors leading to the decision to terminate the Lunar Orbiter I extended mission prior to the launch of Lunar Orbiter II. Nighttime leakage current through the shunt regulator was experienced by Lunar Orbiters II, III, and V but had no effect on extended-mission objectives.

Telemetry data analysis of the photo subsystems during the extended-mission periods was primarily concerned with the environmental control performance except for special experiments and exercises listed in Table 6-1. Analysis showed the leakage rate from pressurization systems to be very low. However, the photo subsystem internal pressure for Lunar Orbiter II began to decrease rather rapidly some time after Day 224 and reached essentially zero psi by Day 253. It was assumed that the loss of pressure was caused either by a small micrometeoroid puncture of the photo subsystem shell or by development of a small crack in a weld seam or around the window, probably due to thermal cycling. A short circuit in the power transformer secondary terminated efforts to advance film in Lunar Orbiter III. Since the film to be moved had been read out previously, the failure did not affect mission operations.

The structure and mechanisms systems, except for thermal control paint, performed within design limits. Deterioration of thermal control coatings required off-Sun attitude operation to maintain thermal control and retard paint deterioration. The addition of mirrors to Lunar Orbiters IV and V covering 20 to 30% of thermal control surfaces resulted in a thermal improvement of 25°F, but continued deterioration of the thermal paint still required off-Sun operation. Lunar Orbiters I and II experienced camera thermal door motor failures. In both cases the failure is attributable to anomalous commands: a wrong sequence of commands for Lunar Orbiter I and a scrambled programmer memory

resulting in a door-open control activation for Lunar Orbiter II.

The velocity and reaction control subsystems performed satisfactorily with no evidence of degradation throughout the extended-mission periods. Nitrogen usage was within predicted limits for the actual maneuvers and limit cycle modes maintained. Lunar Orbiters II, III, IV, and V all experienced slow leakage across the nitrogen shutoff squib valve. However, this was not detrimental to the missions. Lunar Orbiter V experienced an anomaly between January 26, 1968, and January 29, 1968, resulting in the depletion of the nitrogen attitude-control gas to an unsatisfactorily low level. The cause of the situation could not be conclusively established. However, because of this depletion the spacecraft was maneuvered to a controlled lunar impact on January 31, 1968

"The aeronautical and space activities of the United States shall be conducted so as to contribute . . . to the expansion of human knowledge of phenomena in the atmosphere and space. The Administration shall provide for the widest practicable and appropriate dissemination of information concerning its activities and the results thereof."

—NATIONAL AERONAUTICS AND SPACE ACT OF 1958

NASA SCIENTIFIC AND TECHNICAL PUBLICATIONS

TECHNICAL REPORTS: Scientific and technical information considered important, complete, and a lasting contribution to existing knowledge.

TECHNICAL NOTES: Information less broad in scope but nevertheless of importance as a contribution to existing knowledge.

TECHNICAL MEMORANDUMS: Information receiving limited distribution because of preliminary data, security classification, or other reasons.

CONTRACTOR REPORTS: Scientific and technical information generated under a NASA contract or grant and considered an important contribution to existing knowledge.

TECHNICAL TRANSLATIONS: Information published in a foreign language considered to merit NASA distribution in English.

SPECIAL PUBLICATIONS: Information derived from or of value to NASA activities. Publications include conference proceedings, monographs, data compilations, handbooks, sourcebooks, and special bibliographies.

TECHNOLOGY UTILIZATION PUBLICATIONS: Information on technology used by NASA that may be of particular interest in commercial and other non-aerospace applications. Publications include Tech Briefs, Technology Utilization Reports and Notes, and Technology Surveys.

Details on the availability of these publications may be obtained from:

SCIENTIFIC AND TECHNICAL INFORMATION DIVISION

NATIONAL AERONAUTICS AND SPACE ADMINISTRATION

Washington, D.C. 20546